PERFORMANCE EVALUATION OF CONVENTIONAL TURBOPROP ENGINES

A

DISSERTATION

Submitted in partial fulfillment of the requirement for the award of the degree of

Doctor of Philosophy

in

MECHANICAL ENGINEERING

by

Rajiv Ranjan
(ID: 12PHME105)

Under the Supervision of

Dr. MOHAMMAD TARIQ
Assistant Professor
Department of Mechanical Engineering
Shepherd Institute of Engineering & Technology

SAM HIGGINBOTTOM UNIVERSITY OF AGRICULTURE, TECHNOLOGY & SCIENCES

ALLAHABAD, UTTAR PRADESH

INDIA

2017

CERTIFICATE

This is certified that the studies conducted by Mr. Rajiv Ranjan, as reported in the thesis were under my guidance and supervision. The result reported by him is genuine and script of the thesis has been written by the candidate himself.

His thesis entitled **"Performance Evaluation of Conventional Turboprop Engines"** is therefore forwarded for the acceptance in the fulfillment of the requirements for the award of degree of **DOCTOR OF PHILOSOPHY IN MECHANICAL ENGINEERING.**

Dr. M. Tariq

Advisor

Assistant Professor

Department of Mechanical Engineering

SIET, SHUATS, Allahabad, India

SELF ATTESTATION

This is to certify that I have personally worked on the research project titled “Performance Evaluation of Conventional Turboprop Engines”. The data given in the project report has been generated during the work, and are genuine. Data/ information obtained from the other agencies have been duly acknowledged. None of the finding/information pertaining to the work has been concealed. The results embodied in this project report have not been submitted to any other university or institution for the award of any degree or diploma.

Place: Allahabad **(RAJIV RANJAN)**

Date: ……

ACKNOWLEDGEMENT

"No Thesis is a solo effort" may be a somewhat overused cliché, but it truly reflects the huge amount of support I have had over the last four years.

Firstly, I'd like to thank my supervisor and mentor Dr. Mohammad Tariq for his guidance throughout both my undergraduate and postgraduate studies. As his first PhD student, I hope that I will always hold a special place in his heart. Similarly, thanks go to Prof (Dr.) Mohammad Imtiyaz, Chairman, DIET for his role of indefatigable problem solver since my initial involvement with the SHUATS University. The research presented in this thesis simply would not have been possible without the efforts of these two.

The SHUATS is something of a family, and as such I'd like to thank its members for their assistance over the years. All deserve an honourable mention. I am indebted to Hon'ble Vice Chancellor, The Most Rev. Prof (Dr.) R. B Lal, Sam Higginbottom University of Agricultural Technology & Sciences, for providing higher studies under doctoral programme in the university.

I express my sincere gratitude to Dr. C. K Shukla, Professor and Dean, Faculty of Engineering & Technology. I am also indebted to Er. Deepak Lal, Dean, Shepherd School of Engineering & Technology for his technical and valuable suggestions.

I am thankful to Prof (Dr.) Anshuka Srivastava, Department of Mechanical Engineering for providing facility and advice needed to complete the work. I am also thankful to all the staff members of Department of Mechanical Engineering for providing the necessary help and encouragement during the work.

I am grateful to my member Dr. L. P Singh, SHUATS for his invaluable guidance, constant encouragement, moral support, and wholehearted co-operation during this research work.

I express my sincere gratitude and indebtedness to Dr. Shakti Suryavanshi, SHUATS for his valuable suggestions and help during the course of study.

I am also grateful to Dr. R. Yadav, (Retired Director General, MIT, Moradabad) and Dr. V.K Neema, (Retired professor, MNNIT, Allahabad) for initiating this work and providing the useful literatures and information regarding turbojet and turbofan engines using gas turbine cycles.

My sincere thanks go to Prof (Dr.) J. D. Mattingly for providing an insight performance data and constructive suggestionson the present analysis. His work on jet propulsion accommodated a great solution for the performance analysis of turboprop engine.

My sister, Bijya and Beauty and brother, Nitish deserves recognition for providing an academic role model.Thanks also go to my parentsfor always supporting me, even when the world seemed to be falling apart. You are the strongest and bravest people that I know, and this thesis is dedicated to you. They have been in the unusual (and arguably unenviable) position of being able to offer me both technical and emotional support, and have provided this in abundance over the last few years.

I thankfully acknowledge the help and support by all the fellow friends Er. V.K Kushwaha, Mr. Donald Denis and all other well wishers for their direct and indirect help at various stages of this research work.

The financial assistance provided by ‘Union Grants Commission’, Govt. of India is gratefully acknowledged.

(RAJIV RANJAN)

TABLE OF CONTENTS

ABSTRACT

Aircraft gas turbine cycles differ from shaft power cycles in that the useful power output is in the form of thrust. The whole of the thrust of the turbojet and turbofan is generated in propelling nozzles whereas with the turboprop, most of the thrust is produced by a propeller with only a small contribution from the exhaust nozzle. A second distinguishing feature is the need to consider the effect of forward speed of flight and altitude on the performance. It was the beneficial aspect of these parameters, together with a vastly superior power/weight ratio that enabled the gas turbine to so rapidly supplant the reciprocating engine for aircraft propulsion except for aircraft propulsion and low powered lighter aircraft.The designer of aircraft engines recognized the various requirements for take-off, climb, cruise and manoeuvring, the relative importance of these being different for civil and military applications and for long and short haul aircraft. In the early days, it was common practice to focus on the take-off thrust, but this is no longer acceptable. Engines for long range civil aircraft, for example, require low SFC at cruise speed and altitude, while the thrust level may be determined either by take-off thrust on the hottest day likely to be encountered or by the thrust required at top of climb. Evidently the selection of design condition is much more complex than for a land- based unit. As examples, ‘design point’ calculations will be shown for take-off (static) and cruise condition.

In turboprop engines a conventional aircraft propeller is usually mounted in front of the jet engine and in one type of engine is driven by a second or free turbine. This is located behind the turbine that is driving the compressor. In other designs the power is obtained by additional stages on the main turbine.Since turbine speeds are much higher than propeller speed, a reduction gear is required between the turbine and the propeller. About 90 percent of the energy in the hot gases is absorbed in the turbine, and only about 10 percent remains to increase the speed of the exhaust jet. Accordingly, only a very small portion of the overall thrust is produced by the jet; most of it comes from the propeller. Turboprops are usually rated on the basis of equivalent power at take-off conditions and the specific fuel consumption and specific power are often expressed in terms of that equivalent power. It is nevertheless desirable to quote both the shaft power and jet thrust available.

Turboprops are advantageous for small and medium-sized planes and at air speeds from 480 to 640 kilometers/hour. They cannot compete with turbojets for very large planes or at higher speeds. The limitations and advantages of the turboprop are those of the propeller. In recent

development of gas turbine cycles, new software for calculating thermal efficiency and power output of the turboprop engine is optimized. The present analysis includes several of the air-breathing engine performance parameters that are useful in aircraft propulsion (i.e., turbine inlet temperature, compressor pressure ratio, thrust specific fuel consumption) for a real turboprop engine. The study is based on design point performance and has been carried out by selecting models for different components of engines. Software in 'MATLAB 14' has been developed, which is capable of predicting engine dependent parameters for two-spool turboprop engine. Two design variables – the compressor pressure ratio and the low- pressure (free or power) turbine temperature ratio is considered to develop the cycle equations in terms of the pressure and temperature ratios across both the high- pressure turbine (drives the compressor) and the low- pressure turbine. The results show the variation in performance of a turboprop engine with compressor pressure ratio and turbine temperature ratio. The figures for the engine cycle with losses can be compared with the performance of the ideal turboprop engines to see the effects of component performance on the overall cycle. The engine with losses that gives the minimum fuel consumption has a compressor pressure ratio of 30 and corresponding turbine temperatures of 0.40 are drawn with dashed curves. The specific thrust developed by the core increases with compressor pressure ratio for a constant turbine temperature ratio. On the other hand, the thrust per unit core mass flow developed by the propeller has a shape similar to the total specific thrust curve.

LIST OF SYMBOLS

a	speed of sound; constant
C	work output co-efficient
C_c	work output co-efficient of core
C_P	pressure co-efficient
C_{prop}	work output co-efficient of propeller
C_{tot}	total work output co-efficient
C_V	velocity co-efficient
c_p	specific heat at constant pressure
c_v	specific heat at constant volume
E	energy; modulus of elasticity
e	polytropic efficiency; energy per unit mass
F	force; uninstalled thrust
g_c	Newton's constant
h	enthalpy per unit mass
h_{PR}	low heating value of fuel
M	Mach number
$\dot{m}$	mass flow rate
R	gas constant; additional drag
S	uninstalled thrust specific fuel consumption
T	temperature; installed thrust
U	internal energy; rotor velocity
u	internal energy per unit mass
V	absolute velocity; volume
$\dot{W}$	power
w	work interaction per unit mass

Subscripts

A	air mass
a	air; atmosphere
b	burner; combustor
C	core stream
c	compressor; chamber; centrifugal
d	diffuser or inlet
g	gearing; gas
j	jet
L	low-pressure
m	mechanical; mean
n	nozzle
O	overall; output
P	propulsive; products
p	propellant
prop	propeller
r	ram; reduced; rotor
SL	sea level
T	thermal
t	total; turbine
σ	control volume
0, 1, 2,.....10	different locations

Greek

α	bypass ratio; angle
γ	ratio of specific heats
Δ	change
Δ	dimensionless pressure; deviation

η	efficiency
μ	Mach angle
π	pressure ratio
ρ	density
Σ	sum
τ	temperature ratio; torque
τ_λ	enthalpy ratio
ω	angular speed

LIST OF TABLE

LIST OF FIGURES

CHAPTER 1

1. INTRODUCTION

This chapter provides an overview of gas turbine performance, applications, recent researches and objectives of the present work. Within this chapter, the issues addressed by the present research work are contextualized in a broader form.

1.1 OVERVIEW

Upcoming world economy is speculated to be truly omnibus where national periphery becomes prevalent by interdependent commerce. This future view can only be considered if there is drastic change in transportation systems, entitling greater mobility of people and products with renovate safety, timeless and vantage. Propulsion and power capabilities are the foundation on which future subsonic transport aircrafts will shape the aviation landscape and establish this global conduit of commerce. The early inclusion of technological and operational scenarios into aircraft design as well as the ability to cover the analysis of competitor aircraft asks for a flexible software system. However, traditional research activities have laid the more emphasis on the development of sophisticated analysis methods for all disciplines involved in the design process rather than on the introduction of modern software technologies in an aircraft design system. A modern design tool has to cope with complex data management and varying input schemes.

Driving force modernity has been the fundamental driver for the progress in air transportation. Plenteous progresses in driving force execution and efficiency have made it possible for aircraft to travel at higher speeds over longer distance while carrying larger payloads. This has enhanced efficiency by orders of magnitude since the arrival of air travel.

Air transportation in the new millennium will require revolutionary key to meet public demand for reforming safety, credibility, environmental consistency and affordability. In the recent years of powered flight, the aviation community is well balanced to meet defiance of new millennium. Safety, capacity, economy and environmental concern remain the themes and challenges for NASA and its industry partners in 21st century. The public needs to get to destinations faster and cheaper with improved quality of travel while allowing aviation to expand to meet the increased demand for service. Future aero-propulsion system will require operating over a wide range of fight

regimes, while providing unprecedented high level of safety and reliability. They will need to be much more energy efficient throughout their flight envelopes.

Ordinarily, airplanes are powered by turboprop engines. These engines are quite reliable, providing years of trouble free services. However, because of the rarity of turboprop engine malfunctions and the limitations of simulating those malfunctions, many flight crew have felt unprepared to diagnose engine malfunctions that have occurred. These turboprop engines are used on many small commercial subsonic aircraft. This engine has typically two spools namely; the core engine spool and the power spool. The pressure ratios across the high pressure turbines and power turbines are normally high enough to have choked flow in the turbine inlet nozzle for most operating conditions of interest. The convergent exhaust nozzle of these turboprop engines has a fixed throat area which will be choked when the exhaust total ambient static pressure ratio is equal. When exhaust nozzle is unchoked, the nozzle exit pressure equals the ambient pressure and the exit Mach number is subsonic, with constant temperature ratio and pressure ratio for the turbine driving the compressor. The analysis of the turboprop's core mass flow rate and compressor pressure ratio follows directly from the single-spool turbojet engine with choked exhaust nozzle. Gas turbine engine designers have attempted to increase thrust to weight ratio and widen the thrust range of engine operation, especially for military engines. The present scenario for combustion is through conventional combustion chamber either for main combustor or afterburner. A new concept has been proposed to achieve combustion in the turbine passages, which in general has been considered to be undesirable.

1.2 EVOLUTION OF TURBOPROP ENGINES

Man-made propulsion devices have existed for many centuries and natural devices have developed through evolution. Most modern engine and gas turbines have one common denominator: compressors and turbines or turbo-machines. Both the turboprop and piston engines are the two commonly known types of engines used to power propelled-driven aircraft. For several decades, the piston engines coupled with propellers have provided the necessary power for early aircrafts. The aviation was once dominated by the piston propeller aircraft through the 1950's until rapid advancement in aircraft engine technology introduced the turbojet (Banach & Reynold's, 1984). The emergence of turbojet and turboprop engines in the 1940's were encouraged by the difficulties encountered in developing advance technology for piston engines (Constant, 1980). As

aircraft safety is greatly improved and these engines allow much faster speed when compared to piston-powered, the air transportation business has also dramatically changed.

As the gas turbine technology continues to develop, it let to the introduction of the turbofan engine to replace turbojet engine. However, a serious energy crisis in the 1970's gave a huge impact to the airlines industry as more than half of the airlines operating costs went to their fuel expenditures (Bowles & Dawson 1998). Realizing that the existing turbine engine consumes more fuel and a significant imporvement in engune fuel consumtion is essential , a new type of engine has been proposed by the United States National Aeronautics and Space Administration (NASA). The proposed engine by NASA which is referred to as 'propfan',has the performance of turboprop engine with an addition of advanced propellers. The advanced propeller feature thin, swept and twisted propeller blades, with complex structural properties (Nethercote et al.,1992). Propfan concept is a trademark of Hamilton-Standard which works on this project together with NASA. It has a bypass ratio of more than 30 and it incoporates some of the characteristics and advantages of a turboprop engine while allowing higher flight speeds (Crane, 2005). In terms of productivity and passenger comfort, it is almost as similar to a ten compared to advanced turbofan (Banach & Reynolds,1984).

1.3 AERO-PROPULSION SYSTEM

The existence of the gas turbine engine's first application for aircraft propulsion is almost 60 years old and a revolution has been vatical to improve their execution. The target has been to mitigate the fuel burn, enhance safety and credibility and slacken the environmental influence of disruptive dispersion and noise. It is believed that further progress in aircraft gas turbine engine technology will continue for another 20-30 years at which point the gas turbine revolution will end with the development of what NASA calls "Intelligent Engines". These engines will be without human interruption and capable to operate at optimum conditions to accomplish pre-specified customer requirements during the entire ground and flight envelope. For example, during take-off and approach, the engine will optimize geometry and air flow to achieve minimum noise and emissions during cruise operation; it will optimize itself to mitigate fuel burn.

At the beginning of this century, steam and internal combustion engines were in existence but were far too heavy for flight application. The Wright brothers recognized

the great future potential of the internal combustion engine and developed both a relatively light weight engine suitable for flight applications. Through the subsequent four decades of evolution, the overall efficiency and power to weight ratio improved substantially, latter by more than one order of magnitude to about 1.3156kW/kg. This great improvement was achieved by engine design structures and materials, advanced fuel injection, aerodynamic shapes of the propeller blades, variable pitch propellers and engine superchargers. The overall efficiency reached about 28% and the power output of the largest engine amounted to 5000hp.

1.4 GAS TURBINE

Gas turbines are an important source of mechanical power not only for air and sea transportation, but also for the cogeneration of electricity. To monitor and control the operation of these complex machines it is necessary to develop high fidelity mathematical models that describe the operating conditions both in steady state and transient operations, predicting simulations that could affect the safety and engine performance. Simulations are also used extensively in the development, testing and turning of the control system, reducing the time and the cost of gas turbine equipment. The primary purpose of gas turbines is to extract mechanical energy from the hot gases delivered to it by the combustion chamber and to supply shaft power to drive the compressor. The turbine also supplies power to the auxiliary equipment, such as fuel pumps, oil pumps, and electrical generators. In turboprop and turboshaft engines, the turbine supplies power to drive the propeller or helicopter rotor. Typically, three-fourths of all the energy available for the products of combustion is necessary to drive the compressor. If the engine is a turboprop or turboshaft, the turbine is designed to extract all the energy possible from the gases passing through the engine. So efficient is the turbine, in this case, that in a turboprop aircraft the propeller provides approximately 90% of the propulsive force, leaving but 10% to be supplied by jet thrust. The axial flow turbine is comprised of two main elements i.e., turbine wheel or rotor and a set of stationary vanes. The stationary section consists of a plane of contoured vanes, concentric with the axis of the turbine, and set at an angle to form a series of small nozzles which discharge the turbine gases onto the blades of the turbine wheel. For this reason, the stationary vane assembly is usually referred to as the turbine nozzle, and the vanes themselves are called nozzle guide vanes. Aerodynamic design of turbine blades is less critical than compressor blades because they operate in a regime

of favourable pressure gradient rather than an adverse pressure gradient. Turbine-nozzle area is a critical part of turbine design because it establishes the engine (compressor operating line). The jets of escaping gases which are formed by the nozzle discharge are directed against the rotating turbine blades in a direction which enables the kinetic energy of the gases to be transformed into mechanical energy which is generated by the rotating turbine wheel. Turbines may be either single or multiple-stage. When the turbine has more than one stage, stationary vanes are inserted between each rotor wheel and the rotor wheel downstream, as well as at the entrance and exit of the turbine unit. Each set of stationary vanes forms a nozzle vane assembly for the turbine wheel that follows. The exit set of vanes serves to straighten the gas flow before passage through the jet nozzle.

1.4.1 PROGRESSION OF THE GAS TURBINE

- It is proficient of producing large amount of expendable power for a comparatively small magnitude and ponderosity.
- Since motion of its entire prime genre involve pure rotation (i.e., no reciprocating motion as in a piston engine), its mechanical life is long and the compatible maintenance cost is relatively low.
- Notwithstanding the gas turbine must be started by some adventitious means (a small external motor or other source ,such as another gas turbine), it can be brought up to full load (peak output) conditions or circumstances in minutes as in proportional to a steam turbine plant whose outset time is measured in hours.
- A wide variety of fuels can be employed. Generally, natural gas is used in land based gas turbine while light distillate (kerosene-like) oils power aircraft gas turbines. Diesel oil or peculiarly treated residual oils can also be used as well as inflammable gases derived from blast furnaces, refineries and the gasification of solid fuel such as wood chips, coal and bagasse.
- Commonly working fluid is atmospheric air. As an ultimate power supply, the gas turbine lacks no coolant (e.g. - water).

Primarily, one of the major deficit of the gas turbine was its lower competency (hence higher fuel usage) when collated to other IC engine and to steam turbine power plants. Notwithstanding, during the last fifty years, sustained engineering progress work has uplifted the thermal efficiency (18% for the 1939 Neuchatel gas turbine) to extant

levels of about 40% for simple cycle operation and about 55% for combined cycle operation. Furthermore, fuel potential gas turbines are in the mapping stages with simple cycle efficiencies predicted as high as 47% and combined cycle machines in the range of 60%. These overhanging values are significantly surpassing the other prime movers, such as steam power plants.

1.4.2 Open Gas-Turbine Cycle

1.4.2.1 Working Principal

Fresh air enters the compressor at ambient temperature where its pressure and temperature are increased. The high pressure air enters the combustion chamber where the fuel is burned at constant pressure. The high temperature (and pressure) gas enters the turbine where it expands to ambient pressure and produces work.

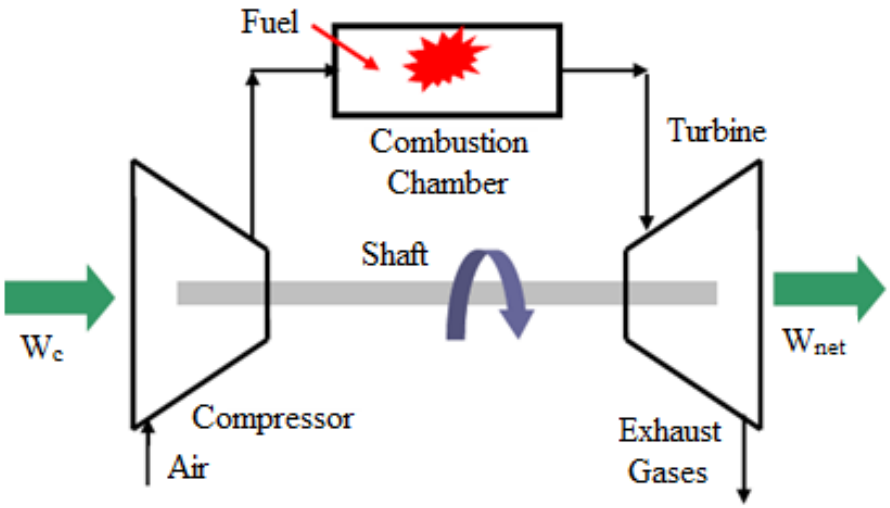

Fig.1.1 Schematic for an open gas-turbine cycle

Features:

- Gas-turbine is used in aircraft propulsion and electric power generation.
- High thermal efficiencies up to 44%.
- Suitable for combined cycles (with steam power plant)
- High power to weight ratio, high reliability, long life
- Fast start up time, about 2 min, compared to 4 hr for steam-propulsion systems
- High back work ratio (ratio of compressor work to the turbine work), up to 50%, compared to few percent in steam power plants.

1.4.3 Closed gas turbine cycle

A closed cycle gas turbine is a turbine in which the air is circulated continuously within the turbine. The components of this turbine are compressor, heating chamber, gas turbine which drives the generator and compressor, and a cooling chamber.

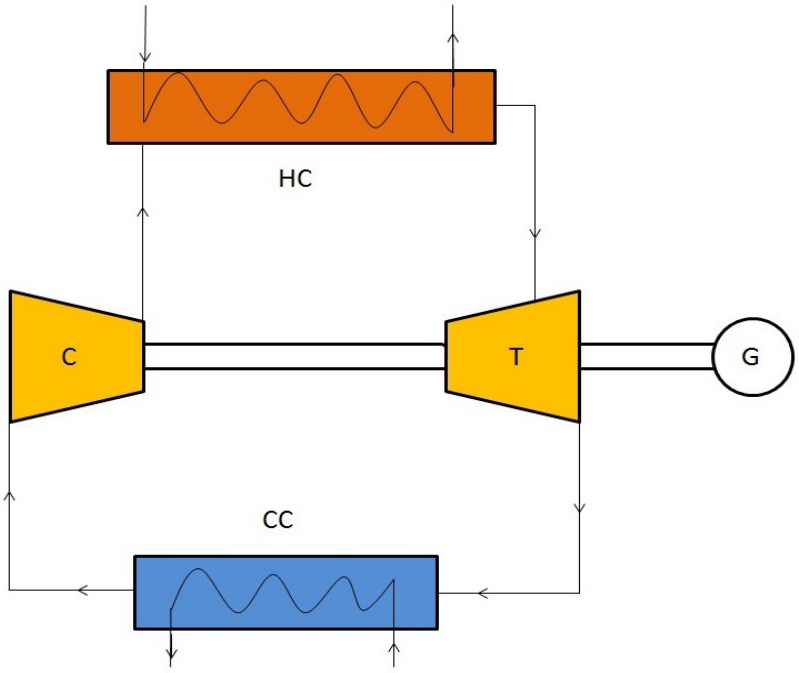

Fig.1.2 Schematic for close gas-turbine cycle

The function of various components of a simplest form of a closed cycle gas turbine is discussed below:

a) **Compressor (C):** It is used to compress the air.
b) **Heating chamber (HC):** The heating of the compressed air is takes place in the heating chamber.
c) **Gas turbine (T):** It is used to produce the useful work which is used by the generator to generate electricity.
d) **Generator (G):** It generates the electricity with the help of the gas turbine.
e) **Cooling chamber (CC):** Cooling of the gas after passing from the turbine takes place in the cooling chamber.

1.4.3.1 Working Principle

The closed cycle gas turbine works on the principle of Joule's or Brayton's cycle. In this turbine, the gas is compressed isentropically and then passed into the heating chamber. The compressor generally used is of rotary type. The compressed air is heated with the help of some external source and then made to flow over the turbine blades. The turbine used here is of reaction type. The gas while flowing over the blades of the turbine gets expanded. From the turbine the gas is passed to the cooling chamber. Here the gas is cooled at constant pressure with the help of circulating water to its original temperature. Now the gas is again made to flow through the compressor to repeat the process. Here the same gas is circulated again and again in the working of a closed cycle gas turbine.

1.4.4 Brayton Cycle

Brayton cycle is the ideal cycle for gas-turbine engines in which the working fluid undergoes a closed loop. That is the combustion and exhaust processes are modelled by constant-pressure heat addition and rejection, respectively.

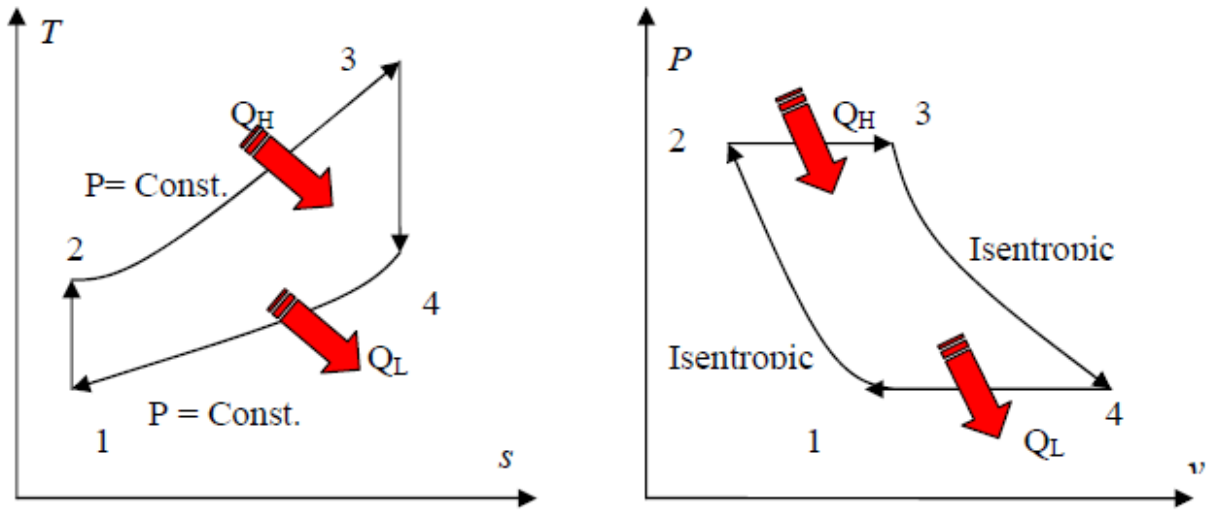

Fig.1.3 T-s and P-v diagrams for ideal Brayton cycle

The Brayton ideal cycle is made up of four internally reversible processes:

1-2 Isentropic compression (in compressor)

2-3 Constant pressure heat-additions (in combustion chamber)

3-4 Isentropic expansion (in turbine)

4-1 Constant pressure heat rejection (exhaust)

1.5 CLASSIFICATION OF JET PROPULSION

The jet propulsion engines are extensively categorised on the basis of their way of using oxygen for the deflagration of the fuel. Accordingly, they are classified as air breathing and non-air breathing engines. Rockets are mainly categorised as non-breathing engines while air-breathing engines include turbojet, turbofan, turboprop, turboshaft and ramjet engines.

The propulsion provided by air-breathing and rocket engines is just similar in that thrust is attend by producing reward momentum is one or more streams of gas. In case of a rocket, the propulsive gas originates on-board the vehicle and is hence independent of atmospheric air whereas in an air-breathing engine most of the propelling gas incepts from the free air surrounding the vehicle. Thus the execution relies upon the weight and the temperature if the climatic air and subsequently to go an awesome range and the height and forward speed of the engine. Rockets are classified relying on the fuel state as liquid and solid propellant rockets. While ramjet, on the basis of type of deflagration are classified as pulse jet with discontinuous combustion and scramjet with supersonic firm state combustion. Aircraft gas turbine cycles differ from shaft power cycles in that useful power output of the former in the form of thrust is cultivated wholly are in part as a result of enhancement in a propelling nozzle: downright in turbojet and turbofan engines and partly in turboprop engines. In the current work our main target is to vaticinate the performance of the turboprop engines.

The gas turbine engine is an intricate accumulation of variety of substantive that is designed on the basis of thermodynamic laws. The design and operation theories of these particular substantive are intricated. The intrication of aero-dynamic analysis make it inaccessible to mathematically solve the optimization equations involved in various gas cycles. When gas turbine engines were designed during the last century, the need to estimate the engine performance at both design point and off design conditions becomes articulate. Manufactures and designers of gas turbine engines became conscious that some tools were needed to predict the performance of the gas turbine engines especially at off design conditions where its performance was significantly affected by the load and the operating conditions. Also, it was assumed that these tools would help in vaticinating the performance of particular substantive such as compressor, turbine and combustion chamber etc.

1.6 PRINCIPLE OF JET PROPULSION

Jet propulsion is a practical application of Sir Isaac Newton's third law of motion which states that, for every force acting on a body there is an opposite and equal reaction'. For aircraft propulsion, the body is atmospheric air that is caused to accelerate as it passes through the engine. The force required to give this acceleration has an equal effect in the opposite direction acting on the apparatus producing the acceleration. A jet engine produces thrust in a similar way to the engine/propeller combination. Both propel the aircraft by thrusting a large weight of air backwards, one in the form of a large air slip stream at comparatively low speed and the other in the form of a jet of gas at very high speed. This same principle of reaction occurs in all forms of movement and has been usefully applied in many ways.

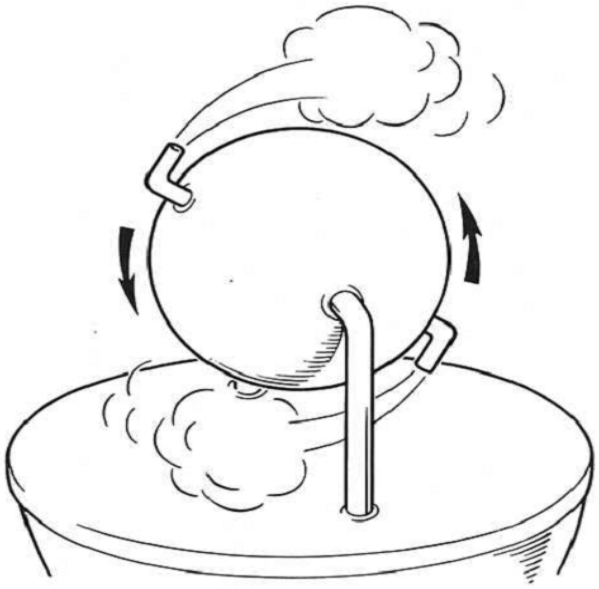

Fig. 1.4 Hero's engine – probably the earliest form of jet reaction

The earliest known example of jet reaction is that of Hero's engine (Fig. 1.4) produced as a toy in120 B.C. This toy showed how the momentum of steam issuing from a number of jets could impart an equal and opposite reaction to the jets themselves, thus causing the engine to revolve.

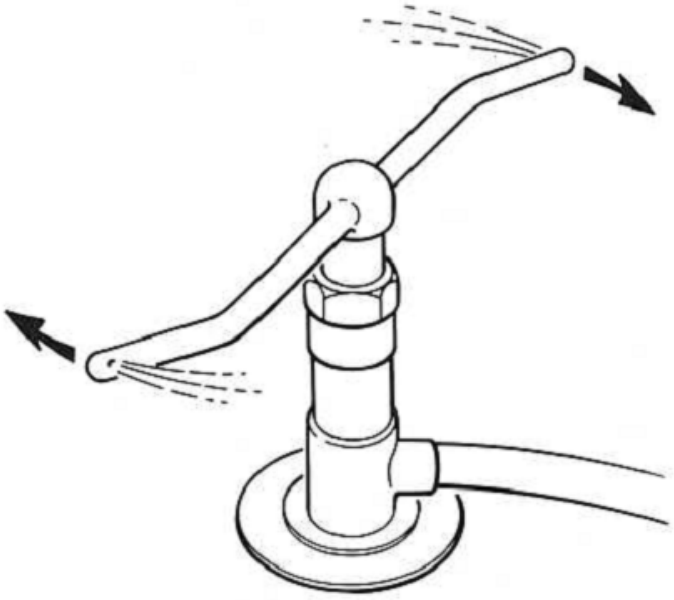

Fig. 1.5 A garden sprinkler rotated by the reaction of the water jets

The familiar whirling garden sprinkler (Fig. 1.5) is a more practical example of this principle, for the mechanism rotates by virtue of the reaction to the water jets. The high pressure jets of modern fire-fighting equipment are also an example of 'jet reaction', for often, due to the reaction of the water jet, the hose cannot be held or controlled by one fireman. Perhaps the simplest illustration of this principle is afforded by the carnival balloon which, when the air or gas is released, rushes rapidly away in the direction opposite to the jet. Jet reaction is definitely an internal phenomenon and does not, as is frequently assumed, result from the pressure of the jet on the atmosphere. In fact the jet propulsion engine, whether rocket, athodyd or turbojet is a piece of apparatus designed to accelerate a stream of air or gas and to expel it at high velocity. There are, of course, a number of ways of doing this but in all instances the resultant reaction or thrust exerted on the engine is proportional to the mass or weight of air expelled by the engine and to the velocity change imparted to it. In other words, the same thrust can be provided either by giving a large mass of air a little extra velocity or a small mass of air a large extra velocity. In practice it is preferred since by lowering the jet velocity relative to the atmosphere a higher propulsive efficiency is obtained.

1.7 TYPES OF JET PROPULSION SYSTEM

There are two general types of jet propulsion engines, namely air-breathing and non-air breathing engines. Air-breathing engines use oxygen from the atmosphere in the

combustion of the fuel. They include turbojet, turboprop, ramjet and pulsejet. The term jet is usually used only in reference to air-breathing engines. Non- breathing engines carry an oxygen supply. They can be used both in the atmosphere and in outer space. They are commonly called rockets and are of two types i.e., liquid propellant and solid propellant.

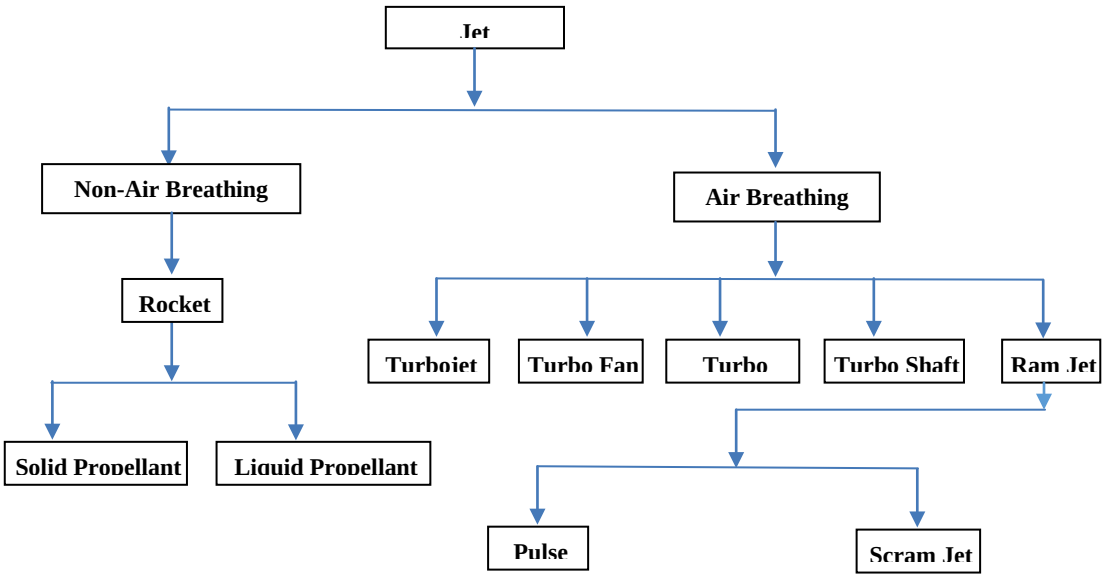

Fig. 1.6 Layout of Jet Propulsion System

1.7.1 Turbojet

The turbojet engine, developed for aircraft in the years prior to World War II, was a departure in thinking from the standard piston engine. Instead of burning fuel in a confined space that is dependent upon precise timing of ignition, the turbojet engine is essentially an open tube that burns fuel continuously. According to Newton's third law, as hot gases expand out from the rear of the engine, the engine is accelerated in the opposite direction. The engine consists of three main parts, the compressor, the burner, and the turbine, along with the inlet, shaft, and nozzle, as shown above. A large mass of air enters the engine through the inlet and is drawn into a rotating compressor. There are two types of compressors, centrifugal and axial. The compressor raises the pressure of the air entering the engine by passing it through a series of rotating and stationary blades. As the gas is forced into smaller and smaller volumes, the pressure of the gas is increased. The gas also heats up as its volume is decreased by the compressor. Today's compressors can have a compression ratio of over 40:1, much higher than a piston

engine. Also, in order to maximize the engine's performance, turbojets will have two different compressors operating on different shafts: a low-pressure compressor followed by a high-pressure compressor.

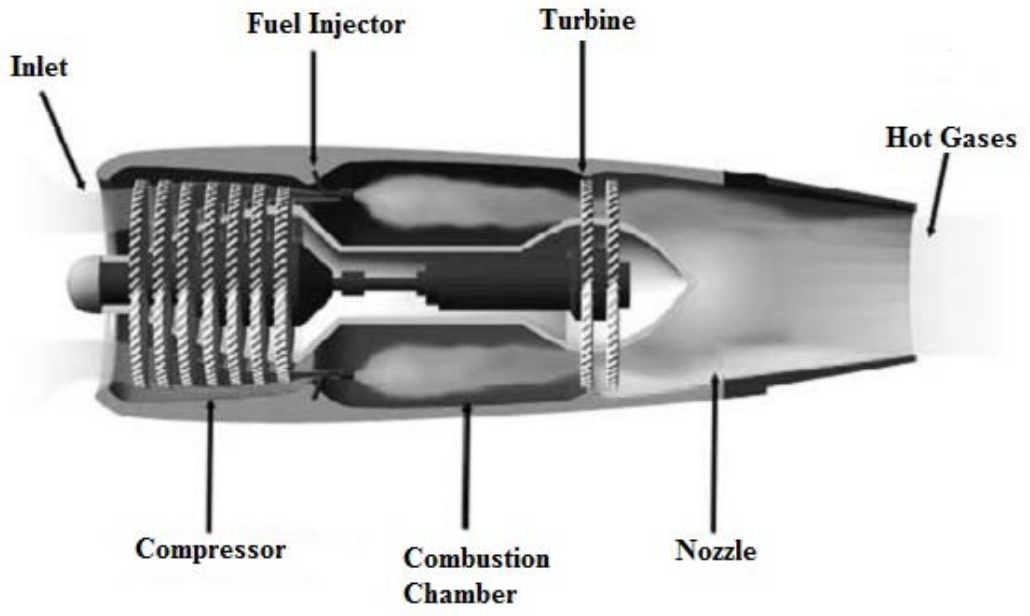

Fig. 1.7 Cutaway view of turbojet engine

At the burner stage fuel is injected and ignited, raising the energy of the gas by raising its temperature. A typical engine will add about 0.9072 kg/s for every 45.36 kg/s. The energy of the gas increases dramatically and is accelerated toward the turbine due to the high pressure created by the compressor. Since these engines can produce temperatures well over the melting points of the materials used to make the turbine, only 12 to 25 percent of the air from the compressor is combusted while the rest cools the combusted gases down to temperatures just below that which would damage the turbine. The larger the difference between the temperature of gas at the turbine face and that of the outside air, the more thrust is created and the more efficient the engine. The next stage is the turbine. Here the heated gas passes over the turbine blades causing them to rotate and, in turn, to rotate a shaft that is connected to the compressor. The turbine removes some energy from the flow to drive the compressor, but there remains sufficient energy in the gas to do work as it exits the nozzle. The purpose of the nozzle is to convert energy into velocity thus producing thrust. The nozzle allows the flow of hot gases to exit the rear of the engine until they reach free-stream pressure, which creates the thrust of the engine. Most nozzles restrict the flow somewhat before allowing it to expand. This creates

additional pressure and thus, additional thrust. It also controls the mass flow through the engine, which along with the velocity, determines the amount of energy the engine produces. Overall, turbine engines have a much higher power-to-weight ratio than piston engines. They can operate at much higher temperatures and can produce much more thrust than propeller engines. However, they are less efficient at low speeds and low altitudes.

1.7.2 Turbofan

A turbofan is a modified version of a turbojet engine. Both shares the same basic core of an inlet, compressor, burner, turbine and nozzle but the turbofan has an additional turbine to turn a large, many-bladed fan located at the front of the engine. This is called a “two-spool” engine. One spool is used to power the compressor and another spool to turn the large fan. Some of the air from this large fan enters the engine core where fuel is burned to provide some thrust, but up to 90 percent of it goes around or “by passes” the core of the engine. As much as 75 percent of the total thrust of the engine comes from the bypass air. Although there is less energy added to this bypass air compared with that going through the core, by moving a very large amount of air the turbofan gets a large boost in thrust for very little additional fuel.

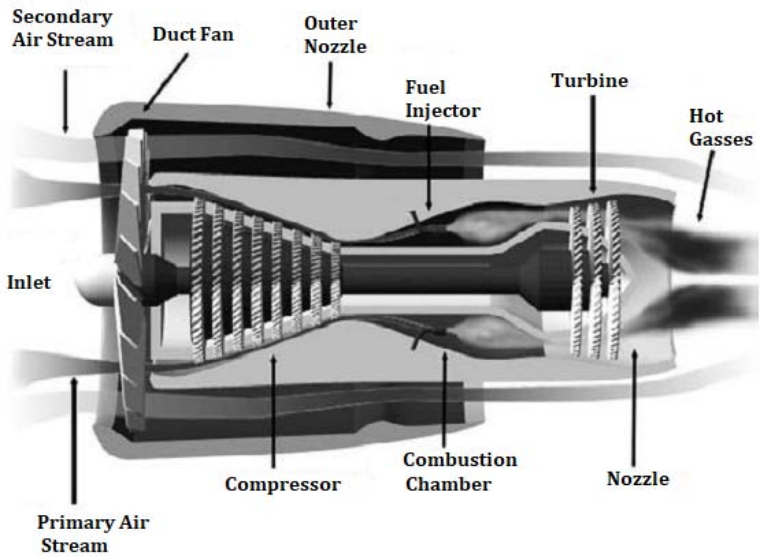

Fig.1.8 Cutaway view of turbofan engine

It is thus a very fuel-efficient engine and good for cruising. Also, since the fan has many blades and the air is ducted, turbofans can operate faster and more efficiently than simple propeller aircraft. The pressure ratio of a 50-blade ducted fan may be 1.4 to 1.6

(i.e., the pressure is increased by a factor of 1.4 to 1.6) whereas a propeller may have a pressure ratio of only 1.02. This is why large passenger planes using turbofans are able to cruise at high subsonic speeds and still use fuel efficiently. Even jet fighters will often use low-bypass. Turbofan engines, where a smaller amount of air bypasses the core, so they can conserve fuel while in cruising mode.

1.7.3 Turboprop

This engine is a hybrid of a turbojet and a propeller engine. It has at its heart a turbojet core to produce power, but with two turbines. The first turbine powers the compressor while the second powers the propeller through a separate shaft and gear reduction. The gears are necessary to keep the propeller from going super-sonic and losing efficiency.

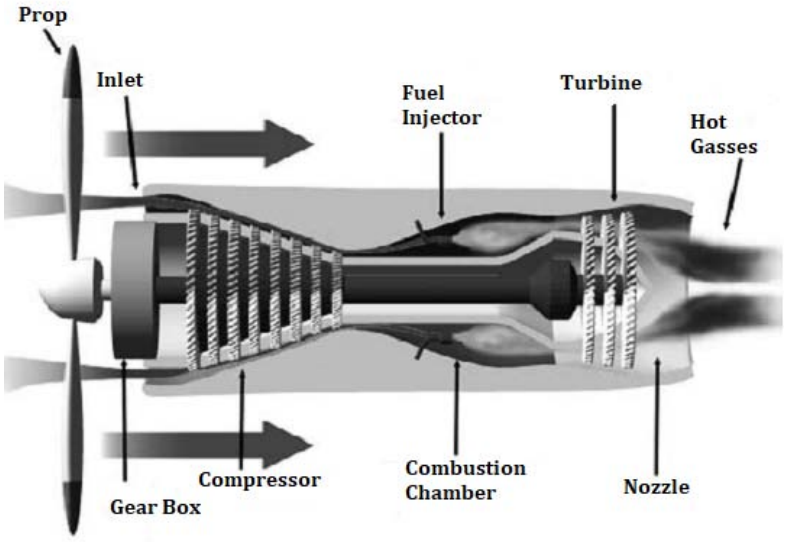

Fig. 1.9 Cutaway view of turboprop engine

Unlike a basic turbojet, the second turbine removes most of the remaining energy from the flow to power the propeller and less than 10 percent of actual thrust is produced by the core. Turboprops operate well in the low subsonic range, with much more power than a piston-driven propeller aircraft. This is why turbojets are used by long-range military cargo planes. Another version of the turboprop is the turbo-shaft engine. Instead of driving a propeller, the shaft is used to power such things as helicopters, tanks, train engines, and etc.

1.7.4 Ramjets

Rockets are a proven way to accelerate crafts to very high speeds, but rockets must carry their own supply of oxidizer as well as fuel. About 82 percent of the mass of the external

tank of the space shuttle is liquid oxygen (oxidizer). Ramjets are designed to scoop up their oxygen from the atmosphere and eliminate this extra weight. Thrust is produced by passing hot, combusted gases through a nozzle where the nozzle accelerates the flow. To maintain flow, combustion must occur at a pressure higher than the nozzle pressure. In a standard turbojet engine this pressure is created by the action of the compressor.

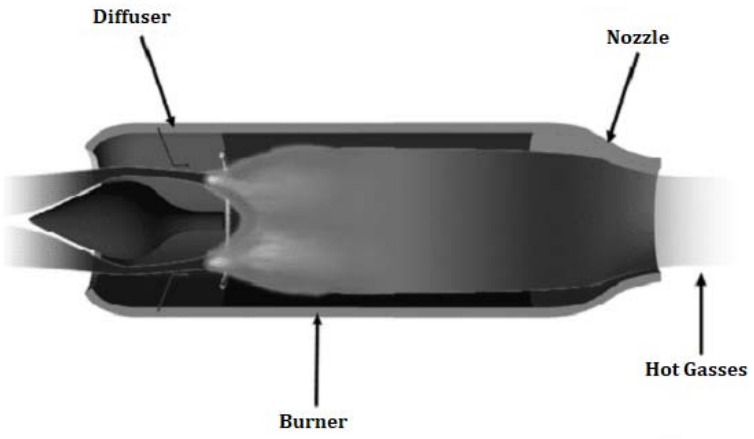

Fig. 1.10 Cutaway view of Ramjet

In a ramjet, however, there is no compressor. Instead, the forward speed of the vehicle is employed to 'ram' air into the combustor. At supersonic speeds air enters the intake where a diffuser nozzle causes the air to slow down to around Mach 0.2 through a series of shock waves. This sudden slowing creates the pressure needed to operate the engine. Fuel is injected and burned with the aid of a flame holder. Since there is no compressor to power, there is no need for a turbine and the hot gases expand directly out the nozzle. It is important to note that, other than an external turbo-pump to inject fuel; the ramjet has no moving parts and is lighter in weight than a turbojet. It also can operate at higher temperatures than a turbojet because there is no turbine that might melt thus it is more efficient.

1.7.5 Pulsejet Engines

A pulse-jet is similar to a ramjet except that a series of spring-loaded, shutter-type valves is located ahead of the combustion section. In a pulse-jet the combustion is intermittent or pulsing rather than continuous as in a ramjet. Air is admitted through the valves, and combustion begins. This increases the pressure and closes the valves, preventing backflow through the inlet. As the gases expand through the rear nozzle to produce thrust, the pressure in the combustion section drops to the point where the

valves open again to admit fresh air. This cycle is then repeated. The most widely known pulse-jet was the German V-1 missile or 'buzz bomb', which was used near the end of World War II and which fired at a frequency of about 40 cycles per second. Pulse-jets are inefficient, noisy, and subject to severe vibration. Their use is now limited to low-cost pilotless vehicles.

1.7.6 Scramjets

When the speed of a ramjet increases above Mach 5, the temperature in the combustion chambers would exceed 2000℃ . At this temperature the air is so hot that not much additional energy can be gained by burning fuel. There would also be some serious material damage to the inside of the engine. Scramjets are a way to overcome this speed limitation. In a scramjet (supersonic combustion ramjets), the incoming air is not slowed down to subsonic speeds, but is burned at supersonic speed. This creates other problems. The biggest of these is getting the fuel to mix efficiently with the air and burn in milliseconds or less before it exits the nozzle. It has been shown that hydrogen gas can be made to mix efficiently and burn under these conditions.

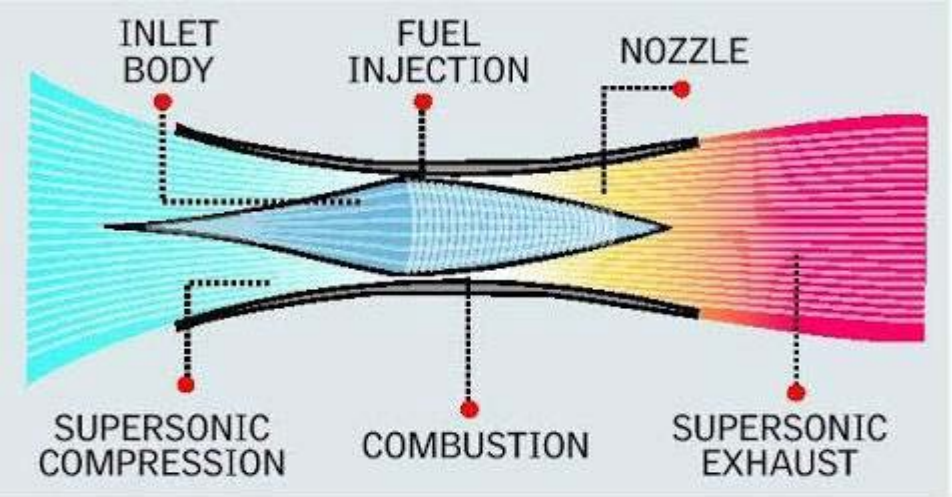

Fig. 1.11 Description of Scram Jet Engine

1.7.7 Jet Propulsion Engine Components

A greater understanding of the gas turbine and its operation can be gained by considering its five major components:

- Inlet/Intake
- Compressor
- Combustor

- Turbine
- Nozzle

The features and characteristics will be stated in concise.

1.7.7.1 Inlets

An inlet detracts the entering air velocity to a level appropriate for the compressor. The air velocity is mitigated by a compression headway which enhances the air pressure. The manipulation and design of the inlet are depicted in terms of the efficiency of the compression process, the outward drag of the inlet and the mass flow into the inlet. The design and the manipulation of the inlet depend on whether the air entering the conduit is subsonic or supersonic. As the aircraft outlooks the speed of sound, the air reclines to be more compressed and at Mach 1, shock wave occurs. Shock waves are compression waves and at higher Mach numbers these compression waves are energetic. Compression by shock wave is incapable.

1.7.7.1.1 Subsonic inlet

The subsonic inlet can be a divergent duct as shown in figure 1.12. This duct is tolerable until the Mach number becomes greater than 1, at which time a shock wave occurs at the mouth and the compression process becomes incapable. The subsonic divergent duct disengage best at one velocity (design point), and at other velocities, the compression process is less accomplished and the external drag is greater. The airflow patterns for the subsonic inlet are shown in figure 1.12.

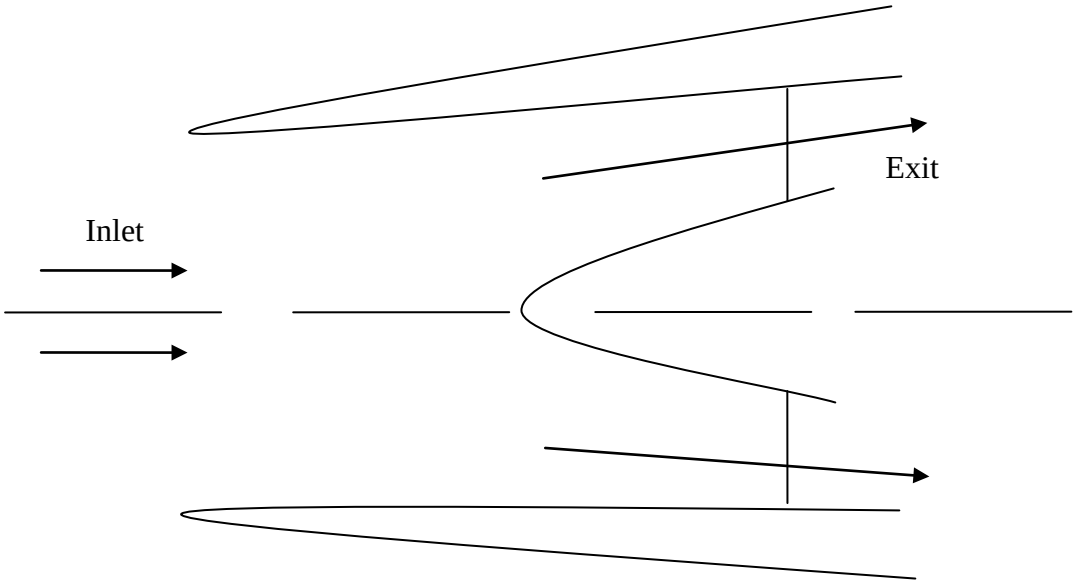

Fig. 1.12 Rough draft of Subsonic Inlet

1.7.7.1.2 Supersonic inlet

Since shock waves occur in supersonic flow, the geometry of such inlets is designed to enlist the most efficient compression with a minimum of weight. If the velocity is reduced from a supersonic speed to subsonic speed with one normal shock wave, the compression process comparatively inefficient. If several oblique shock waves are deputed to detract the velocity, the compression process is more efficient.

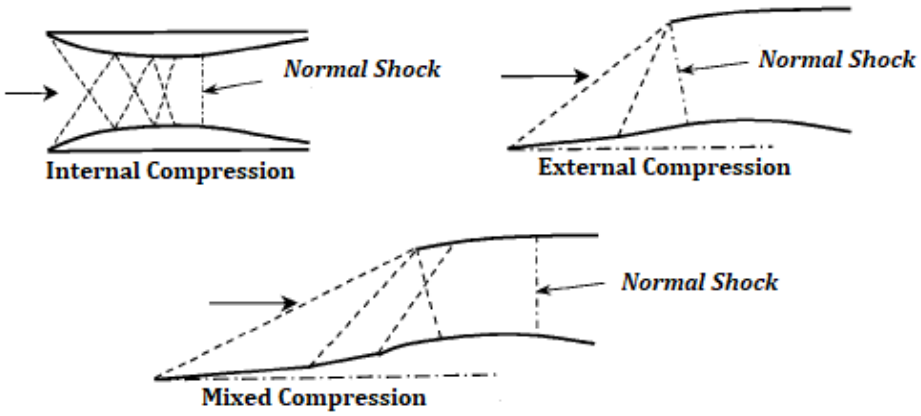

Fig.1.13 Schematic of Supersonic Inlet

Generally there are two types of supersonic inlets i.e., the ramp (two-dimensional wedge) and the centre body (three dimensional spikes). At off-design Mach numbers, the location of the shock waves change thus possessing the external drag and the efficiency of the compression.

1.7.7.2 Compressors

Compressors are an example of a negative shaft work machines. They increase both the temperatures and pressures of the working fluid. Increasing the pressure of the fluid requires a negative shaft work transfer. The compressor components are connected to the turbine by a shaft in order to allow to the turbine to the compressor. A signal shaft gas turbine has only one shaft connecting the compressor and turbine components. A twin spool gas turbine has two concentric shafts, a longer one connecting a low pressure compressor to a low pressure turbine (the low spool) which rotates inside a shorter, larger diameter shaft. The shorter, larger diameter shaft connects the high pressure turbine with the higher pressure compressor (the high spool) which rotates at higher speeds than the low spool. A triple spool engine would have a third intermediate pressure compressor turbine spool.

1.7.7.2.1 Axial compressors

The purpose of a compressor is to increase the total pressure of the gas stream to that required by the cycle while absorbing the minimum shaft power possible. Gas turbine compressors are either centrifugal or axial, can be a combination of both.

Centrifugal compressors (with compressed air output around the outer of the machine) are robust, generally cost less and limited to pressure ratios of 6 or 7 to 1. They are found in early gas turbines or in modern, smaller gas turbines.

The more efficient, higher capacity axial flow compressors (with compressed air output directed along the centre line of the machine) are used in most gas turbines. An axial compressor is made up of a relatively large number of stages, each stage, consisting of a row rotating blades (airfoils) and a row of stationary blades (stators), arranged so that the air is compressed as it passes through each stage.

Figure 1.14, illustrates the typical blading configuration for an axial flow compressor. One stage comprises a row of rotor blades followed by a row of stator vanes. A number of stages, with the rotors on a common shaft, form a compressor. Often an additional row of outlet guide vanes (OGVs) are required downstream of the last stator row to carry structural load, or remove any residual swirl prior to the flow entering the downstream duct. These are a row of stators vanes whose angle may be changed by control system action to improve off design operation. Some of the stator rows may also be of variable angle and these are referred to as variable stator vanes (VSVs). As a first order rule 1 stage of VIGVs or VSVs is required per each additional compressor stage beyond 5 to provide a satisfactory part speed surge line. This ratio will be reduced if handling bleed valves are available.

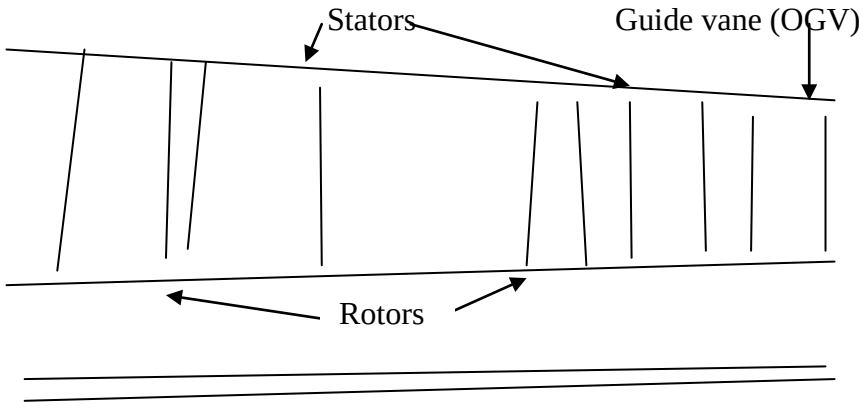

Fig. 1.14 Schematic of Axial Compressor

1.7.7.3 Combustion chamber (Combustor)

The combustion chamber is the component of the gas turbine in which fuel is combined with air from the compressor and burned. The combustion chamber functions like a heat exchanger and can be modelled as a constant pressure device. In the combustion chamber, large amount of fuel is burnt with a huge amount of compressed air supplied by the compressor, which results in release of heat. Generally, the air fuel ratio in an open cycle gas turbine varies from 50:1 to 200:1 to get efficient combustion and to keep the turbine inlet temperature down to a permission level. In actual situation, combustion is never complete and is accompanied by chemical dissociation of gages and throttling losses etc. Also, there is as pressure drop in gas steam.

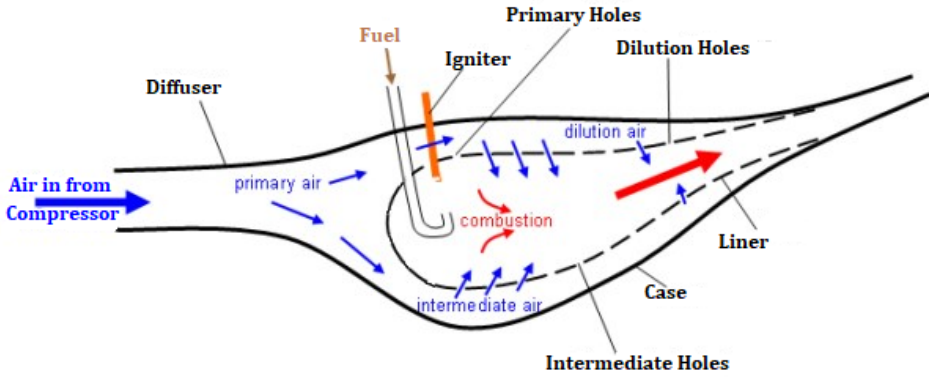

Fig.1.15 Schematic diagram of combustor

A successful combustor design must satisfy many requirements and has a challenge from the earliest gas turbines of Whittle and Von Ohains. The relative importance of each requirement varies with the application of the gas turbine, and of course, some requirements are conflicting, requiring design compromises to be made. Most design requirements reflect concerns over engine costs, efficiency and the environment. The basic requirement can be classified as follows:

- High combustion efficiency at all operating conditions.
- Low levels of unburned hydrocarbons and carbon monoxide, low oxides of nitrogen at high power and no visible smoke (Minimized pollutants and emissions).
- Low pressure drop (3-4% is common).
- Combustion must be stable under all operation conditions.

- Consistently reliable ignition must be attained at very low temperatures, and at high altitudes (for aircraft).
- Smooth combustion, with no pulsation or rough burning.
- A low temperature variation for good turbine life requirements.
- Useful life (thousands of hours), particularly for industrial use.
- Characteristically natural gas diesel fuels are used for industrial application and kerosene for aircraft.
- Length and diameter compatible with engine envelope (outside dimensions).
- Designed for minimum cost, repair and maintenance.
- Minimum weight (for aircraft application).

A combustor consists of at least three basic parts: a casing, a flame tube and a fuel injection system. The casing must withstand the cycle pressures and may be a part of the structure of the gas turbine. It encloses a relatively thin-walled flame tube within which combustion takes place, and a fuel injection system. Figure represents the combustion zone of a combustor.

1.7.7.4 Turbines

Turbines are an example of positive shaft work machines. They decrease both the temperature and pressure of the working fluid. This decrease creates positive work transfer. They are commonly convenient to design and operate than compressors since the hot air flow enlarging rather than being compressed.

Turbine design and manufacture is enigmatic by the need to enlarge turbine component life in the hot air flow. The problem of securing tenability is especially critical in the first turbine stage where temperatures are highest. Specific materials and described cooling schemes must be used to permit turbine airfoils that melt at 1255-1310 K to subsist in air flows with temperatures as high as 1922 K.

1.7.7.4.1 Axial flow turbine

A turbine extracts power from the gas stream to drive either engine compressor or, in the case of a power turbine, a load such as a propeller or electrical generator. Fewer stages are expected in axial flow turbines in comparison to an axial compressor. The axial flow turbine consists of a turbine wheel rotor and a set of stationary vanes stator. The set of stationary vanes of the turbine is plane of vanes (concentric with the axis of

the turbine) that are set at an angle to form a series of small nozzles which discharge the gases onto the blades of the turbine wheel. The discharge of the gases onto the rotor allows the kinetic energy of the gases to be transformed to mechanical shaft energy.

1.7.7.4.2 Impulse turbine

In the impulsive type, the relative discharge velocity of the rotor is the same as the relative inlet velocity since there is no net change in pressure between the rotor inlet and rotor exit. The stator nozzles of the impulse turbines are shaped to form passages which increase the velocity and reduce the pressure of the escaping gases as illustrated in figure 1.16.

1.7.7.4.3 Reaction turbine

In the reaction turbine, the relative discharge velocity of the rotor increases and the pressure decreases in the passages between the rotor blades. The stator nozzle passages of the reaction turbine simply alter the direction of the flow which is shown in figure 1.16. Most turbines in the jet engines are a combination of impulse and reaction turbines.

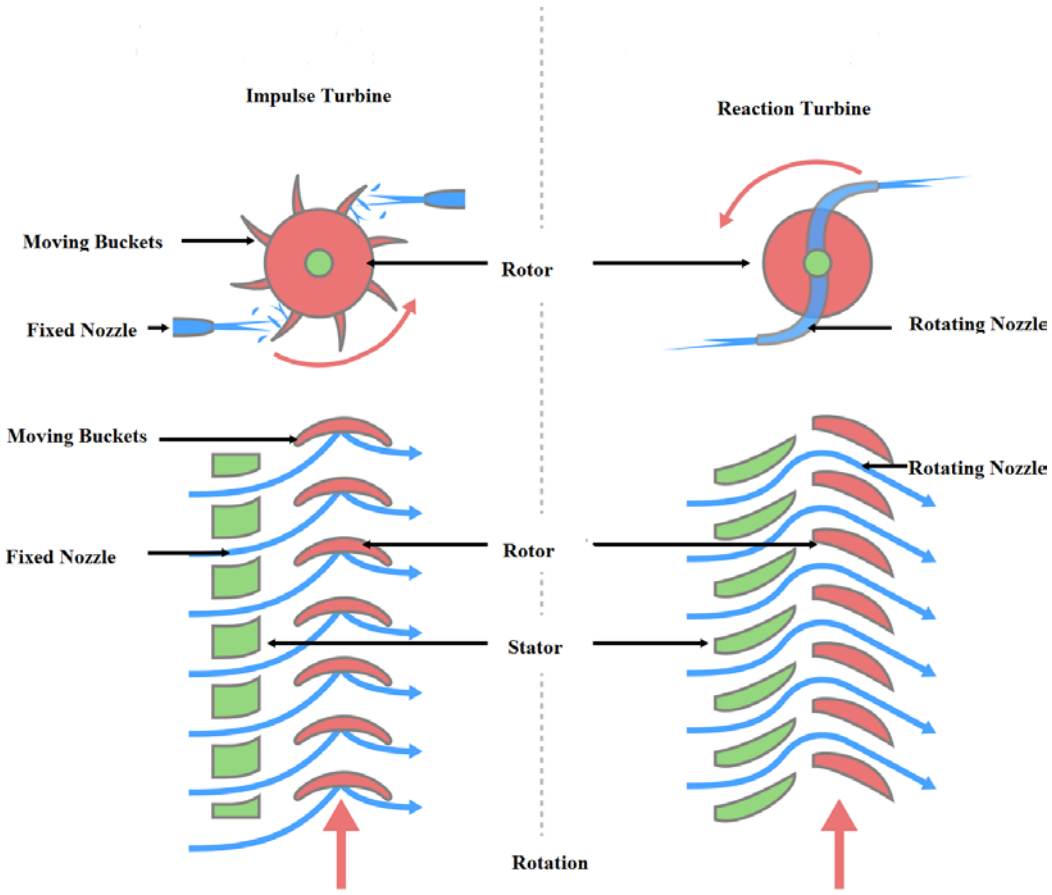

Fig.1.16 Cross sectional view of Impulse and Reaction Turbine

1.7.7.5 Nozzle

The motive of the nozzle is to enhance the velocity of the exhaust gas prior to discharge from the nozzle and to hoard and disarm gas flow from the turbine. In operating the gas turbine engine convert the internal energy of the fuel to kinetic energy in the exhaust gas stream. The net thrust of the engine is the outcome of this operation and is calculated by the Newton's second law of motion.

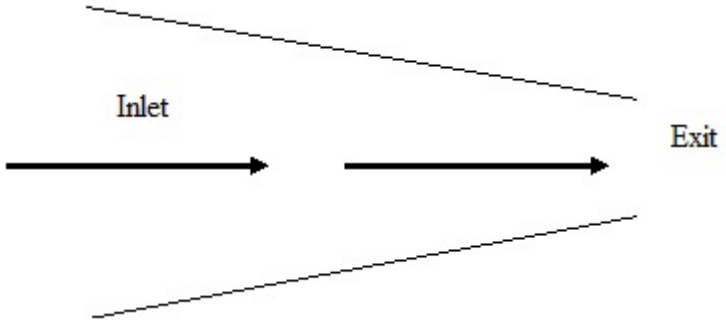

Fig.1.17 Simplified model of nozzle

For volumetric values of specific thrust, the kinetic energy of the exhaust gas must be sublimate, which notifies a high exhaust velocity. The nozzle supplies a high exit velocity by expanding the exhaust gas in an expansion process which lacks a decrease in pressure. The pressure ratio across the nozzle controls the expansion process and the maximum thrust for a given engine is procured when the exit pressure equals the ambient pressure. Further they are classified on the basis of their operation as convergent and convergent-divergent nozzles.

1.7.7.5.1 Convergent nozzle

The convergent nozzle is an ingenious convergent duct, as shown in figure 15. When the nozzle pressure ratio (turbine exit pressure to nozzle exit pressure) is less i.e., less than about 2, the convergent nozzle is employed. These nozzles have generally being used in low thrust engines are subsonic aircrafts.

.

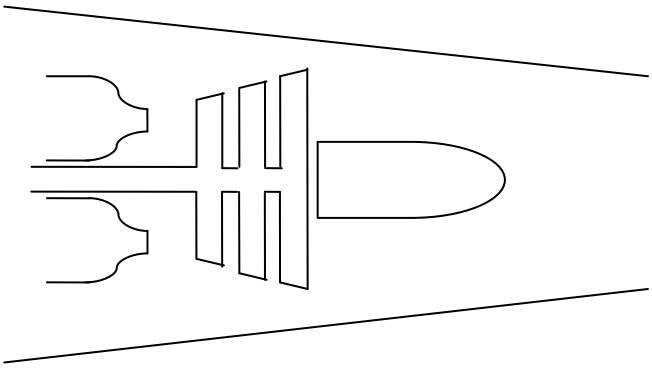

Fig.1.18 Convergent exhaust nozzle

1.7.7.5.2 Convergent-divergent nozzle

The convergent-divergent nozzle can be a convergent duct pursued by divergent duct where the cross-sectional area of the duct is least, the nozzle is said to have a gullet at that position. Most convergent-divergent nozzles used in supersonic aircrafts are not simple ducts, but synoptic variable geometry and other aerodynamic characteristics as shown in figure 1.19.

Only the throat area and the exit area of the nozzle are set mechanically, the nozzle walls being apprized aerodynamically by the gas flow. These nozzles are used if the pressure ratio is high (or high specific thrust). If the engine comprehends an afterburner, the nozzle throat and exit area must be diverged to match the multiple flow conditions and to output utmost extant.

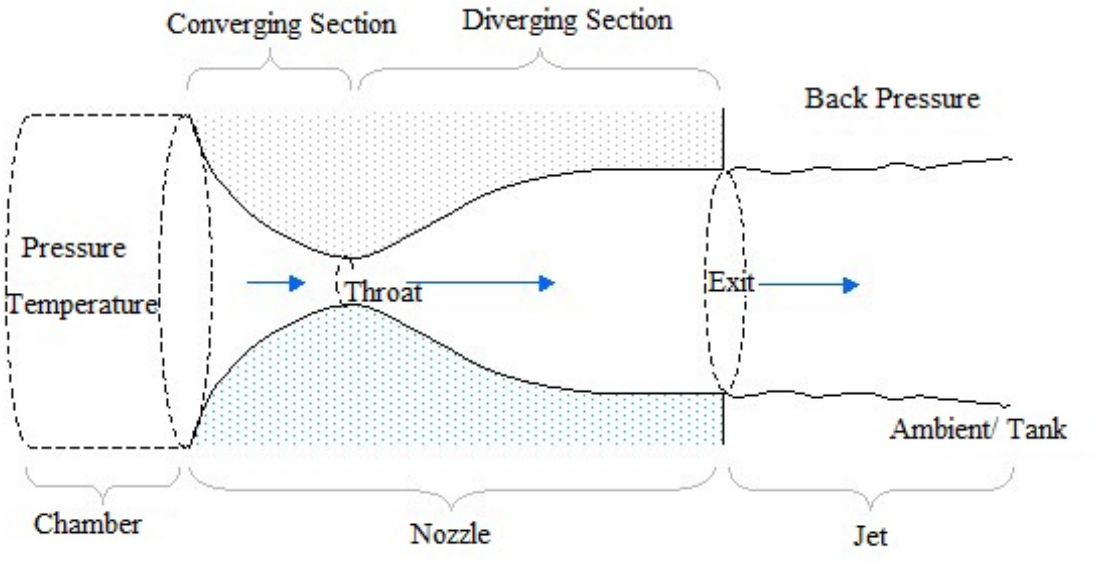

Fig.1.19 Schematic of convergent-divergent nozzle

1.8 Outline of the thesis

This thesis is organised in five chapters. Chapter 1 gives the detailed inspection of jet propulsion system, thereby enabling to know how it came into existence and their various aspects. It also defines the context and rationale of the work presented in this thesis. In chapter 2, a literature review is carried out. This chapter provides an overview of the gas turbine operating system, at the same time that gives a special focus to the past efforts with respect to gas turbine design and performance. Apart from that, it also introduces the approaches used to predict the fuel efficiency. Chapter 3 includes the description of the modelling procedures adopted for turboprop engine. It includes the description of the software used, as well as the limitations associated to the approach adopted. In chapter 4, the analysis results are exposed and discussed. The results analysis is done on the basis of the software introduced i.e., Matlab 14. In chapter 5, the conclusions on the conventional turboprops are discussed, as well as some proposals and recommendation of future work is also provided.

1.9 Objectives

1) To develop and adopt mathematical models for various components of turboprop engine under real conditions.
2) To construct computer software for parametric analysis based on modelling and governing equation in Matlab 10.
3) To perform parametric thermodynamic analysis.

CHAPTER 2

2. REVIEW OF LITERATURE

This chapter deals with the review of literature on major areas of the present study. Major areas include the design models, brief history of jet propulsion development. Historical development in the performance characteristics interlinking in Indian context with respect to the present scenario is also discussed in the terms of the reviews. A general gap in the research was found which is envisaged in the present perusal.

2.1 HISTORY

It has been more than 60 years since the gas turbine was developed and successfully applied. The initial applications included both aircraft propulsion and land-based power generation. The greatest impact of the gas turbine engine has been on aviation with the development of the jet engine. Aircraft gas turbines were developed by the former piston aero engine manufacturers, while steam turbine manufacturers started developing gas turbines for land based applications. Later, aircraft gas turbine derived engines were used for industrial use as well. From the very start, modeling the processes inside the gas turbine has been critical for successful development towards a working concept. Models were required to predict performance of the Joule-Brayton cycle that takes place in the gas turbine, to predict performance of the components and to predict structural and thermal loads. Obviously, the first models consisted of only manual cycle and component performance and structural stress calculations. These models had limited potential and consequently in those early days a lot of experimental work was needed for development of optimized gas turbine designs. At the same time, the rapidly growing scientific gas turbine community was working hard to minimize this trial-and-error approach, developing new modeling techniques and, after the introduction of computers, exploiting the utmost from available computer power.

2.2 INCEPTION OF JET PROPULSION

Jet propulsion is based on Newton’s second and third law of motion. Momentum is imparted to a mass of fluid in such a manner that the reaction of imparted momentum gives propulsive force. This is done by expanding the gas which is at high temperature and pressure through a nozzle so that the gas with markedly increased velocity in the form of jet comes out in the atmosphere and its reaction in the opposite direction gives the propulsive force. The open cycle gas turbine is more suited for the jet propulsion.

The idea of air-breathing jet propulsion originated at the beginning of 20th century. Several patents regarding air-breathing jet engines had been applied for by various inventors of different nationalities who worked independently of each other.

Air-breathing jet propulsion can be defined as a special type of internal combustion engine which produces its net output power as the rate change in the kinetic energy of the working fluid. The working fluid enters as environmental air which is ducted through an inlet diffuser into the engine. Few examples of early air-breathing jet propulsion patents are mentioned below:

1. In 1908, Lorin patented a jet engine which was based upon piston machinery.
2. In 1913, Lorin patented a jet engine based on ram compressors in supersonic flights.
3. In 1923, M. Guillaume patented a jet engine based on turbo-machinery; the intake air was compressed by an axial-flow compressor followed by a combustor and an axial flow turbine driving the compressor.

2.3 PAST CONTRIBUTIONS

Many studies have been conducted by various authors on this particular topic including the experimental studies of various jet engines.

G. Kraft and W. Strack (1975) calculated the fuel savings potential of advanced turboprops and compared with that of an advanced turbofan for use in an advanced subsonic transport. All the engines were designed for cruise at 10.67 km with a turbine-rotor inlet temperature of 1590 K. The regular turboprops had overall pressure ratios of 25 and 50. However, the regenerative turboprop had an optimum pressure ratio of only 10, and a ceramic rotary heat exchanger which had a design effectiveness of 85 percent and a pressure loss and leakage on 4%. The propeller efficiency was assumed to be 85 percent which implies an advanced low camber or variable camber propeller technology for the high cruise speeds studied (Mach 0.65 to 0.90). The mission called for a payload of 18144 kg at a range of 10200 and 5500 km. The results of this study indicated that, relative to the reference turbofan, the turboprops saved 31 to 33 percent of the fuel on the long range mission and about 27 to 28 percent on the medium range mission. With the high propeller efficiencies assumed, the direct operating cost comparison at Mach 0.80 is also favourable toward the turboprop by 14 to 18 percent. The minimum direct operating cost occurs at about Mach 0.76 for both engine types.

These important benefits for the turboprop engine are not substantially reduced by rather pessimistic perturbations in the propeller, gearbox, and heat exchanger assumptions. The regenerative turboprop cycle yields about the same fuel and takeoff gross weight results as the best regular turboprop.

Bencze, D. P. and Williams, I. J. (1977) focused on the future plans for continued development of the technology for advanced turboprop transport aircraft and focused on the fuel savings of advanced turboprop aircraft which appeared to be 10 to 20 percent relative to equivalent technology turbofan aircraft. These fuel savings are certainly large enough to warrant further research to establish the viability of turboprop transport aircraft. They identified the technology requirements in propeller design for high efficiency and low noise, fuselage noise attenuation, propeller and gear box maintenance, and engine-airframe integration. In order for new short-medium range transports to offer significantly lower operating costs than potential derivatives of current designs using advanced technology, the efficiency improvements of high speed turboprop propulsion system may be required.

Gearhart, W. S. (1983) focused on the efficiency of aircraft propulsion as the cost of fuel has risen. Studies conducted by NASA to obtain fuel efficient aircraft have considered relatively highly loaded turboprop systems. The higher disc loadings result in greater slipstream swirl and higher energy losses. Of primary importance is the radial distribution of the energy losses across the slipstream due to the tangential and axial velocities. This study presents the results of analysis defining the various sources of energy loss resulting from a swirling slipstream downstream of a propeller. Experimental data is presented demonstrating the presence of such losses and a propeller configuration discussed which offers improved propulsive performance when relatively highly loaded propellers arc employed.

Stoten, M. D. and Harvey, R. A. (1983) developed a new technology for the design of each engine component and assessed the influences of some of the factors on profitability. The regional airline operator has a unique set of requirements which maximize his operating profit. For a new turboprop engine these can be translated into a set of design goals, which address operating cost in the context of a relatively small airline operating a short-haul route network at high utilization rates. The PW-lOO was used as an example to show how design choices can be made on a new engine and how future developments may allow engines in this class to evolve.

Hirschkron and James (1984) evaluated (for NASA Lewis by General Electric Co.) the merits of special design features to provide a 2.5 minute contingency power rating, permitting an engine size reduction. Twin helicopter engines are often sized by power requirement of safe mission completion after the failure of one of the two engines. The merits of water injection, cooling flow Modulation, throttle push and an auxiliary power plant were evaluated using military life and commercial helicopter direct operating cost merit factors in a "rubber engine/rubber aircraft" scenario.

Mclntire, W. L. (1985) had improved power and fuel consumption of the T56 Series IV turboprop engine. Development program was incorporated for the improvements while retaining the long term durability and cost effective design of the T56 family. The initial full-scale demonstration in this program confirmed a 10.5% reduction in specific fuel consumption (sfc) and a power growth of 21% in the basic T56 frame. Continued early demonstrations and development by IR&D, Navy funds, and Allison discretionary funds showed a further (sfc) reduction to 13% and power increase of 28%.

Hirschkron, R. and Russo, C. J. (1986) conducted a study on turboshaft / turboprop engines in a nominal 850 shp size to determine advanced technology payoff in typical aircraft missions. Payoff was evaluated using a reference engine based on current technology. The results indicated worthwhile areas of development in compressor and turbine aerodynamic viscous codes, ceramic composite materials, and advanced ceramic recuperators. An advanced simple cycle engine could demonstrated a 20% fuel saving and a 24% Life Cycle Cost (LCC) reduction vs. current engines. An advanced recuperative engine increases the fuel reduction potential to 37% but with a smaller LCC improvement. An engine incorporating far term, post year 2000 technologies could reach fuel saving reductions of 50%.

Becker, M. G. (1991) tested a modern turboprop system ‘Allison’ was selected to provide the Propulsion System Package for the Saab 2000 aircraft and has used the tools and facilities available to improve the overall aircraft quality. By using an early nacelle in a large turboprop test facility, an early assessment of the engine/installation compatibility can be made. A production configuration nacelle was installed and tested both for system compatibility and endurance capabilities. This provided an early assessment of the system and an opportunity for early "fixes" prior to problems developing in the field that could lead to poor customer satisfaction and eventually lower unit sales.

Nitzsche, F. (1991) conducted a parametric study using a 15 degree of freedom model. He emphasizes that it is not an easy task to develop a safe engine suspension for a modern turboprop or propfan configuration The new aircraft configurations that have two pusher propellers or propfans located at the rear fuselage are susceptible to a whirl-flutter related instability characterized by a complex dynamic coupling involving not only the propeller-nacelle whirl modes but also the natural modes of the supporting backup structure. It was shown that the single-engine classical whirl-flutter formulation does not correctly predict these particular situations of instability, which were called whirl induced flutter. The main stiffness properties of both the supporting backup structure and the engine mounting system are systematically changed and the mechanism of the aforementioned phenomenon is explained on simple physical grounds.

Nitzsche, F. (1994) investigated the feasibility of using the active control technique to suppress the whirl-flutter instability of advanced turboprops. Aerodynamic vanes are incorporated at the engine nacelle to generate control air-loads. The actuator system is driven by a control law that is based on the Kalman filter estimation of the critical aero-elastic modes of the structure. The results demonstrated that the compensator provides enough controllability to prevent the whirl-flutter onset well beyond the design speed. His study suggested that a very efficient vibration isolation in advanced turboprops may be achieved both by optimizing the engine-propeller suspension in the actual flying envelope and by employing the active control technique to deal with the safe margins.

Yuan-Hu et al. (1995) developed a new method for predicting the off-design performance and the surge line of axial-flow compressors. In this method, the stall points of stages were determined by generalized curves, which are derived from the criterion of rotating stall based on the neutral condition of stability, and the off-design characteristic of stages is calculated by a reasonable iterative method. The stage-stacking method was adopted to obtain the off-design performance of a multistage compressor. The surge line of the compressor was predicted with the "actuator-delay-volume" model and the method of numerical integration. The results were found satisfactory.

Klein (1995) has dealt in a general fashion with flow phenomena in diffusers, explain problems the designer is confronted with and then discusses the results of tests conducted on various combustor diffusers. In addition to the evidence available in the

open literature, unpublished material of extensive research work carried out at MTU (Motoren and Turbinen-Union Miinchen) was presented and future developments are outlined. A short summary of CFD methods is included. Combustor diffusers in aircraft engines are required to maintain stable and efficient combustion, to provide the turbine nozzles with an acceptable temperature profile as well as with sufficient cooling air and to minimize total pressure losses. Their importance was growing as compressor discharge velocities increase and combustion requirements become more challenging. In spite of the progress of computational fluid dynamics (CFD) in recent years, the development of combustor diffusers is still mainly based on experimental work.

Campos et al. (1995) reviewed the longitudinal motion of an airplane, starting a dive at an arbitrary speed, and flown on a constant glide slope; this non-linear longitudinal speed stability problem is solved analytically to provide groundspeed as a function of time.

- Three restrictions were made.
- Neglect of the short period mode.
- Low Mach number flight, i.e. omission of drag due to compressibility small altitude change, so that the air density could be taken as constant.

The predicted stability curves were compared with flight test data obtained using a CASA 212 Aviocar twin-turboprop transport. The flight data records showed that lateral motion was negligible. The effects of wind were compensated and the possible errors were estimated. An extension was made of the stability theory from still air to account for the presence of winds; the latter were assumed not to exceed 30% of the groundspeed. The comparison of the theoretical stability curves with flight test data can be automated, as can the identification of the relevant data record. The disturbance intensity can be used as a parameter which indicates the start and end of flight manoeuvre. This parameter is defined as the relative lift change and for longitudinal flight it can be obtained from the wind velocity, vorticity components and changes of airspeed, angle-of-attack and vertical acceleration. It similarly has applications to perturbations of a horizontal turn.

Tryon et al. (1996) have presented a case study in which structural reliability based methodologies are used to assess cyclic fatigue life. The study involves the high pressure turbine of a turboprop engine. The response surface approach is used to

construct a fatigue performance function. This performance function is used with the first order reliability method (FORM) to determine the probability of failure and the sensitivity of the fatigue life to the engine parameters for the first stage disk rim of a two stage turbine. A hybrid combination of perturbation analysis and Monte Carlo simulation is used to incorporate time dependent random variables. System reliability is used to determine the system probability of failure, and the sensitivity of the system fatigue life to the engine parameters of the high pressure turbine. The variation in the primary hot gas and secondary cooling air, the uncertainty of the complex mission loading and the scatter in the material data are considered. The analysis incorporates standard modeling techniques used in the deterministic analysis of the fatigue life.

Hoheisel (1997) has contributed different aspects of engine airframe integration and summarizes areas of concern for engine installation such as, engine development trends, turbofan integration with respect to advanced engine concepts, programs and investigations on propeller integration, application of theoretical methods in particular with respect to viscous effects, engine location, nacelle design and flow aspects as well as jet flows.

Schiitze et al. (1998) have developed a lightweight engine mounting for turboprop aircraft which allowed for active suppression of disturbing vibrations. It consists of an advanced carbon fiber reinforced polymer (CFRP) truss structure based upon high-load CFRP struts which enable an optimal integration of piezo-electric stack actuators. The dynamic behaviour of the truss structure was analyzed by a 3D-simulation and the optimal position of active struts was evaluated. The experimental results of static and dynamic tests showed very good agreement with the analytical predictions. First investigations of the active vibration suppression by means of a simple feedback controller exhibited an excellent functionality of the adaptive structure and a promising potential to future improvements.

Pantand Fielding (1999) have discussed the application of simulated annealing in the conceptual design and optimization of twin-turboprop Commuter & Regional aircraft to obtain the optimum configuration and flight profile of such aircraft for operation over a given stage length. Generalized cost of travel incurred by a passenger for air travel between two cities is considered as the objective function to be minimized. Generalized cost is assumed to consist of four cost terms i.e., access cost, flight cost, time cost and airport cost. A computational methodology was developed for the estimation of these

cost terms for short-haul air travel, as a function of seventeen design variables and nine constraints. A simulated annealing optimization method was coupled to this methodology and a case study for short-haul business travel in India was carried out. A modified optimization strategy was adopted to reduce the overall computation time required. The results obtained in this case study were discussed in the paper.

Xieand Haberland (1999) have developed the design system Visual CAPDA on the basis of the former CAPDA system by evolutionarily introducing modern software standards under the premise of maximum reusability of existing FORTRAN coded methods. The new system plays the role of a workbench, which has to provide the analysis methods and necessary data. Through a graphical user interface the application of the system comes along as comfortable for the user as possible. In order to cover turboprop aircraft, new modules with respect to cabin layout, propeller aerodynamic and acoustic analysis, propeller slip stream, engine modeling, geometry modeling are integrated into the design tool. The flexibility of the new system is demonstrated by applying it to the configurational development of propeller aircraft, investigating actual problems such as Twin or Quad, Turboprop or Turbofan and finally, dealing with typical optimization problems. Besides the conceptual configuration development of an aircraft, a modern design tool should cover the evaluation of competitor aircraft, allow the assessment of technological and operational scenarios and thus should have the potential to right first time design.

Filippone (2000) has provided a synthetic and comparative view of selected aircraft and rotorcraft (nearly 300) from past and present. It has been reported geometric characteristics of wings (wing span, areas, aspect-ratios, sweep angles, dihedral/anhedral angles, thickness ratios at root and tips, taper ratios) and rotor blades (type of rotor, diameter, number of blades, solidity, rpm, tip Mach numbers); aerodynamic data (drag coefficients at zero lift, cruise and maximum absolute glide ratio); performances (wing and disk loadings, maximum absolute Mach number, cruise Mach number, service ceiling, rate of climb, centrifugal acceleration limits, maximum take-off weight, maximum payload, thrust-to-weight ratios). There are additional data on wing types, high-lift devices, noise levels at take-off and landing. The data are presented on tables for each aircraft class. A graphic analysis offers a comparative look at all types of data. Accuracy levels are provided wherever available.

Coiro and Nicolosi (2001) have developed experimental tools in his department and devoted to aircraft design for low subsonic flow. These tools comprise numerical codes for analysis, design and simulation, and experimental tests performed in our tunnel and particularly devoted to light aircraft design. The importance of developing such tools in house was highlighted. Examples of light aircraft designed using such tools was presented and some attention was paid to the design of a three-surface R/C model aircraft and on the adaptation of numerical codes to the prediction of its behaviour in the non-linear range of angles of attack.

Bousquet and Gardarein (2003) have presented the application of the CANARI (Code for the Analysis Necessary for Arpege for Its Rejects and Its Initialization) flow solver to the computation of unsteady effects in the aerodynamic interaction of a high speed propeller with the aircraft. The method is first validated on the APIAN (Advanced Propulsion Integration Aerodynamics and Noise) isolated propeller test case by comparison with experiment at M=0.7. The method is then applied to the time accurate 3D Euler computation of a generic transport aircraft at M=0.68. Analysis of the results shows significant unsteady effects both on the propeller forces and on the wing aerodynamic flows, by comparison with steady computations.

Kong et al. (2003) developed a steady state performance simulation program for a turboprop engine and performance analysis was performed at uninstalled and installed conditions. The analysis results were compared with performance data provided by engine manufacturer and with analysis results by GASTURB program. It was confirm that the developed program was reliable because the results by the developed program were well agreed with those by GASTURB within 5%. Linear and nonlinear GPA (Gas Path Analysis) programs for performance diagnosis were proposed, and selection of optimal measurement variables was studied by using the programs. Multiple faults of compressor, compressor turbine and power turbine, which may occur damages of the engine, were also considered.

Levy et al. (2004) has developed thermodynamic relationship with the gas turbine flameless oxidation. A detailed analysis of the different operational scheme options was described. It is shown that the thermodynamic process and operational parameters within the present low-NO_x gas turbine combustor are principally different to those of industrial furnace operating in the flameless oxidation mode of combustion. The project was aimed to develop technology for clean and efficient gas turbines, operating at high

temperatures. It is based on the technologically innovative combustion solution-flameless oxidation. The investigation was directed towards the validation of engineering feasibility of the flameless oxidation technology for the production of operating pilot combustors that will demonstrate, advantages including among others, improved performance relating to low NO_x levels, maintaining uniform combustor wall temperatures, uniform fuel stream injection and more, resulting in an increased mean time between failure and reliability of the gas turbine. Combustion chambers for gas turbines and jet engines differ from conventional industrial furnace design by being 'adiabatic'(without heat extraction inside the combustor) and by operating at elevated pressures.

Pathak et al. (2005) analyzed the performance of a gas turbine cycle at various off-design conditions by using a matching technique. They developed a computer code from the available algorithm and made flexible by using a multidimensional regression package. The equilibrium running line was generated to compare its trend with the available results. The prediction of some important parameters of the cycle like specific fuel consumption (SFC), compressor work, power output, compressor efficiency, gas generator (GG) turbine inlet temperature are made at various equilibrium running condition at various off-design condition.

López-Díez et al. (2005) The improvement of the front end area of the TP400D6 motor for the A400M military transport aircraft has been a standout amongst the most difficult points of the plan of this motor. Further, they portray the discoveries and conclusions of the work performed amid the diverse periods of the procedure: the pre-advancement stage, the applied stage and the detail configuration phase.

Gaertner (2005) has dealt with two tasks within the development and production of MTU Aero-Engines (German Aircraft Engine Manufacturer). The development of application-software for the engine-control unit together with the complete development of the engine monitoring unit has been done. The aerodynamic and structural design aspects for a five stage intermediate pressure compressor have also been developed. Both tasks comprise the design-work for the individual components.

Raghunathan *et al.* (2006) have reviewed the current state of art in system engineering approach to aircraft design and identify some of the major challenges, the current state of the art and visions for the future. The review moves from an initial basis in

traditional engineering design processes to consideration of costs and manufacturing in this integrated environment. Issues related to the implementation of integration in design at the detailed physics level are discussed in the case studies. The challenge in Aerospace Engineering, in the next two decades as set by Vision 2020, is to meet the targets of reduction of nitric oxide emission by 80%, carbon monoxide and carbon dioxide both by 50%, reduce noise by 50% and of course with reduced cost and improved safety. All this must be achieved with expected increase in capacity and demand. Such a challenge has to be in a background where the understanding of physics of flight has changed very little over the years and where industrial growth is driven primarily by cost rather than new technology. The way forward to meet the challenges is to introduce innovative technologies and develop an integrated, effective and efficient process for the life cycle design of aircraft, known as systems engineering (SE). The key contribution of the paper will be to review this formalization and to present the very latest knowledge and technology that facilitates SE theory. Typically, research into SE provides a deeper understanding of the core principles and interactions and helps one to appreciate the required technical architecture for fully exploiting it as a process, rather than a series of events. There are major issues as regards to systems approach to aircraft design and these include lack of basic scientific practical models and tools for interfacing and integrating the components of SE and within a given component, for example, life cycle cost, basic models for linking the key drivers

Meherwan P. Boyce (2006) has discussed the performance of gas turbines and the mechanical standards used for them. The American Society of Mechanical Engineers (ASME) performance test codes are written to ensure that tests are conducted in a manner that guarantees that all turbines are tested under the same set of rules and conditions to ensure that the test results can be compared in a judicious manner. The mechanical standards and codes have been written by both the ASME and American Petroleum Institute (API). The ASME PTC 46 1996 code is written to establish the overall plant performance. Power plants that produce secondary energy output, such as cogeneration facilities, are included within the scope of this code. The PTC 46 has been designed to determine the performance of the entire heat cycle as an integrated system. The PTC 19.1 1988 code specifies procedures for the evaluation of uncertainties in individual test measurements, arising from both random errors and systematic errors, and for the propagation of random and systematic uncertainties into the uncertainty of a

test result. The object of the ASME PTC 22 1997 code is to detail the test to determine the power output and thermal efficiency of the gas turbine while operating at the test conditions, and correcting these test results to standard or specified operating and control conditions. The tests of gas turbines with water or steam injection for emission control and/or power augmentation are also included. The tests can be applied to gas turbines in combined cycle power plants or with other heat recovery systems.

F.W Geels (2006) dealt with system innovation in Freeman and Perez's innovation typology (incremental, radical, system, and techno-economic paradigm) and conceptualizes these changes as transitions from one socio-technical system to another. These transitions are co-evolution processes that are not only about technological discontinuities, but also about markets, user practices, regulation, culture, infrastructure and science. To understand transitions, these insights are combined in a multi-level perspective, consisting of niche, regime and landscape levels. Transitions come about when co-evolutionary dynamics at these three levels link up and reinforce each other. The perspective is illustrated with a historical case study: the transition from aviation systems based on propeller-aircraft to aviation systems based on turbojet aircraft (1930–1970). The case study provides not just an evolutionary economic analysis of technological change, but also deals with the long-run evolution of technology and the socio-economic system.

Lemoult et al. (2007) dealt with the noise that is emitted from the exhaust of these engines. The two noise sources suspected that are direct and indirect combustion noise. Direct noise is the noise due to the flame and its possible interaction with the combustion chamber, whereas indirect noise is generated when turbulence and temperature eddies are convected through the turbine blade rows. The study focuses on the propagation of direct combustion noise trough turbine stages and generation of indirect combustion noise. Since the acoustic wavelength is much higher than the blade dimensions in Turbomeca turbines due to low studied frequencies and high temperatures (i.e. high speed of sound), analytical models based on actuator disc assumptions are developed. After a presentation of these models, the paper presents the investigations made in the case of the transmission and reflection of an acoustic wave through a representative turbine distributor. In particular, analytical models are compared to ACTRAN numeric calculations. This study demonstrates the ability to predict noise in Turbomeca with the very simple actuator disc model. The influence of

the blades themselves is weak and the blade row response is mainly due to the velocity mismatch on both sides.

Adel Ghenaiet and Tayeb Boulekraa (2009) describes an approach that gives the freedom to select or optimize the design of new turboprops to match the power requirements of a propeller-drivenL100-30 aircraft powered by four turboprops, for which flight performance and a diagram of constraints were established. In such thermal systems, the Pareto solutions provide more insights into the competing objectives: the minimum power specific fuel consumption can be directly translated into increased range and payload, whereas, the high specific power leads to reducing engine size, weight, and installation losses. Three configurations of turboprops included a single-spool fixed turbine, a single-spool free turbine, and a twin-spool fixed turbine that were modeled within the developed engine performance analyzer. The obtained results based on the model of aircraft have indicated that we could preserve the diversity of non-dominated individuals and the quality of the Pareto front, and the decision variables related to the propulsion cycle could be determined easily.

Tie-lin and Dong-li (2009) have established a relationship between multidisciplinary design optimization (MDO) for aircrafts and the large-scale system theory was expatiated. Using the large-scale system theory, the system was decomposed gradually based on the different classification standards and the system characteristics. At the same time, the MDO methods for aircrafts were classified according to the decomposition-coordination method of the large-scale system theory. The theory background and applicable range of each algorithm were elucidated. Aircraft design system is a typical engineering large-scale system, and the basic of MDO for aircrafts is the large-scale system theory. Therefore, the large-scale system theory and MDO for aircrafts should be studied simultaneously to improve the MDO.

Viet Van Pham et al. (2010) presented an aviation emission inventory using real time air traffic trajectory data. An up to date and accurate aviation emission inventory is a prerequisite for any detailed analysis of aviation emission impact on greenhouse gases and local air quality around airports The reported inventory is in the form of a 4D database which provides resolution of (1x1x1000) feet for temporal and spatial emission analysis. The inventory is for an ongoing period of six months starting from October 2008 for Australian Airspace. In this study we show 6 months of data, with 492,936 flights (inbound, outbound and over flying). These flights used about 2515.83

kt of fuel and emitted 114.59 kt of HC, 200.95 kt of CO, 45.92 kt of NOx, 7929.89 kt of CO2, and 2.11 kt of SOx. From the spatial analysis of emissions data, we found that the CO2 concentration in some parts of Australia is much higher than other parts, especially in some major cities. The emission results also show that NOx emission of aviation may have a significant impact on the ozone layer in the upper troposphere, but not in the stratosphere. It is expected that with the availability of this real time aviation emission database, environmental analysts and aviation experts will have an indispensable source of information for making timely decisions regarding expansion of runways, building new airports, applying route charges based on environmentally congested airways, and restructuring air traffic flow to achieve sustainable air traffic growth.

Schertz et al. (2010) have studied CFD (Computation fluid dynamics) to perform on two-dimensional wing sections in transonic, viscous flow to investigate the effect of jet-wing on propulsion efficiency and the flow field, determine design changes for achieving efficient distributed propulsion, and investigate the effect of jet-flaps with small jet deflection angles on aerodynamic parameters. The jet-wing distributed propulsion can give propulsive efficiencies on the order of turbofan engine aircraft and if the trailing edge of a conventional Outboard airfoil is expanded, efficiency can be increased by 7.5%. An increase in propulsion efficiency was achieved without expanding the trailing edge for a thicker Inboard airfoil. Distributed propulsion is the idea of redistributing the thrust across the drag producing elements of a vehicle. Our configuration has a modest number of engines with part of the exhaust flow vented from thick trailing edges of the wings to cancel the local profile drag and the rest of the exhaust flow providing thrust to cancel the induced drag and drag of the fuselage and tails.

Yunos (2011) has evaluated the actual performance of turboprop engine. The performance evaluation is also important for the development, of preliminary requirements for the engine test cell. Faculty of Mechanical and Manufacturing Engineering, Universiti Tun Hussein Onn Malaysia (UTHM) has acquired a Pratt and Whitney PT6A-20 turboprop engine to be used in its aeronautical engineering technology programme. However, to fully utilize the engine, a solid familiarity with its current performance and a proper testing arrangement are important. The main concern on the engine is the age of the engine and lack of information on its previous

performance. A better performance investigation and testing can be conducted in an engine test cell. Altogether, a total of three engine tests were performed by varying engine speed from 55 percent rpm to 75 percent rpm. Performance data obtained include the engine's torque, propeller speed, fuel flow rate, and inter-turbine temperature. They were captured by using data acquisition software from Aero Train Corp. An averaging was done to the data in order to study engine shaft horsepower, specific fuel consumption, and thermal efficiency. From the result of manual calculation, the engine can produce power up to 34.8 kW while running at 75 percent rpm. The specific fuel consumption is 7.07 kg/kW-hr while the thermal efficiency is at 1.19 percent. On the other hand, the data acquisition system shows that the engine managed to deliver 89.5 kW of power, 3.15 kg/kW-hr of specific fuel consumption and thermal efficiency of 19.5 percent. It was found that the results of manual calculation were significantly lower than the percent different in specific fuel consumption. Although the current engine performance is acceptable and satisfactory to be used for aircraft propulsion education, a safer and more reliable testing arrangement is still needed. Considering that a proper test facility will be essential to obtain a highly accurate result on the engine performance, an engine test cell was proposed to be built. The test cell was proposed to be an indoor test cell and it was planned to accommodate engine testing on small turboprop engine with power range between 200 to 450kW.

Andriani et al. (2011) developed a thermodynamic code that simulates the behaviour of a gas turbine engine at different engine and operating conditions. They presented the main results obtained with the code, simulating the behaviour at take-off and cruise of a turboprop engine in which both intercooling and regeneration are introduced. The reduction of fuel consumption and pollutant emissions has become one of the main requirements of modern gas turbine aero engines. To pursue this aim engineers are developing new techniques to improve the efficiency of the thermodynamic cycle of new engines. In particular the attention was focused on the possibility to introduce practices as heat regeneration and staged-intercooled compression process on these engines. These techniques, that change considerably the engine working cycle features, are well known and widely used in ground based power plants, but until now they have not been transferred on aero engines, mainly for extra weight and size problems. However these problems now seem to be overcome by new technology, and the

possibility to have intercooled-regenerated gas turbine engines on an aircraft has become real.

Gohardani et al. (2011) highlighted the role of distributed propulsion technology for future commercial aircraft. After an initial historical perspective on the conceptual aspects of distributed propulsion technology and a glimpse at numerous aircraft that have taken distributed propulsion technology to flight, the focal point of the review is shifted towards a potential role this technology may entail for future commercial aircraft. Technological limitations and challenges of this specific technology are also considered in combination with an all electric aircraft concept, as means of predicting the challenges associated with the design process of a next generation commercial aircraft.

Rahman et al. (2011) presented the parametric study of thermodynamic performance on gas turbine power plant. The variation of operating conditions (compression ratio, turbine inlet and exhaust temperature, air to fuel ratio, isentropic compressor and turbine efficiency, and ambient temperature) on the performance of gas turbine (thermal efficiency, compressor work, power, specific fuel consumption, heat rate) were investigated. The analytical formula for the specific work and efficiency were derived and analyzed. The programming of performance model for gas turbine was developed utilizing the MATLAB software. The results show that the compression ratio, ambient temperature, air to fuel ratio as well as the isentropic efficiencies are strongly influence on the thermal efficiency. In addition, the thermal efficiency and power output decreases linearly with increase of the ambient temperature and air to fuel ratio. However, the specific fuel consumption and heat rate increases linearly with increase of both ambient temperature and air to fuel ratio.

Povazan, J. et al. (2012) presented the basic description of turboprop engines as a special class of turbine engines – advanced approaches in its modeling and control. A brief description of analytical and experimental approaches in modeling of individual parts of the engine with description of their thermo-dynamics and states were introduced by them. Such engines are systems with two degrees of freedom and demand advanced control algorithm in case of control with single control lever. It also extant the design of such control algorithm with perspective use of advanced control methods. Such approaches will increase efficiency, fuel consumption, safety and control comfort for the pilot.

Filho et al. (2012) has described a turboshaft nonlinear dynamic model and its control system used for electric power generation. The dynamic modeling of the gas turbine was developed in a modular form considering each engine component, in such a way that the dynamic equations describe the real conditions of operation during start up, load change, shutdown and steady state regimes. The control strategy seeks to operate in the regions of best performance, keeping the prescribed reference speed, while protecting the engine operation from surge, flameout, over speed and overheat. Simulation results are presented for normal operating conditions and under the effect of disturbances, observing the control action of the turboshaft.

Lee et al. (2013) have investigated the S-shaped diffuser which connects the exit of the compressor to the inlet of the combustion chamber of the Allison 250 gas turbine using the Shear-Stress Transport turbulence model (SST) and the commercial code ANSYS-CFX. The diffuser geometry includes an initial conical diffuser which smoothly transitions into a constant cross-section S-duct. The numerical model and setup were validated using both in-house processed experimental data and experimental data from the literature on a similar geometry. The stream-wise velocity profile was observed to flatten in the initial divergent section, and then the region of the flow with the highest velocity is pushed toward the outer surface of the first bend, with a secondary-flow in the plane of the cross-section. This distortion of the stream-wise velocity intensified when the inlet turbulence intensity was decreased or when the Reynolds number was increased. An increase of the Reynolds number also translated into higher static pressure recovery potential and lower wall friction coefficients. Six variations of the diffuser geometry were considered, all having the same total cross-sectional area ratio and centreline offset. The qualitative results were the same as those of the Allison 250 diffuser, but unlike the base geometry, all the considered variants showed separated-flow regions (and reversed-flow regions in some cases) of different sizes and at different locations. The performance indicators for the Allison 250 S-shaped diffuser were the highest overall. Most interestingly, the current duct geometry outperformed its variant with a cross-sectional area expansion extending over its entire length, which is the most common inlet duct configuration.

Hassan et al. (2013) presented an experimental investigation of the Heat Transfer Coefficient (HTC) performance of a Micro-Tangential-Jet (MTJ) Film cooling scheme on a gas turbine vane using transient Thermo chromic Liquid Crystal (TLC) technique.

The MTJ scheme is a micro-shaped scheme designed so that the secondary jet is supplied parallel to the vane surface. In order to supply the jet in a direction parallel to the vane surface, extra material was added on both pressure and suction sides. The film cooling performance of one row of holes on both pressure and suction sides were investigated at a blowing ratio ranging from 0.5 to 1.5 on the pressure side and 0.25 to 0.625 on the suction side, calculated based on the MTJ scheme exit area. The average density ratio during the investigations was 0.93, and the Reynolds number was 1.4E+5, based on the free stream velocity and the main duct hydraulic diameter. The pitch to diameter ratio of the cooling holes is 5 on the pressure side and 6.5 on the suction side. The turbulence intensity during all investigations was 8.5% and was measure two chords upstream the vane leading edge using the PIV technique. The investigations showed that the increase in the HTC ratio due to the presence of the MTJ scheme is very close to that resulting from the presence of normal traditional shaped schemes on the pressure side. Meanwhile, a reduction in the HTC ratio is recorded on the suction side. Such performance is attributed to the small overall height of the scheme which helped keep the resulting turbulence to a minimum. Moreover, the HTC distribution downstream the MTJ scheme is uniform in the lateral directions which helps minimize the thermal stresses. The Net Heat Flux Reduction (NHFR) parameter is used to judge the overall performance of the MTJ scheme. The NHFR represents a combination of the effects of both the cooling effectiveness and the HTC. Great enhancement in the NHFR performance of the MTJ was observed compared to traditional shaped schemes. With the current MTJ scheme design and dimensions and under the previously mentioned Reynolds number and turbulence intensity it was observed that a blowing ratio close to unity, calculated based on the scheme exit area, provides an optimal film cooling performance on both pressure and suction sides.

Villace and Paniagua (2013) deduced the engine thermal and airframe transfer effectivenesses based on thermodynamic availability, related to the overall losses of the thermally integrated vehicle for a given mission. The engine overall effectiveness, derived from the propulsive efficiency and the engine thermal effectiveness, was found to be a generalization of the Breguet equation. The developed methodology was demonstrated in a combined cycle engine operating at flight speeds from Mach 2.5 to 5. In particular, the propulsive efficiency, thermal effectiveness, total loss and subcomponent losses were evaluated using the common framework of thermodynamic

availability. Air-breathing engines are utilized in the hypersonic regime through thermal integration of the fuel into the propulsive cycle, which improves the efficiency by recovering thermal energy from the free stream and the aero-shell. The classical efficiency figures based on first principle analyses are inaccurate performance indicators of the resulting combined cycle**.**

Aydın et al. (2013) presented the exergetic sustainability indicators of the turboprop engine for eight flight phases. The results show that exergetic efficiency approaches a maximum value (29.2%), waste exergy ratio (70.8%), exergetic destruction ratio (0.41) and environmental effect factor (2.43) become minimum values, whereas exergetic sustainability index approaches a maximum value (0.41). The phases of taxi and landing for the turboprop aircraft have minimum exergy efficiency (20.6%) and minimum exergetic sustainability index (0.26). Accordingly, the exergetic efficiency, waste exergy ratio and exergetic sustainability index of the aircraft are reasonably well in the climb, maximum cruise/continuous, normal/maximum take-off and APR (automatic power reverse) phases. Finally, it is supposed that studying exergetic indicators for an aircraft enables how much improvement is possible for aircraft engines to achieve better sustainable aviation. One of the key challenges for sustainable aviation is to reduce global and local environmental impacts. The scope of this study is analyzed and discussed in detail for better understanding of sustainability performances of a turboprop aircraft.

Balli and Hepbasli (2013) assessed the performance of T56 turboprop engine using the exergo-economic, sustainability and environmental damage cost analysis methods at different power loadings. The unit exergy cost of the shaft power decreases from 76.34 $/GJ at 75%-mode to 58.32 $/GJ at Takeoff-mode due to increasing the shaft power. The unit exergy cost of the kinetic exergy increases 599.43 $/GJ at 75%-mode to 666.76 $/GJ at Takeoff-mode because of the unit exergy cost of the exhaust gaseous with the increase in the fuel flow. The sustainability analysis indicates that the gas turbine has the highest sustainability index. Increasing the fuel flow rate raises the environmental pollutants and the environmental damage cost rate. The environmental damage cost rates of the engine are calculated to be 423.94 $/h at 75%-mode, 576.97 $/h at 100%-mode, 634.93 $/h at military-mode and 665.85 $/h at Takeoff-mode. The total cost rate consists of the sum of the fuel cost, the capital investment cost, the operating and maintenance costs, and the environmental damage cost. The total cost

rates of the engine are determined to be 1702.59 $/h at 75%-mode, 2100.26 $/h at 100%-mode, 2220.42 $/h at military-mode and 2284.50 $/h at Takeoff-mode.

Ujam, A. J. (2013) developed a real-time turbojet engine integrating aero-thermodynamics together with principles of jet propulsion and inters component volume dynamics represented in 1-D non-linear equations. As jet engines are required to operate at a higher rpm for the same thrust values in cases such as aircraft landing and military loitering. High rpm reflects higher efficiency with increased pressure ratio. This work was focused on performance characteristics of turbojet with reduced inlet pressure to the compressor engine. Specific fuel consumption, specific thrust, component pressure ratios, thermal and propulsive efficiencies are the performance parameters of the engine that were analyzed on the model with reduced inlet pressure for the real-time test cases of desired thrust range. A flow control mechanism that produces a pressure drop across inlet was assumed and the analyses were carried out with reduced compressor inlet pressure for matching thrust. The result of the findings showed that with increase in shaft rpm, pressure and temperature ratio values across the compressor turbine assembly increases. Performance parameters of the engine are analyzed with the increase in compressor pressure ratio and shaft rpm.

Ahmed, A. M and Tariq, M. (2013) presented work on the parametric study of a gas turbine cycle model power plant with intercooler compression process and regeneration turbine. The thermal efficiency, specific fuel consumption and net power output are simulated with respect to the temperature limits and compressor pressure ratio for a typical set of operating conditions. Simple gas turbine cycle calculations with realistic parameters are made and confirmed that increasing the turbine inlet temperature no longer means an increase in cycle efficiency, but increases the work done. Regenerative gas turbine engine cycle was presented that yields higher cycle efficiencies than simple cycle operating under the same conditions. The analytical formulae about the relation to determine the thermal efficiency were derived taking into account the effected operation conditions (ambient temperature, compression ratio, intercooled effectiveness, regenerator effectiveness, compressor efficiency, turbine efficiency, air to fuel ratio and turbine inlet temperature).The analytical study was done to investigate the performance improvement by intercooling and regeneration. The analytical formula for specific work and thermal efficiency are derived and analyzed. The simulation results showed that increasing turbine inlet temperature and pressure ratio can still improve the

performance of the intercooled gas turbine cycle. The power output and thermal efficiency are found to be increasing with the regenerative effectiveness, and the compressor and turbine efficiencies. The efficiency increased with increasing the compression ratio to 5, then efficiency decreased with increased compression ratio, but in simple cycle the thermal efficiency always increases with increased in compression ratio. The increased in ambient temperature caused decreased thermal efficiency, but the increased in turbine inlet temperature increase thermal efficiency.

Mohammed Jasim Mohammed and Tariq, M. (2014) developed software for calculating thermal efficiency and power output of a reheat and regenerative cycles which was used to calculate the various parameters of a combined gas turbine cycle. The temperature after reheating assumes to be reaching at the same temperature of HPT inlet. The combination of the reheat and regenerative cycle was taken and the thermodynamic analysis was performed using MATLAB 10 software. The parameters were selected in the well defined range for overall pressure ratio, turbine inlet temperatures and ambient temperature. The cycle performed the analysis for various regenerative effectiveness and it was found that the thermal efficiency increases on increasing the regenerative effectiveness and the heat required in the burner decreases for higher regenerative effectiveness.

Rana Adil Abdul-Nabe and Tariq, M. (2014) developed software in "C++" which was capable of predicting engine dependent parameters for turbojet engine at varying independent parameters. The work was based on detailed parametric thermodynamic analysis of the single spool turbojet engine with transpiration air cooling techniques for turbine. The analysis was carried out by selecting models for different components of engines which included the application of a gas turbine engine for a single spool turbojet engine. As the design and operation theories of the components used in the jet engines are complicated, the complexity of thermodynamic analysis makes it impossible to mathematically solve the optimization equations involve in turbojet engine cycle. It was expected that these tools would help in predicting the performance of individual components such as compressors, combustion chamber, turbine, nozzle etc. In conventional configurations, the high temperature and high pressure gas expand through the turbines which provide just enough power to drive the compressor and other engine auxiliaries. Further expansion of the gases takes place in the nozzle to produce the high speed jet. Transpiration cooling technique was taken for the turbine

blade in their analysis. Also the amount of the air bled from the high pressure compressor as a fraction of the mainstream flow was calculated. The cooling of turbine blades (first stator only) was also examined at various altitudes and Mach numbers for the various configurations of turbojet and turbofan engines.

Armendariz et al. (2014) focused on the response of the structure after the break of a propeller blade until the end of the phenomenon. The detached propeller blade is also studied in terms of the size that is lost and its influence on the system behaviour. Moreover the effects of stiffness and strength changes on the engine mounting system are analyzed. The research covers different parameters which can influence the phenomenon, including flight condition, propeller rotational frequency, and angular position where the blade is lost. The engine and the engine mounting system have been modeled in a finite element method (FEM). The simulations are run in an explicit solver and the simulation methodology includes failure of elements and non-linear behaviour .One of the most severe failures in an aircraft provided with turboprops is an airscrew blade loss. Design precautions must be taken to minimize the hazards to the airplane in the event of a propeller blade failure. One of the hazards which must be considered includes structural damage, and the airplane must be designed for the imbalance loads resulting from the failure. The structure must absorb the dynamic loads while the rest of the aircraft continues flying. If the energy of the phenomenon increases until it behaves uncontrollably, the engine could be detached from the structure. There must be devices which react to decrease the risks of critical failure for the rest of the structure.

Tariq, M. (2014) presented a regenerative gas turbine engine cycle that yields higher cycle efficiencies than simple cycle operating under the same conditions. The power output, efficiency and specific fuel consumption are simulated with respect to operating conditions. They determined the thermal efficiency taking into account the effected operating conditions (ambient temperature, compression ratio, regenerator effectiveness, compressor efficiency and turbine inlet temperature). Model calculations for a wide range of parameters are presented, as are comparisons with simple gas turbine cycle. They found that the power output and thermal efficiency increases with the regenerative effectiveness, and the compressor efficiency. The efficiency increases with increasing the compression ratio to 15, then efficiency decreased with increased compression ratio, but in simple cycle the thermal efficiency always increases with

increased in compression ratio. The increased in ambient temperature caused decreased thermal efficiency, but the increased in turbine inlet temperature increase thermal efficiency.

Yi Guang Li (2015) developed a novel gas turbine performance estimation method using engine gas path measurements to predict and track engine performance parameters at different ambient, flight, degraded, and part-load operating conditions. The method was based on the influence coefficient matrix of thermodynamic performance parameters of gas turbine engines and the Newton–Raphson mathematical algorithm. Contrary to the conventional gas turbine off-design performance predictions where component characteristic maps are essential, it has the advantage that no component characteristic maps are required for the predictions and, therefore, it is relatively simple thermodynamically, fast in calculation, and desirable in engineering applications. It is able to make important in visible performance parameters visible to gas turbine users, which is a useful complement to current engine condition monitoring techniques.

Sheng et al. (2016) designed an integrated controller on the basis of Matlab/Simulink, which can realize the entire process control of the engine from start-up to maximum power till stop. At the end, on the basis of RT-LAB platform, the real-time digital simulation of the designed control system was studied, different regulating plans were tried and more ideal control effects have been obtained. They studied the real-time digital simulation of turboprop engine control system. The architecture, work principles and external interfaces of RT-LAB real-time simulation platform are introduced firstly. Then based on a turboprop engine model, the control laws of propeller control loop and fuel control loop were studied reduce development cost, shorten development cycle and avert testing risks.

2.4 Research Gap

Gone through various literatures, it is found that the analysis of turboprop engine has not been done using advanced software. The data availability, required output accuracy, plays important roles in the selection of the appropriate model. Therefore, the results published by the literatures are limited and analysis has been performed for particular parameters. It is also found that the cooling of the turbine blade is a major parameter to consider for improving the efficiency and life of the turbine blade. In the present work, general software in Matlab 14 has to be developed which will optimize the input parameters of turboprop engine for better efficiency.

CHAPTER 3

3. MATERIALS AND METHOD

Traditionally, in gas turbine performance simulation, an engine thermodynamic performance model may be set up first at a chosen “design point”, where the performance information such as compressor pressure ratios, compressor isentropic efficiencies, turbine inlet temperature, turbine isentropic efficiencies, airflow rate, etc of the engine at this specific operating points are given and the engine design point performance is calculated. The performance of the engine at off-design conditions (i.e., at different ambient, flight conditions or at different power levels) can be predicted by using thermodynamics, empirical component maps and mathematical algorithms to achieve a new engine thermodynamic equilibrium condition, where the continuity of mass, momentum and energy is satisfied. With the development of advanced gas turbine thermodynamic performance modeling techniques such as off-design performance simulation has been very successful as long as the engine component characteristic maps are accurate and kept unchanged during engine operation. However, prediction errors for individual engines may appear even for the same fleet engines due to manufacturing and assembly tolerance and even for the same engines when their performance degrades during their operation. This is because of the difference between the component characteristic maps used in the performance models and those of real engines.

3.1 MODELING OF TURBOPROP ENGINE CONFIGURATIONS

In the present work the configuration used for turboprop engine is listed below. The schematic and T-s diagram of respective configurations are also given in the following articles.

3.1.1 Mathematical Modeling

In case of air breathing engines when engine has to fly at different altitudes the ambient air property namely pressure and temperature as a function of altitudes should be modeled. These models are discussed below.

3.1.1.1 Atmospheric Model

Cycle performance at an altitude for jet engine, it is needed to know the variation of ambient pressure and temperature with height above sea level. The variation depends, to some extent, upon the season and latitude, but it is usual to work with an average or

standard atmosphere [66]. The International Standard Atmosphere (ISA) corresponds the average of values at middling latitudes and yields that the temperature decreases altitude up to 11000 m after which it is constant until 25000 m. Above this height the temperature starts to increase again slowly. Once the temperature is known, the variation of pressure follows the laws of hydrostatics. However, actual ambient conditions can vary widely from I.S.A. It may be noted that for a given speed the Mach number will rise with altitude up to 11000 m because the temperature is falling as shown in the figure 3.1.

The level of ambient pressure at a point defines the pressure altitude. As per the ISA, pressure altitude is not set by the elevation of the point above sea level.

Pressure falls exponentially from sea level value of 1.01325 bar to 0.035339 bar at 30000 m as shown in figure 3.2.

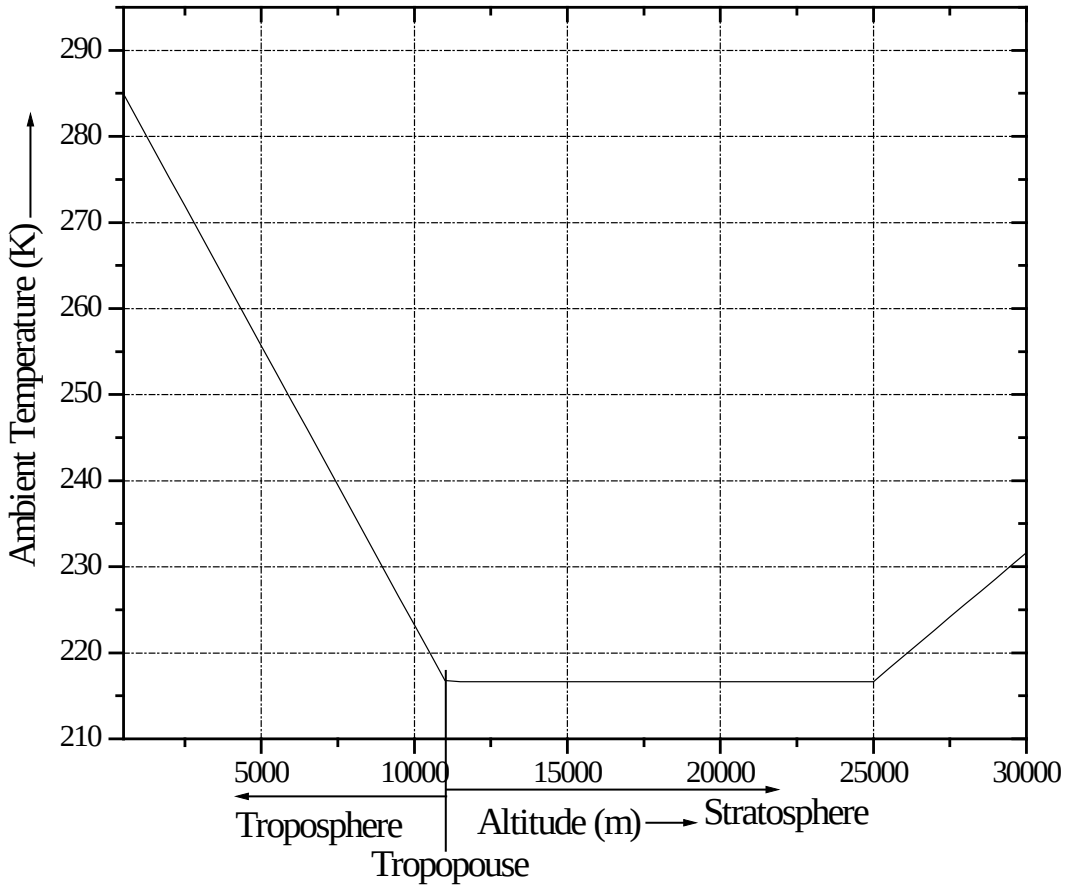

Fig. 3.1 Variation of ambient temperature with altitude for ISA [55]

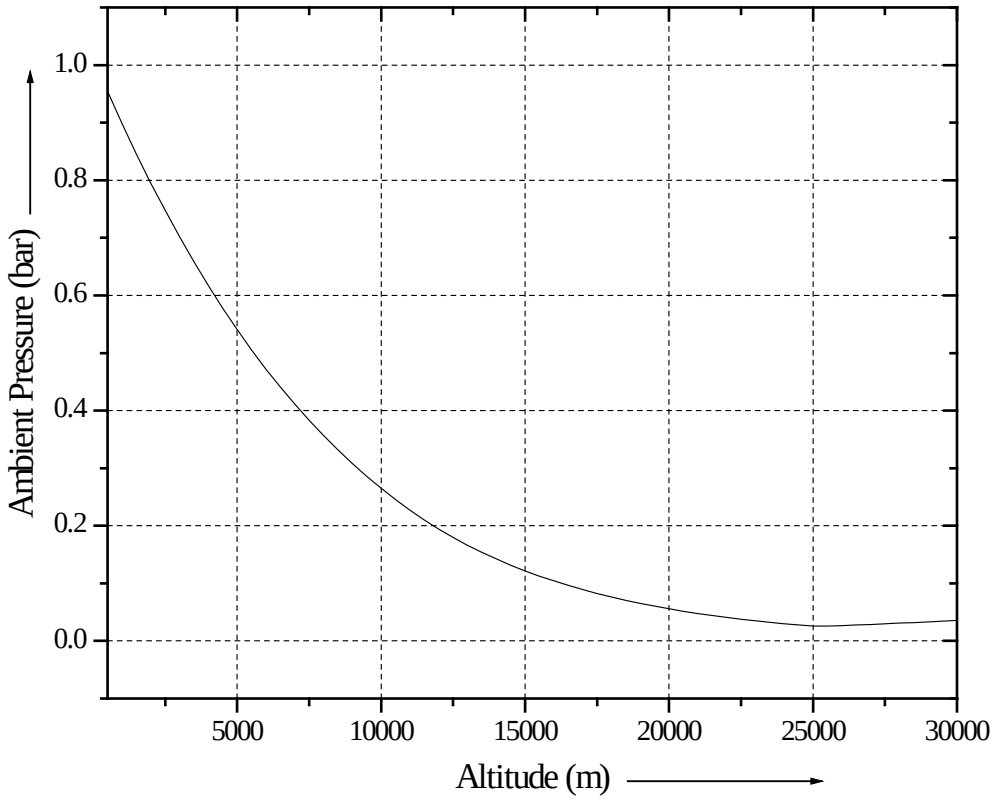

Fig. 3.2 Variation of ambient pressure with altitude for ISA [55]

3.1.1.2 Gas Model

The thermodynamic properties of air and gases are the function of temperature. The specific heat is the function of temperature and hence it varies with temperature. Following equations are used to calculate the gas constant as a function of specific heats of air and gas.

$$R_c = \frac{\gamma_c - 1}{\gamma_c} C_{pc} \qquad 3.1.1$$

$$R_t = \frac{\gamma_t - 1}{\gamma_t} C_{pt} \qquad 3.1.2$$

Speed of sound will be given by,

$$a_0 = \sqrt{\gamma_c R_c g_c} T_0 \qquad 3.1.3$$

Absolute velocity of jet/air is given by,

$$V_0 = a_0 M_0 \qquad 3.1.4$$

3.1.2 Modeling of individual components

In order to carry out the thermodynamic analysis for predicting the performance of a turboprop engine, it is necessary to model its various components at a given operating conditions. Now modeling of various components of turboprop engine has been generated.

Following are the various components of turboprop engine.

Turboprop Engine Components

1. Inlet/Diffuser
2. Propeller and Compressors
3. Combustion Chamber / Combustor
4. Gas turbines
5. Nozzle

Modeling of the above mentioned five components are taken up in the following sections.

3.1.2.1 Intake/Diffuser

The intake in the turboprop engine is an important part and has a significant effect on engine efficiency and aircraft safety. The focus is to minimize the pressure loss up to the propeller inlet and ensure that the flow enters the compressor with a uniform pressure and velocity, at given altitude. Non-uniform or distorted flow may cause compressor surge which can result in either engine flame-out or severe mechanical damage due to blade vibration induced by unsteady aerodynamic effects. Even with a well-designed intake, it is difficult to avoid some flow distortion during rapid manoeuvring.

Current designs of compressors require the flow to enter the first stage at an axial Mach number in the region of 0.4 to 0.5. Subsonic aircraft will typically cruise at a Mach number in the range 0.8 to 0.85, while supersonic aircraft may operate at speeds from Mach number 2 to 2.5. At take-off, with zero forward speed, the engine will operate at maximum power and air flow.

The intake is the duct through which free stream air enters in the engine. The intake can be a convergent duct for subsonic engine. The duct for the turboprop engine is rounded at the entrance in order to avoid flow separation and aerodynamic losses. The intake would thus follow an isentropic process. Thus it may be thought of as a

compressor with no moving parts. The stagnation temperature is constant although there will be a loss of stagnation pressure due to friction and due to shock waves at supersonic flight speeds.

At very low forward speeds, the intake acts as a nozzle in which the air accelerates from zero velocity or low velocity V_1 to V_2at the intake exit and hence at compressor inlet. At normal forward speeds, however, the intake performs as a diffuser with the air decelerating from V_1 to V_2 and the static pressure rising from $P_1$to P_2.Since it is the stagnation pressure at the compressor inlet which is required for cycle calculations, it is the pressure rise $(p_{02} - p_1)$ which is of interest and which is referred to as the 'ram pressure rise'. At supersonic speeds it will comprise the pressure rise across a system of shock waves at the inlet followed by that due to subsonic diffusion in the remainder of the duct.

Ram action takes place in diffuser. The concept of intake efficiency (η_i) is incorporated in the model to account for the inefficiency of diffuser caused by aerodynamic losses.

The intake efficiency can be expressed in a variety of ways, but the two most commonly used ways are the 'isentropic efficiency η_i (defined in terms of temperature rises)' and the 'ram efficiency η_r (defined in terms of pressure rises)'. The ram efficiency is defined by the ratio of the ram pressure rise to the inlet dynamic head and can be expressed as

$$\eta_{ram} = \frac{P_{02} - P_1}{P_{02} - P_1} \qquad 3.1.5$$

While isentropic efficiency of diffuser is expressed as

$$\eta_{ise} = \frac{T'_{02} - T_1}{T_{02} - T_1} \qquad 3.1.6$$

where, T'_{02} is the temperature that would have been reached after an isentropic ram compression to p_{02}

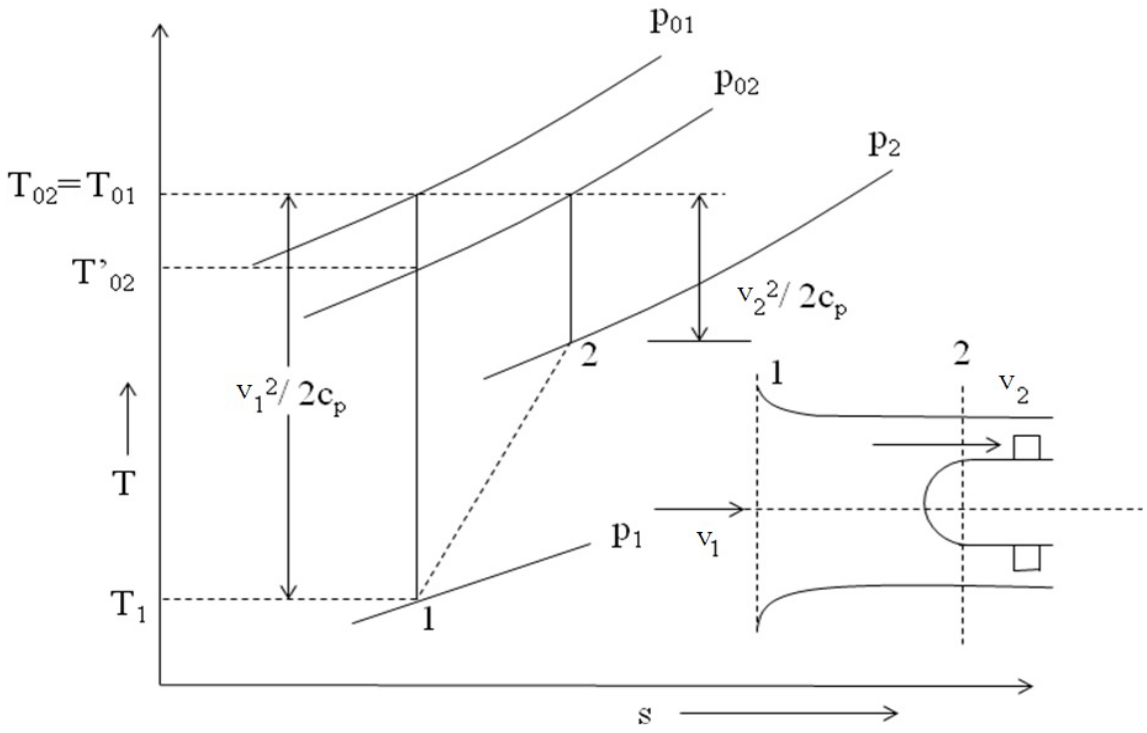

Fig. 3.3 T-s representation of intake loss in diffuser

Isentropic efficiency (η_{ise}) can be regarded as the fraction of the dynamic temperature which should be required for isentropic compression in the intake. Ram efficiency (η_{ram}) can be shown to be almost identical in magnitude to η_{ise} and these are interchangeable.

Though η_{ram} is easier to measure experimentally, it has no advantage over η_{isen} and the latter is used here for the calculation. They both suffer equally from the drawback of implying zero stagnation pressure loss when V_1 is zero, because then $\frac{p_{02}}{p_1} = 1$ and $p_1 = p_{01}$. This is not serious because under these conditions the average velocity in the intake is low, and the flow is accelerating, so that the effect of friction is very small.

The inlet and exit conditions of diffuser are expressed by,

At inlet,

$$\frac{T_{01}}{T_1} = \left[1 + \left(\frac{\gamma_c - 1}{2}\right).M^2\right] \qquad 3.1.7$$

The intake efficiency will depend upon the location of the engine in the aircraft (in wing, pod or fuselage), but here it is assumed a constant value for subsonic intake. In practice, neither η_r nor η_i is used for supersonic intakes and it is more usual to quote the values of stagnation pressure ratio $\frac{p_{02}}{p_{01}}$ as a function of Mach number where, $\frac{p_{02}}{p_{01}}$ is also known as pressure recovery factor of the intake.

$$\frac{p_{0,2}}{p_1} = \left(\frac{T_{0,1}}{T_1}\right)^{\frac{\gamma_c}{\gamma_c - 1}} \quad \text{for } M \leq 1 \qquad 3.1.8$$

At exit,

$$T_{0,2} = T_{0,1} \qquad 3.1.9$$

$$\frac{p_{0,2}}{p_1} = \left[1 + \eta_d . \left(\frac{\gamma_c - 1}{2}\right) . M^2\right]^{\frac{\gamma_c}{\gamma_c - 1}} \qquad 3.1.10$$

For the definition of the total enthalpy and total pressure, it can be expressed as

$$\tau_r = 1 + \frac{\gamma_c - 1}{2} M_0^2 \qquad 3.1.11$$

$$\pi_r = \tau_r^{\gamma_c/(\gamma_c - 1)} \qquad 3.1.12$$

Because of shocks, only a portion of the ram total pressure can be recovered. Now, π_{dmax} is that portion of π_d which is due to wall friction and defines η_r as that portion of π_d due to ram recovery. Thus,

$$\eta_r = 1 \qquad 3.1.13$$

$$\pi_d = \pi_{d\max} \times \eta_r \qquad 3.1.14$$

3.1.2.2 Propeller and Compressor

The purpose of a compressor is to increase the total pressure of the gas stream that required by the cycle by absorbing the minimum possible shaft power. Propeller is the term given to the first compressor in a turbofan engine and is usually a single stage compressor. The term reflects the fact that it has a high flow and low pressure ratio

compared with core compressors. For a multistage fan the term low pressure compressor is more frequently used.

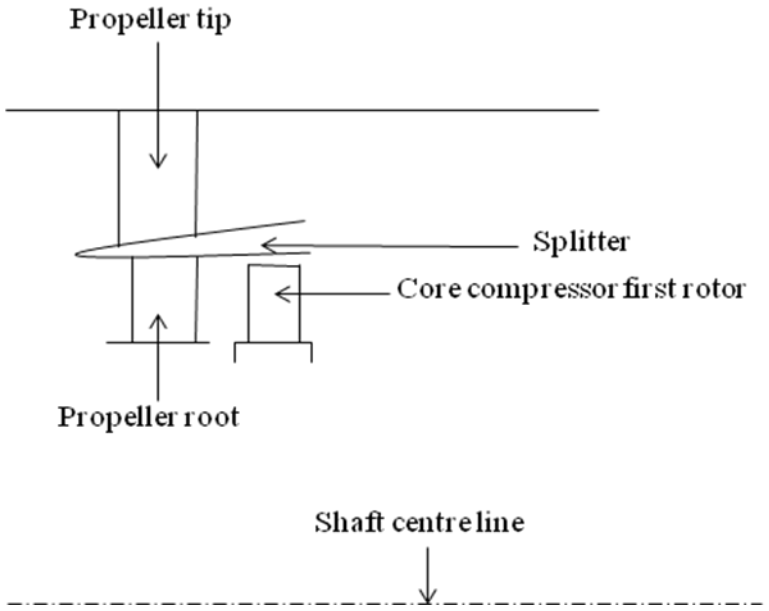

Fig. 3.4 Schematic of Propeller tip and root arrangement

Propellers Fans are always axial flow unit. The diameter and downstream ducting required for a centrifugal stage make its use prohibitive. The typical arrangement of a single stage fan is shown in figure 3.4.

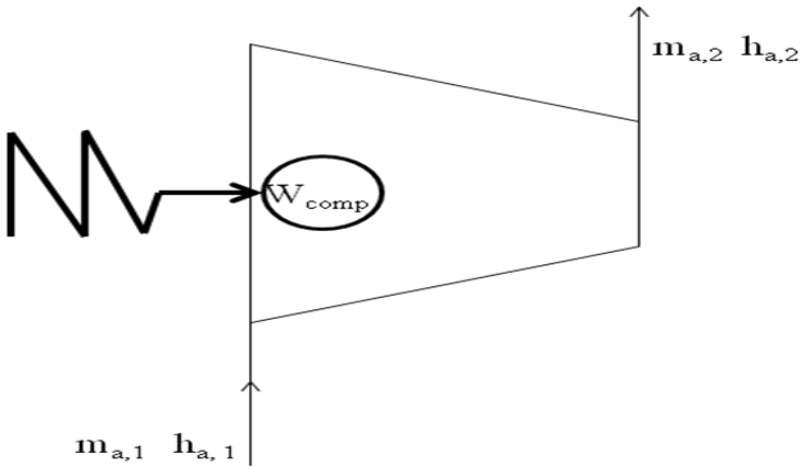

Fig. 3.5 Simplified model of compressor

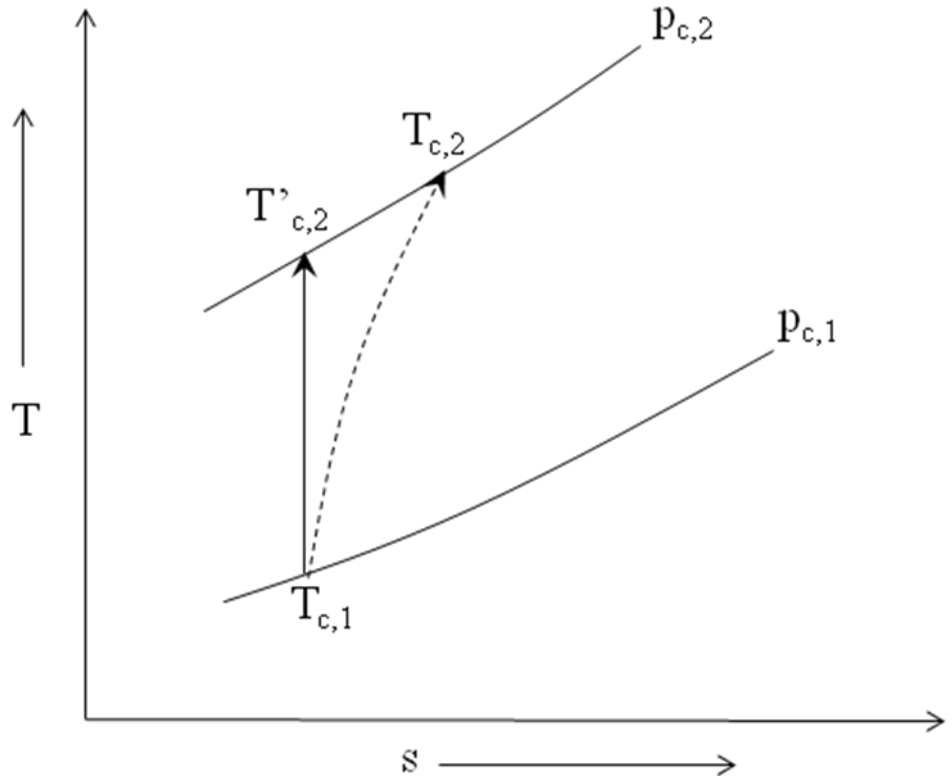

Fig. 3.6 T-s representation of compression process (isentropic & actual process)

Propeller/Compressor are subjected to various aerodynamic losses which are accounted here by introducing the concept of polytropic efficiency. For a given polytropic efficiency, pressure ratio, temperature and other variables for each stream are calculated.

The mass and energy balances yield the compressor work, as given below

Mass balance:

$$\dot{m}_{a1} = \dot{m}_{a2} \qquad 3.1.15$$

Energy balance:

$$W_{comp} = \dot{m}_{a,2} . h_{a,2} - \dot{m}_{a,1} . h_{a,1} \qquad 3.1.16$$

Further, the temperature ration of compressor can be calculated by:

$$\tau_c = 1 + \frac{T_{t4}/T_0}{(T_{t4}/T_0)_R} \frac{(\tau_r)_R}{\tau_r} (\tau_c - 1)_R \qquad 3.1.17$$

Pressure Ratio is given by:

$$\pi_c = [1+\eta_c(\tau_c - 1)]^{\gamma_c/(\gamma_c - 1)} \qquad 3.1.18$$

Enthalpy Ratio is given by:

$$\tau_\lambda = \frac{C_{pt}T_{t4}}{C_{pc}T_0} \qquad 3.1.19$$

where, π_c is the pressure ratio of compressor and η_c is isentropic efficiency of the compressor.

3.1.2.3 Combustor

The purpose of the combustion system of a turboprop engine is to increase the thermal energy of a flowing gas stream by combustion which is an exothermic chemical reaction between the hydrocarbon fuel and oxygen in the air-stream. Principal features of a combustor are shown schematically in figure 3.7. Inflowing air is diffused at the entrance of the burner. The burner is divided in to three zones namely, primary-, secondary-, and dilution-zone. In the primary zone the fuel, atomized and partially or completely vaporized by the fuel nozzle, is mixed with the primary air coming through the air swirler. In the secondary zone the primary zone effluent gases continue to burn and incoming secondary air leans out the main gas stream. The combustion process completes at the downstream end of the intermediate zone. In the dilution zone any remaining annulus airflow is dumped through the dilution holes in to the liner hot gas stream.

During modeling, incomplete combustion is taken care by the combustion efficiency (η_b) and pressure loss which is calculated from the combustion loading.

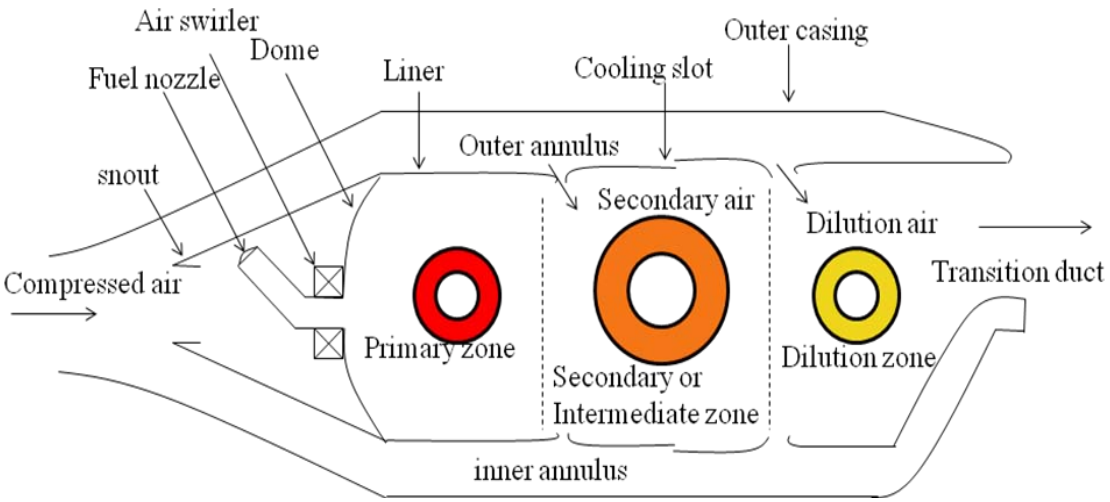

Fig. 3.7 Schematic diagram of Combustor

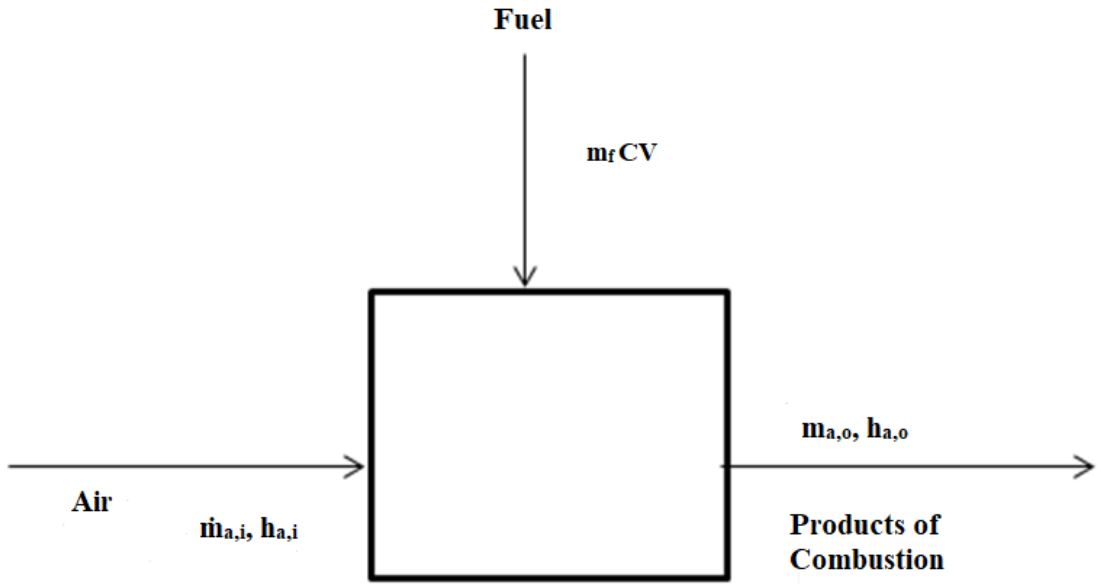

Fig. 3.8 Simplified representation of combustor model

The highly distilled form of diesel issued which makes little difference in performance compared to kerosene. Therefore, it has been used in the present analysis.

The mass and energy balances for combustor with suffixes 1and 2 denoting its inlet and exit sections, are given by

Mass balance:

$$\dot{m}_g = \dot{m}_{a1} + \dot{m}_{f,b} \qquad 3.1.20$$

Energy balance:

$$\eta_b . \dot{m}_b . CV = \dot{m}_{g,2} . h_{g,2} - \dot{m}_{a,1} . h_{a,1} \quad 3.1.21$$

The pressure at combustion chamber exit is given by

$$p_{b2} = P_{b1} - \Delta p_b \quad 3.1.22$$

Where, ΔP_b is the pressure loss in the combustion chamber taken as 2% of p_{b1}, for calculation

The fuel to air ratio (FAR) is calculated as,

$$\frac{\dot{m}_{f,b}}{\dot{m}_a} = \frac{c_{pg} . T_{0,2} - c_{pa} . T_{0,1}}{\eta_b CV - c_{pg} . T_{0,2}} \quad 3.1.23$$

or,

$$f = \frac{\tau_\lambda - \tau_r \tau_c}{CV\eta_b / (C_p T_0) - \tau_\lambda} \quad 3.1.24$$

Mass flow rate is given by:

$$\dot{m} = \dot{m}_{0\,R} \frac{P_0 \pi_r \pi_d \pi_c}{(P_0 \pi_r \pi_d \pi_c)_R} \frac{\sqrt{T_{t4R}}}{\sqrt{T_{t4}}} \quad 3.1.25$$

In this equation $T_{0,2}$ is the turbine inlet temperature, $T_{0,1}$ is stagnation or total exit temperature of compressor, η_b is the combustion efficiency of the combustor, normally taken between (0.98 to 0.99) and CV is the lower calorific value of the fuel taken as 42800 kJ/kg.K assuming fuel as diesel. Values of specific heat of air and gases are assumed for the present analysis.

3.1.2.4 Gas Turbine

There are two turbines used to drive separately compressor and propeller. Turbine produced power to drive engine compressor due to expansion of gas stream. A general model that represents the gas turbine has been developed. The model is intended for use in cycle analysis applications. Aerodynamic losses and hence the inefficiency of gas turbine is taken care by considering polytropic efficiency of turbine.

$$\frac{T_{0,1}}{T_{0,2}} = \left(\frac{p_{0,1}}{p_{0,2}}\right)^{\frac{\eta_{pg}(\gamma_g - 1)}{\gamma_g}} \quad 3.1.26$$

Pressure ratio, the temperature and other variables for each stream are calculated for a given polytropic efficiency.

Work compatibility of turbine and compressor is given as follows:

$$W_{hp,c} + W_{ax} = \eta_m W_{hp,t} \qquad 3.1.27$$

$W_{ax,}$ auxiliary power, required for powering accessories is tapped out from the high pressure turbine. It is assumed to be 10% of the compressor work. Therefore,

$$W_{hp,t} = \frac{W_{hp,c}}{\eta_m} \times 1.10 \qquad 3.1.28$$

Here, $W_{hp,t}$ is the work developed by high pressure turbine, $W_{hp,c}$ is the work required by the high pressure compressor and $\eta_m$is the mechanical efficiency which is used to account for the losses due to windage, bearing friction, and seal drag and is defined as

$$\eta_m = \frac{\text{mechanical power output}}{\text{mechanical power input}}$$

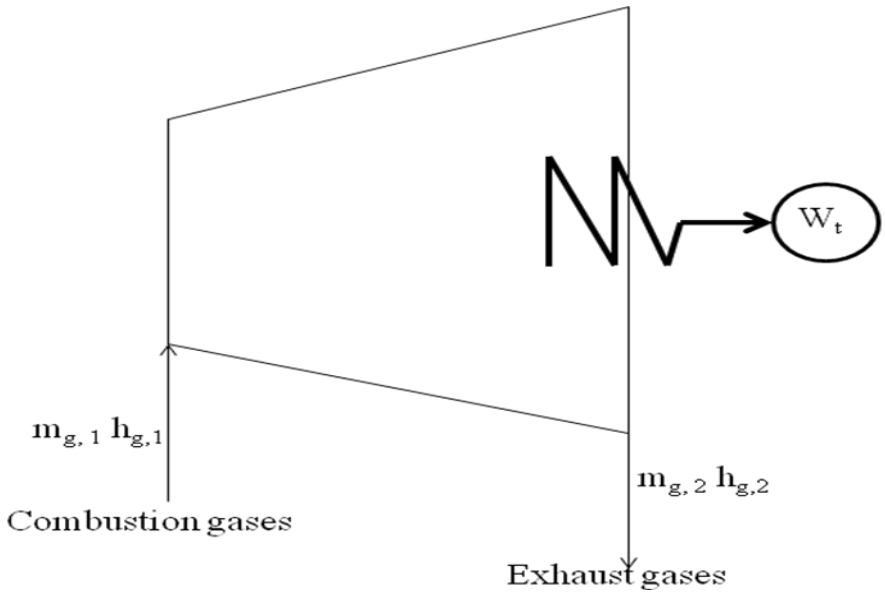

Fig. 3.9 Simplified turbine model

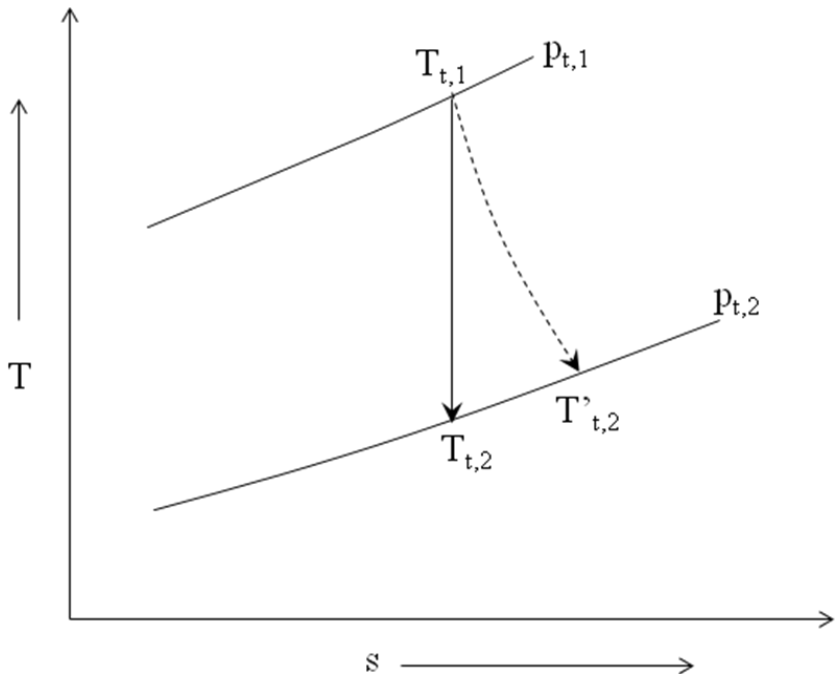

Fig. 3.10 T-s representation of expansion in turbine

It is to be noticed that the auxiliary work taken should be balanced only once with high pressure turbine work.

Mass and energy balances yield the turbine work, as given below.

Mass balance:

$$\dot{m}_{g,i} = \dot{m}_{g,e} \qquad 3.1.29$$

where,

$$\dot{m}_{g,i} = \dot{m}_{a,i} + \dot{m}_{f,cc} \qquad 3.1.30$$

Energy balance:

$$\dot{m}_{g,i}.h_{g,i} = \dot{m}_{g,e}.h_{g,e} + W_T \qquad 3.1.31$$

Kerosene is the standard aviation fuel but the highly distilled forms of diesel used make little difference to performance compared to kerosene and hence diesel is used here for the analysis.

$$\dot{m}_g.c_{pg}.T_{0,i} + \dot{m}_{f,ab}.LCV_f = (\dot{m}_g + \dot{m}_{fab}).c_{pg}.T_{0,e} \qquad 3.1.32$$

Initial value of low pressure turbine (π_{tL})

$\pi_{tL} = \pi_{tLR}$

Turbine temperature and exhaust nozzle has been specified:

$$\tau_{tL} = 1 - \eta_{tL}(1 - \pi_{tL}^{(\gamma_t - 1)/\gamma_t}) \quad 3.1.33$$

$$\pi_{tLN} = \pi_{tLR}\sqrt{\frac{\tau_{tL}}{\tau_{tLR}}}\frac{MFP(M_{9R})}{MFP(M_9)} \quad 3.1.34$$

Check for $\tau_{tLN} - \pi_{tL} \leq 0.0001$. If so, then continue….If not, let $\pi_{tL} = \pi_{tLN}$ and return to Eq.3.1.34

3.1.2.5 Exhaust Nozzle

The purpose of the exhaust nozzle is to increase the velocity of the exhaust gas before discharge from the nozzle. For large values of thrust, the kinetic energy of the exhaust gas must be high, which implies a high exhaust velocity. The pressure ratio across the nozzle controls the expansion process and the maximum thrust for a given engine is obtained when the exit pressure equals the ambient pressure, i.e. pressure thrust is zero.

The function of the nozzle may be summarized in the following list:

- Accelerate the flow to a high velocity with minimum total pressure loss thus converting thermal energy of the gas into kinetic energy.
- Match exit and atmospheric pressure as closely as desired. This serves as back pressure control for the engine.
- Permit afterburner operation without affecting main engine operation–requires variable throat area nozzle.
- Allow for cooling of walls if necessary.
- Mix core and bypass streams of turbofan if necessary.
- Allow for thrust reversal if desired.
- Suppress jet noise, radar reflection, and infrared radiation (IR) if desired.
- Two-dimensional and axial-symmetric nozzles, thrust vector control if desired.
- Do all the above with minimal cost, weight, and drag while meeting life and reliability goals.

The nozzle may be thought of as a device that converts enthalpy into kinetic energy with no moving parts. The two basic types of nozzles used in jet engines are the convergent and convergent-divergent (C-D) nozzle.

3.1.3 Propelling Nozzle

Here, the term "propelling nozzle" refers to the component in which the working fluid is expanded to give a high velocity jet. In a simple turbojet engine there is a single nozzle downstream of the turbine. In the transition from the turbine annulus to circular jet pipe some increase in area is provided to reduce the velocity, and hence friction loss, in the jet pipe.

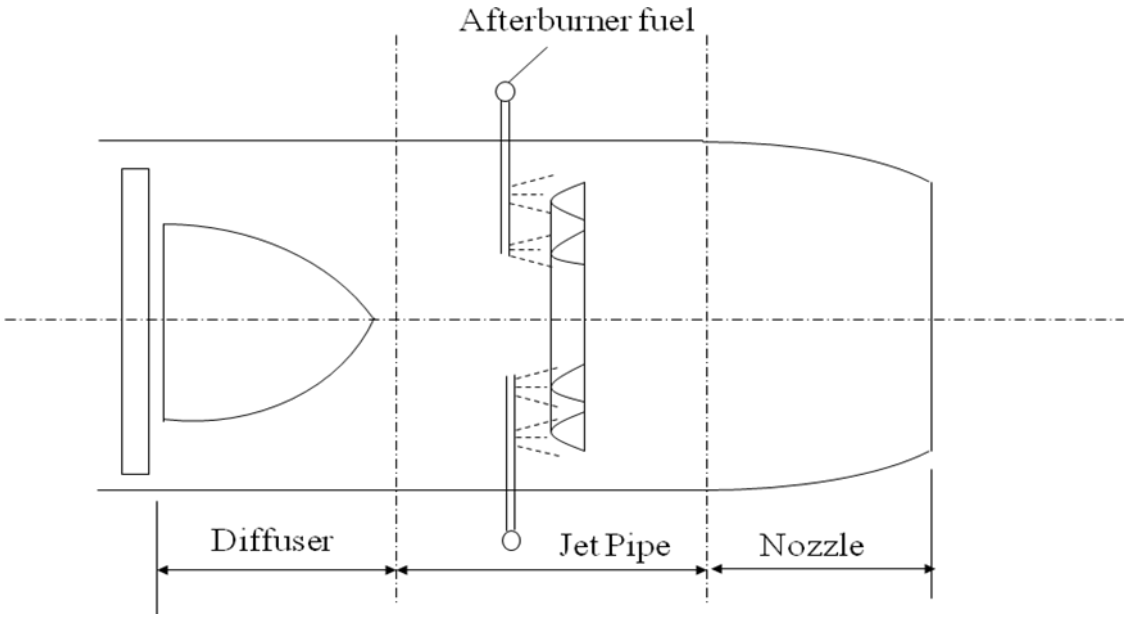

Fig. 3.11 Schematic representation of Propelling Nozzle System

The question immediately arises as to whether a simple convergent nozzle is adequate or whether a convergent-divergent nozzle should be employed. As it will be seen from the subsequent thermodynamic cycle calculations, even with moderate cycle pressure ratios the pressure ratio $\frac{P_{01}}{P_{atm}}$ will be greater than the critical pressure ratio over at least part of the operational range of forward speed and altitude. Although a convergent divergent nozzle might therefore appear to be necessary, it is to be noted that the thrust which is required and not maximum possible jet velocity. Certainly it can be shown that for an isentropic expansion the thrust produced is maximum when complete expansion to P_{atm} occur in the nozzle. Furthermore the use of a convergent-divergent nozzle

would result in significant increase in engine weight, length and diameter which would in turn result in major installation difficulties and a penalty in aircraft weight.

At operating pressure ratios less than the design value, a convergent-divergent nozzle of fixed proportions would certainly be less efficient because of the loss incurred by the formation of the shock wave in the divergent portion. For these reasons aircraft gas turbine normally employs a convergent propelling nozzle.

It should not be thought that convergent-divergent nozzles are never used. At high supersonic speeds, the large ram pressure rise in the intake results in a very high nozzle pressure ratio. The value of $\frac{p_{0,i}}{p_a}$ is then many times larger than the critical pressure ratio and may be as high as 10-20 for flight Mach number in the range 2-3.

3.1.3.1 Convergent Nozzle

This is a simple convergent duct as shown in figure 1.18 when the pressure ratio is low (less than about 4), the convergent nozzle is used. It has generally been used in engines for subsonic aircrafts.

3.1.3.2 Convergent-divergent (C-D) Nozzle

A Convergent-divergent nozzle is used if the nozzle pressure ratio is high (greater than about 4). If the engine incorporates an afterburner, the nozzle throat is usually scheduled to leave the operating conditions of the engine upstream of the afterburner unchanged. In other words, the exit nozzle area is varied so that the engine does not feel that the afterburner is operating. Also, the exit area must be varied to match the internal and external static pressures at exit for different flow conditions in order to produce the maximum available uninstalled thrust.

A convergent nozzle is used in the present analysis. One advantage of the variable area exhaust nozzle is that it improves the starting of the engine. Operating the engine at the maximum throat area reduces the back pressure, which helps in starting the compressor at a low engine speed. This reduces the required size of the engine starter.

Steady state operation close to stall or surge is not desirable as transient operation may cause the compressor to stall. The operating line can be moved away from the stall line by increasing the exhaust nozzle throat area. This increase in nozzle throat area reduces the engine backpressure and increases the corrected mass flow rate through the compressor. Thus change in the nozzle throat area from its

original design value will change the engine design and the operating characteristics of the engine.

The jet nozzle suffers from the aerodynamic losses mainly due to skin friction, which is modeled by introducing the concept of nozzle efficiency. The nozzle may be choked or unchoked and may be decided using the critical pressure ratio.

The critical pressure ratio is expressed as

$$\frac{p_c}{p_{0,i}} = \left[1 - \frac{1}{\eta_n}\left\{\frac{\gamma_g - 1}{\gamma_g + 1}\right\}\right]^{\frac{\gamma_g}{\gamma_g - 1}} \qquad 3.1.35$$

where, η_n is the nozzle efficiency.

3.1.3.3 Choked Nozzle

If $\frac{p_{0,i}}{p_a} > \frac{p_{0,i}}{p_c}$, then nozzle is choked where a Mach number of 1 is reached at the minimum area section along the duct and reducing exit pressure further provides no increase in mass flow.

3.1.3.4 Unchoked Nozzle

If the Nozzle pressure ratio is less than critical pressure ratio i.e. $\frac{p_{0i}}{p_a} < \frac{p_{0i}}{p_c}$ the nozzle is unchoked. Fig. 3.14 shows the T-s representation for unchoked nozzle. In this work, unchoked nozzle is used for the analysis.

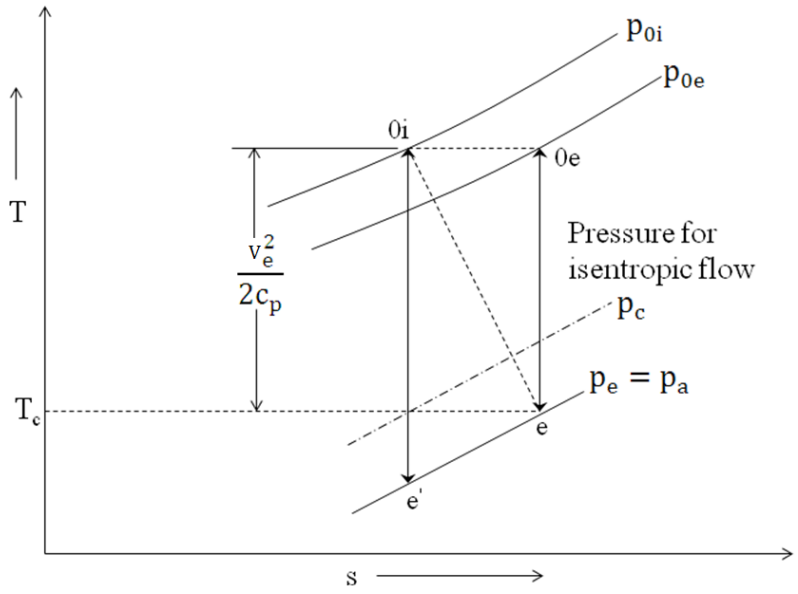

Fig. 3.12 T-s representation of unchoked nozzle when $\left(\frac{p_{0i}}{p_a}\right) < \left(\frac{p_{0i}}{p_c}\right)$

3.2 CYCLE ANALYSIS

The analysis of the turboprop engine cycle calculation is performed by using following equations.

$$p_{0,e} = p_a \tag{3.1.36}$$

$$T_{0,i} - T_e = \eta_j . T_{0i} \left\{ 1 - \left[\frac{1}{\left(\frac{p_{0i}}{p_a}\right)} \right]^{\frac{\gamma_n - 1}{\gamma_n}} \right\} \tag{3.1.37}$$

The jet velocity is given by

$$C_{n,e} = \sqrt{2 c_{pg} . (T_{0,i} - T_e)} \tag{3.1.38}$$

For the thrust of the core stream, the work output co-efficient is give by:

$$C_c = (\gamma_c - 1) M_0 \left[(1+f) \frac{V_9}{a_0} - M_0 + (1+f) \frac{R_t}{R_c} \frac{T_9 / T_0}{V_9 / a_0} \frac{1 - P_0 / P_9}{\gamma_c} \right] \tag{3.1.39}$$

The work output co-efficient of propeller is given by

$$C_{prop} = \eta_{prop} \eta_g \eta_{mL} (1+f) \tau_\lambda \tau_{tH} (1 - \tau_{tL}) \tag{3.1.40}$$

Thus the total work output co-efficient for the turboprop engine is

$$C_{tot} = C_{prop} + C_c \tag{3.1.41}$$

and the corresponding thrust is

$$F = \dot{m}_0 \left(\frac{F}{\dot{m}_0} \right) \tag{3.1.42}$$

It is usual with turboprop engine to have the core stream exit nozzles unchoked, so the pressure imbalance term doesn't contribute in the expression for the thrust. Here, the stations indicated in fig. 3.13 with station 5 being the exit from the high-pressure turbine and the entrance to the low-pressure or power turbine is considered. For a turboprop engine, two design variables: the compressor pressure ratio and the low-pressure (free or power) turbine temperature ratio. The cycle equations in terms of the

pressure and temperature ratios across both the high-pressure turbine (drives the compressor) and the low-pressure turbine is developed.

$$\frac{V_9}{a_0} = M_9\sqrt{\gamma_t R_t T_9 / \gamma_c R_c T_0} \qquad 3.1.43$$

Two flow regimes exist for flow through the convergent exhaust nozzle: choked flow and unchoked flow. For unchoked flow, the exit static pressure P_9 is equal to the ambient pressure P_0 and the exit Mach number is less than or equal to one. Unchoked flow will exist when

$$\frac{P_{t9}}{P_0} = \pi_r \pi_d \pi_c \pi_b \pi_{tH} \pi_{tL} \pi_n \qquad 3.1.44$$

$$\text{If, } \frac{P_{t9}}{P_0} \le \left(\frac{\gamma_t + 1}{2}\right)^{\frac{\gamma_t}{\gamma_t - 1}} \qquad 3.1.45$$

Then,

$$M_9 = 1;\ \frac{P_{t9}}{P_9} = \left(\frac{\gamma_t + 1}{2}\right)^{\frac{\gamma_t}{\gamma_t - 1}} \qquad 3.1.46$$

and,

$$\frac{P_0}{P_9} = \frac{P_{t9}/P_9}{P_{t9}/P_0} \qquad 3.1.47$$

Else,

$$\frac{P_0}{P_9} = 1\,\frac{P_{t9}}{P_9} = \frac{P_{t9}}{P_0} \qquad 3.1.48$$

and,

$$M_9 = \sqrt{\frac{2}{\gamma_t - 1}\left(\frac{P_{t9}}{P_0}\right)^{\gamma_t - 1/\gamma_t} - 1} \qquad 3.1.49$$

and the exit Mach number is given by Equation with $P_9 = P_0$. On the other hand, choked flow will exist when

$$\frac{P_{t9}}{P_0} > \left(\frac{\gamma_t + 1}{2}\right)^{\frac{\gamma_t}{\gamma_t - 1}} \quad 3.1.50$$

Then, $M_9 = 1$; $\frac{P_{t9}}{P_9} = \left(\frac{\gamma_t + 1}{2}\right)^{\frac{\gamma_t}{\gamma_t - 1}}$ 3.1.51

$$\frac{P_0}{P_9} = \frac{\frac{P_{t9}}{P_9}}{\frac{P_{t9}}{P_0}} \quad 3.1.52$$

and,

$$\frac{T_9}{T_0} = \frac{T_{t4}\tau_{tH}\tau_{tL}}{\left(P_{t9}/P_9\right)^{(\gamma_t - 1)/\gamma_t}} \quad 3.1.53$$

For the turboprop engine, both the specific power and the specific thrust are considered

$$\frac{\dot{W}}{\dot{m}_0} = C_{tot} c_{pc} T_0 \quad 3.1.54$$

$$\frac{F}{\dot{m}_0} = \frac{C_{tot} C_{pc} T_0}{V_0} \quad 3.1.55$$

It should also be noted that it is more usual when it is referred to propeller aircraft to refer to the power specific fuel consumption in terms of S_P, where it is defined as

$$S = \frac{f}{F/\dot{m}_0} \quad 3.1.56$$

$$S_P = \frac{f}{C_{tot} c_{pc} T_0} \quad 3.1.57$$

The propulsive efficiency of the turboprop engine is defined as the ratio of the total power interaction with the vehicle producing propulsive power to the total energy available for producing propulsive power. Thus,

$$\eta_p = \frac{C_{tot}}{C_{prop}/\eta_{prop} + ([\gamma_c - 1)/2][(1 + f)(V_9/a_0)^2 - M_0^2]} \quad 3.1.58$$

$$\eta_T = \frac{C_{tot} c_{pc} T_0}{f h_{PR}} \quad 3.1.59$$

The overall efficiency of the engine can be simply expressed as

$$\eta_O = \eta_P \eta_T \quad 3.1.60$$

$$\left(\frac{N}{N_R}\right)_{corespool} = \sqrt{\frac{T_0 \tau_r (\tau_c - 1)}{T_{0R} \tau_{rR} (\tau_{cR} - 1)}} \quad 3.1.61$$

$$\left(\frac{N}{N_R}\right)_{powerspool} = \sqrt{\frac{T_{t4} (1 - \tau_{tL})}{T_{t4R} (1 - \tau_{tLR})}} \quad 3.1.62$$

3.3 Governing equations for performance prediction and software development

Based on the modeling of turboprop engine described in the foregoing sections, the governing equation for performance predictions are discussed in following paragraphs. These equations are used to calculate specific thrust and thrust specific fuel consumption. The cycle performance and optimization are achieved through software developed in MATLAB and then graphs are plotted.

On the basis of nozzle condition, it is expressed as given below:

If nozzle is unchoked, pressure thrust will be zero and the net specific thrust is directly expressed as

$$\mathbf{F_s = \dot{m}_g . \left(C_{n,e} - C_a\right)} \quad 3.1.63$$

Thrust Specific Fuel Consumption: This is the thrust produced by the unit consumption of fuel and is expressed as

$$\mathbf{TSFC = \frac{\dot{m}_f}{F_s}} \quad 3.1.64$$

where, $\mathbf{\dot{m}_f = \dot{m}_{f,cc} + \dot{m}_{f,ab}}$ 3.1.65

In case of no afterburner, $\mathbf{\dot{m}_{f,ab} = 0}$

3.3.1 MATLAB

MATLAB is an interactive, matrix-based system for scientific and engineering calculations. All of the data that enter into MATLAB is stored in the form of a matrix or a multidimensional array. Complex numerical problems can be solved without actually writing a program. The name MATLAB is an abbreviation for matrix laboratory. A numerical analyst called Cleve Moler wrote the first version of MATLAB in 1970s. It has since evolved into a successful commercial software package. MATLAB makes use of highly respected algorithms and we can be confident about results. Powerful operations can be performed using just one or two commands; we can build up our own set of functions for a particular application. Excellent graphics facilities are available, and the pictures can be inserted into LATEX and Word documents.

3.3.2 MATLAB Simulink

MATLAB has an extensive set of build-in functions as well as additional toolboxes that consist of functions related to more specialized topics like fuzzy logic, neural networks, signal processing, and optimization technique. It can be used in tow different ways: as a traditional programming environment and as an interactive calculator. In a calculator mode, the built-in and toolbox function provide a convenient means of programming modes, it provides a programming environment (editor, debugger and profiler) that enables the user to write their own functions and scripts. Expressions consisting of operators and functions that operate on variables are executed at the command line prompt (>>) in the command window. All of the variables that are created are stored in the workspace and are visible in the Workspace panel. Information about any function or toolbox is available via the command-line help function (or from the Help Browser launched from the Help menu). MATLAB, a multi-panel window appears containing command window, workspace, current directory, and command history panels, among others. This, along with windows foe the Editor/ Debugger, Array Editor and help Browser that can be invoked as needed, is the MATLAB environment.

3.3.3 MATLAB System

The MATLAB system consists of five main parts which are discussed below:

- Development environment is the set of tools and facilities that help you use MATLAB functions and files. Many of these tools are graphical user interfaces. It includes the MATLAB desktop and Command Window, a command history,

an editor and debugger and browsers for viewing help, the workspace, files and the search path.

- The MATLAB Mathematical Function Library is a vast collection of computational algorithms ranging from elementary functions like sum, sine, cosine and complex arithmetic, to more sophisticated functions like matrix inverse, matrix Eigen values, Bessel functions and fast Fourier transforms.
- The MATLAB language is high-level matrix/array language with control flow statements, functions, and data structures, input/output and object-oriented programming features. It allows both "programming in the small "into rapidly create quick and dirty throw- away programs and "programming in the large" to create large and complex application programs.
- Graphics has extensive facilities for displaying vectors and matrices as graphs, as well as annotating and printing these graphs. It includes high-level functions for two-dimensional data visualization, image processing, and animation and presentation graphics. It also includes low-level functions that allow you to fully customize the appearance of graphics as well as well as to build complete graphical user interfaces on your MATLAB applications.

The MATLAB external interface is a library that allows you to write C and FORTRAN programs that interact with MATLAB. It includes facilities for calling routines from MATLAB (dynamic linking) called MATLAB as computational engine and for reading and writing MAT-files.

3.4 TWO-SPOOL TURBOPROP ENGINE

Schematic diagram and the T-s representation of the various processes involved in a turboprop engine are given in the figs. 3.3.1 and 3.3.2, respectively.

3.4.1 Atmospheric model:

For calculation of the atmospheric condition the equations used has been chosen from the work of Dr. Tariq & Prof. Nema (Ref. 55).

3.4.2 Intake / Diffuser model (0-1)

To calculate the temperature and pressure changes in the diffuser, equations 3.1.5 to 3.1.14 are used.

3.4.3 Propeller / Compressor model (1-3)

To calculate the pressure and temperature changes of propeller, equations 3.1.15 to 3.1.19 are used.

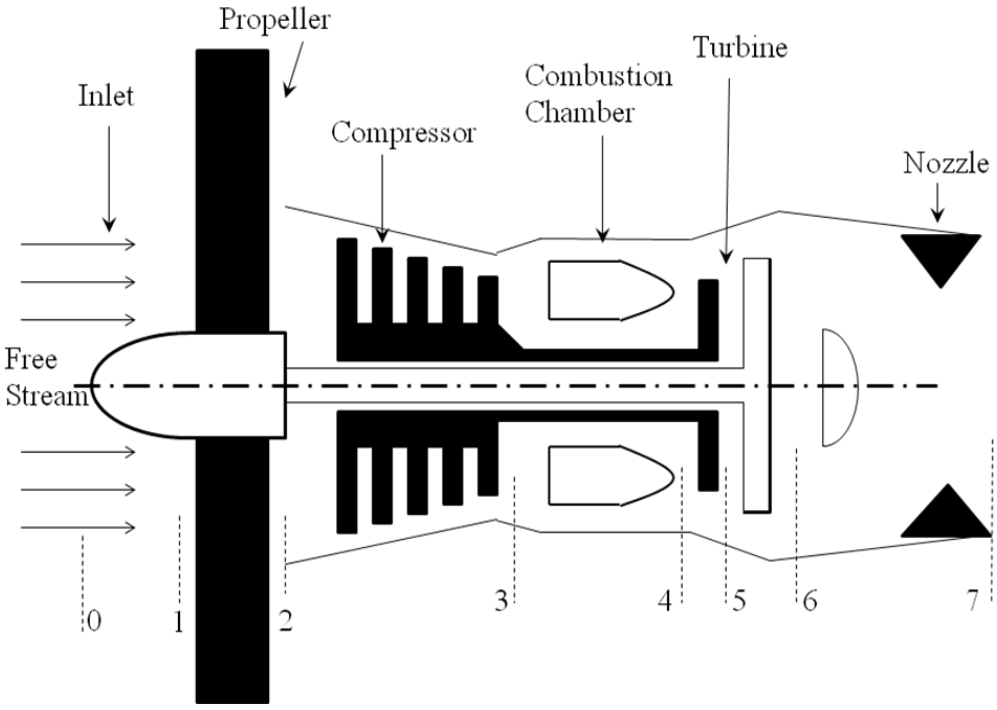

Fig. 3.13 Schematic of two-spool turboprop engine

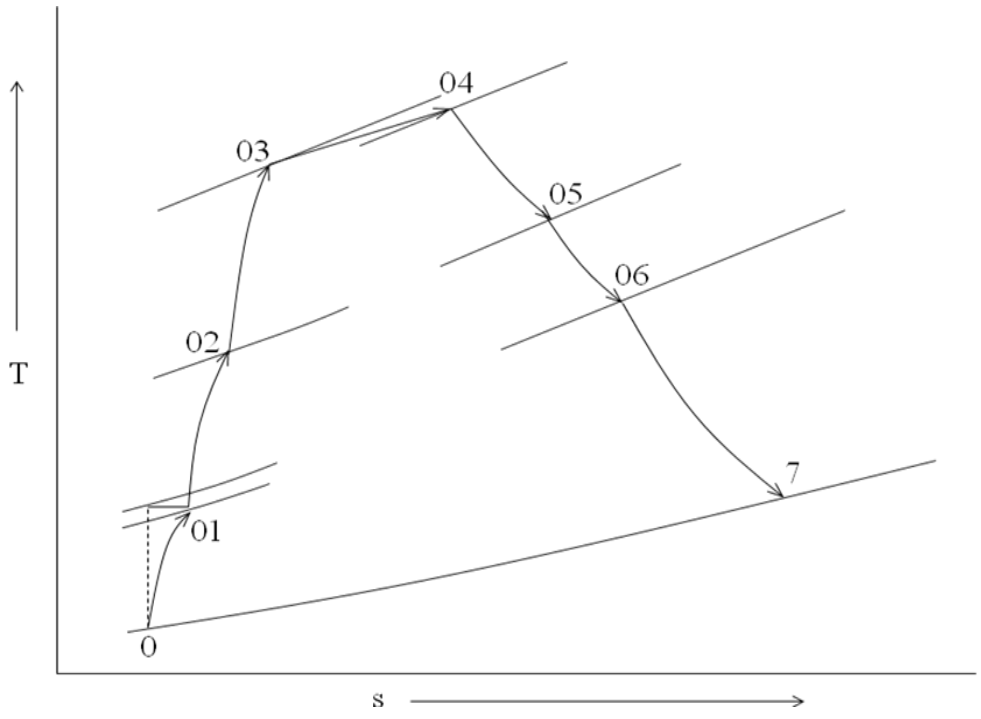

Fig. 3.14 T-s representation of two-spool turboprop engine

3.4.4 Combustor model (3-4)

To calculate the mass of fuel required per kg of air in the combustion chamber, equations 3.1.20 to 3.1.25 are used.

3.4.5 Turbine Model (4-5)

To calculate the temperature and pressure changes in high pressure turbine, equations 3.1.26 to 3.1.34 are used.

3.4.6 Jet Nozzle model (6-7)

To calculate the pressure and temperature at the exit plane of nozzle, equations 3.1.35 to 3.1.53 are used. These would be needed to determine the thrust from the engine.

CHAPTER 4

4. RESULTS AND DISCUSSION

This chapter deals with the findings based on the MATLAB software which validate the procured results with the genuine input data. Various graphical representations show the basic phenomena known from the analysis of existing designs, ways to gain benefits from analysing the wing that interacts with the propeller.

Table 1. Input data for present work

Sl. No.	Parameters	Values
1	Mach number (M_o)	0.8
2	Temperature (T_o)	240 K
3	Ratio of specific heat of air (γ_c)	1.4
4	Specific heat at constant pressure of air (c_{pc})	1.004kJ/kg.K
5	Ratio of specific heat of gas (γ_t)	1.35
6	Specific heat at constant pressure of gas (c_{pt})	1.108 kJ/kg.K
7	Low heating value of fuel (h_{PR})	42800 kJ/kg
8	Polytropic efficiency of compressor (e_c)	0.90
9	Polytropic efficiency of high pressure turbine (e_{tH})	0.89
10	Polytropic efficiency of low pressure turbine (e_{tL})	0.91
11	Pressure ratio of diffuser or inlet (π_d)	0.98
12	Pressure ratio of burner or combustor (π_b)	0.96
13	Pressure ratio of nozzle (π_n)	0.99
14	Efficiency of burner or combustor (η_b)	0.99
15	Mechanical efficiency of high-pressure turbine (η_{mH})	0.99
16	Mechanical efficiency of low-pressure turbine (η_{mH})	0.99
17	Efficiency of propeller (η_{prop})	0.83
18	Efficiency of gear-reduction box (η_{gr})	0.99
19	Turbine inlet temperature (T_{t4})	1370 K

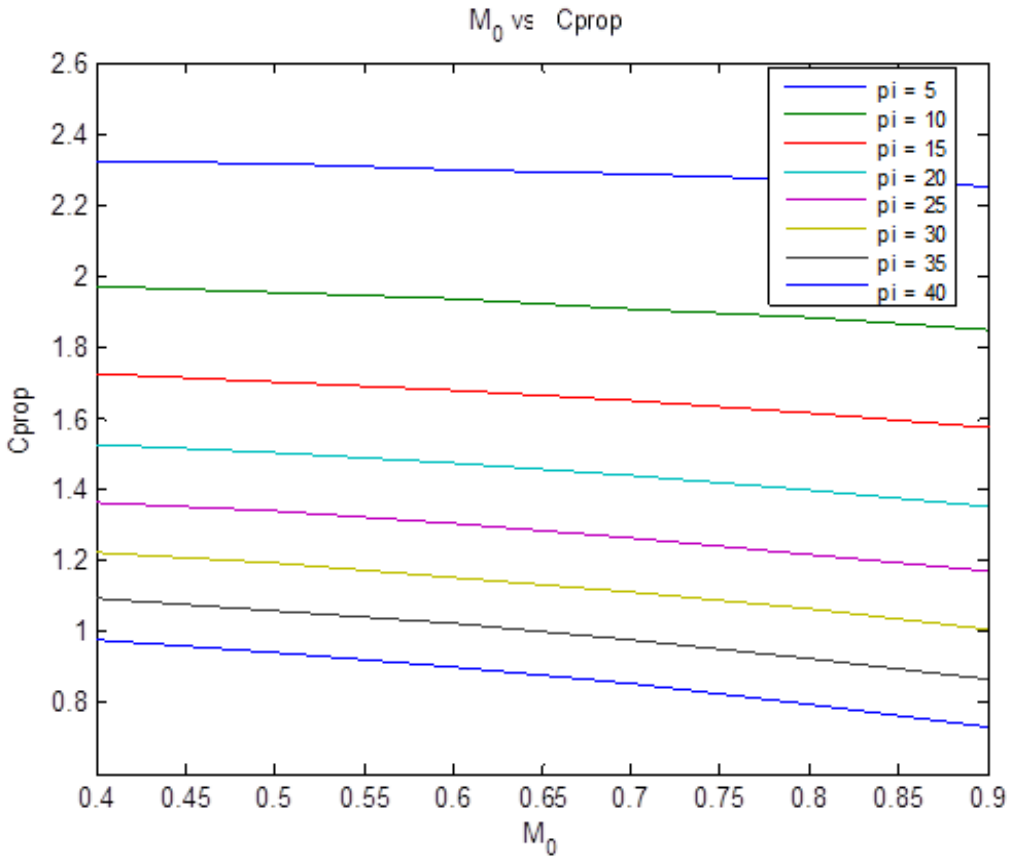

Fig 4.1 Variation of the work output co-efficient (C_{prop}) of propeller with (M_0) at varying compressor pressure ratios

From fig 4.1 it has been observed that the value of the work output co-efficient of propeller decreases on increasing the compressor pressure ratio (π_c) for a given Mach number. It is due to fact that, on increasing the compressor pressure ratio, the temperature ratio of compressor (τ_c) also increases and therefore fuel air ratio decreases. Due to decrease in fuel air ratio, the work output co-efficient of propeller also decreases. It also shows the value of work output co-efficient of propeller (C_{prop}) decreases on increasing the Mach number. Though, the rate of decrease is low at lower pressure ratio. This decrease in C_{prop} with the increase in Mach number is due to fact that the temperature ratio will increase with the increase of Mach number and hence the fuel air ratio will decrease.

Fig 4.2 shows the variation of work output core (C_c) with Mach number (M_0) for various compressor pressure ratios. It has been found that the value of C_c increases on increasing the compressor pressure ratios for a given Mach number. On the other hand, the decrease in work output co-efficient of core (C_c) for a pressure ratio of 25 or below

have been found for a fixed value of Mach no. Though there is an increase in work output co-efficient of core (C_c) for a pressure ratio of 25 beyond Mach number 0.6.

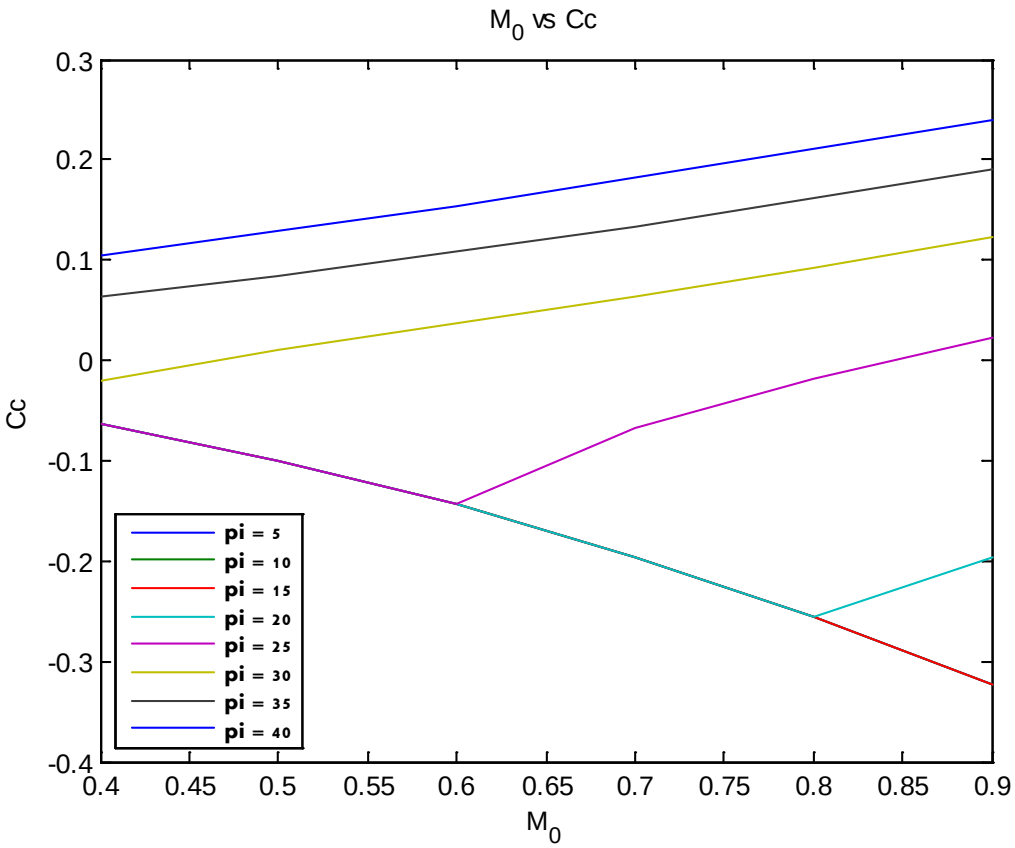

Fig 4.2 Variation of the work output of core (C_c) of propeller with (M_0) at varying compressor pressure ratios

The value of C_c is very low for pressure ratio below 25 and it cannot be considered for a turboprop engine. The fuel consumption increases on increasing the pressure ratio but absolute velocity of the engine will increase the value of C_c for a given value of Mach number. The Mach number is directly proportional to work output co-efficient of core (C_c). Therefore, the value of C_c increases on increasing the value of Mach number. So, moderate Mach no. and higher pressure ratio is available for a better work output co-efficient of core of turboprop engine.

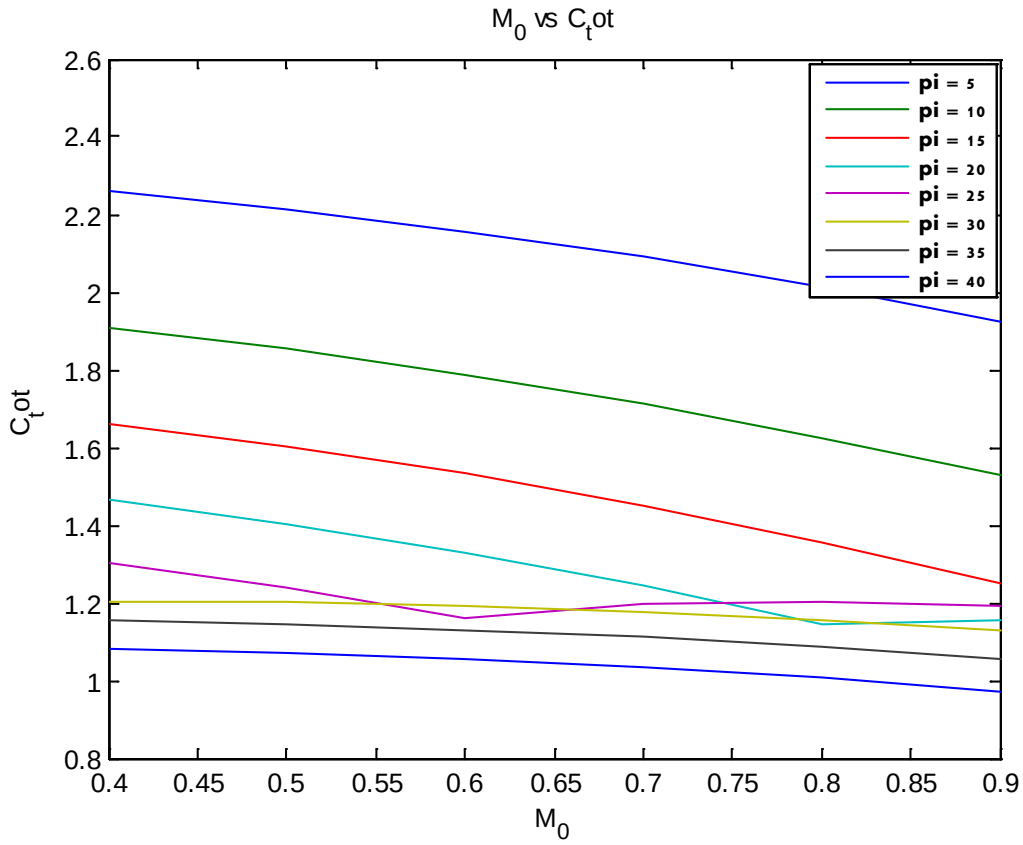

Fig 4.3 Variation of the total work output co-efficient (C_{tot}) of propeller with (M_0) at varying compressor pressure ratios

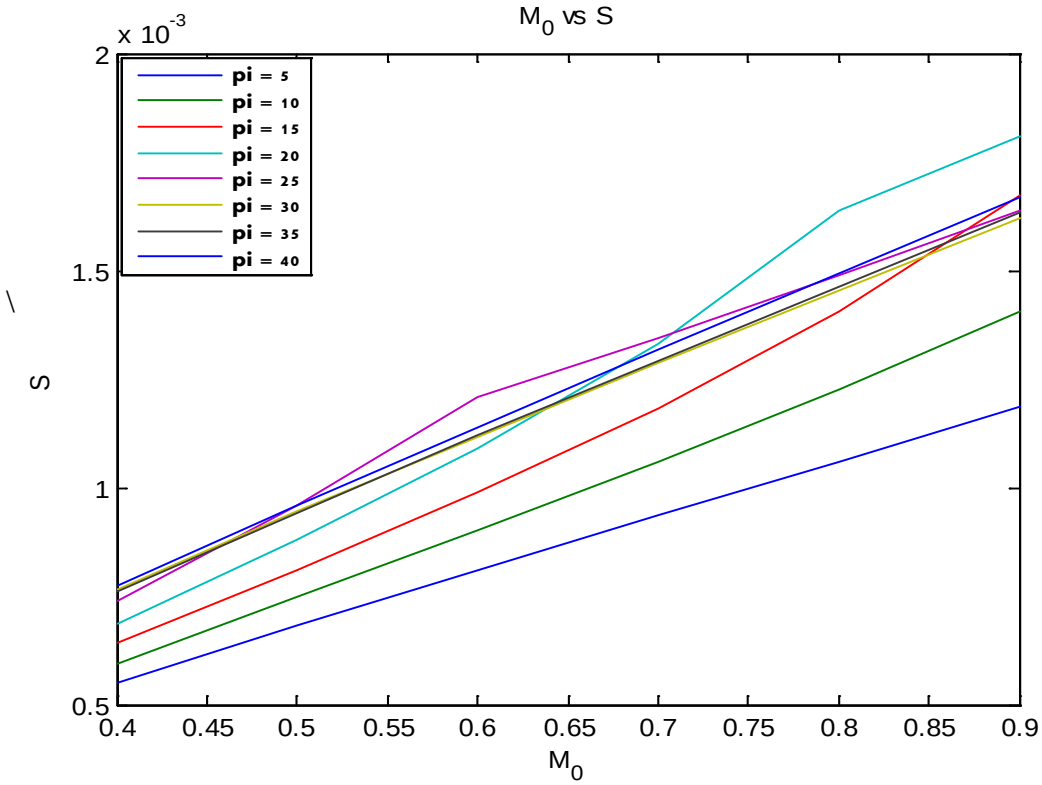

Fig 4.4 Variation of (S) of propeller with (M_0) at varying compressor pressure ratios

Fig 4.3 shows the variation of total work output co-efficient (C_{tot}) with Mach no. for different pressure ratio (π_c). The value of C_{tot} decreases with increase in Mach no. for a given pressure ratio. This is due to fact that on increasing the Mach number, the value of temperature ratio of compressor increases and hence fuel-air ratio decreases. There are two salient points in the figure where the value of C_{tot} increases on increasing the Mach no. above 0.6 at a compressor pressure ratio 25 and above Mach no. 0.8 at a pressure ratio 20. This may be the effect of work output co-efficient of core (C_c) which has absurd value below the pressure ratio 25. It has also been observed that the value of total work output co-efficient (C_{tot}) is higher for low pressure range.

Fig 4.4 represents the variation of S with Mach number for different compressor pressure ratio. The thrust specific fuel consumption, S increases on increasing the Mach no. for the same reason discussed in the above paragraph. It has been observed that the uninstalled specific fuel consumption is very high for pressure ratio ranging between (20 – 25) for Mach no. beyond 0.6 but it has an optimum value for compressor pressure ratio ranging between 30 and 40.

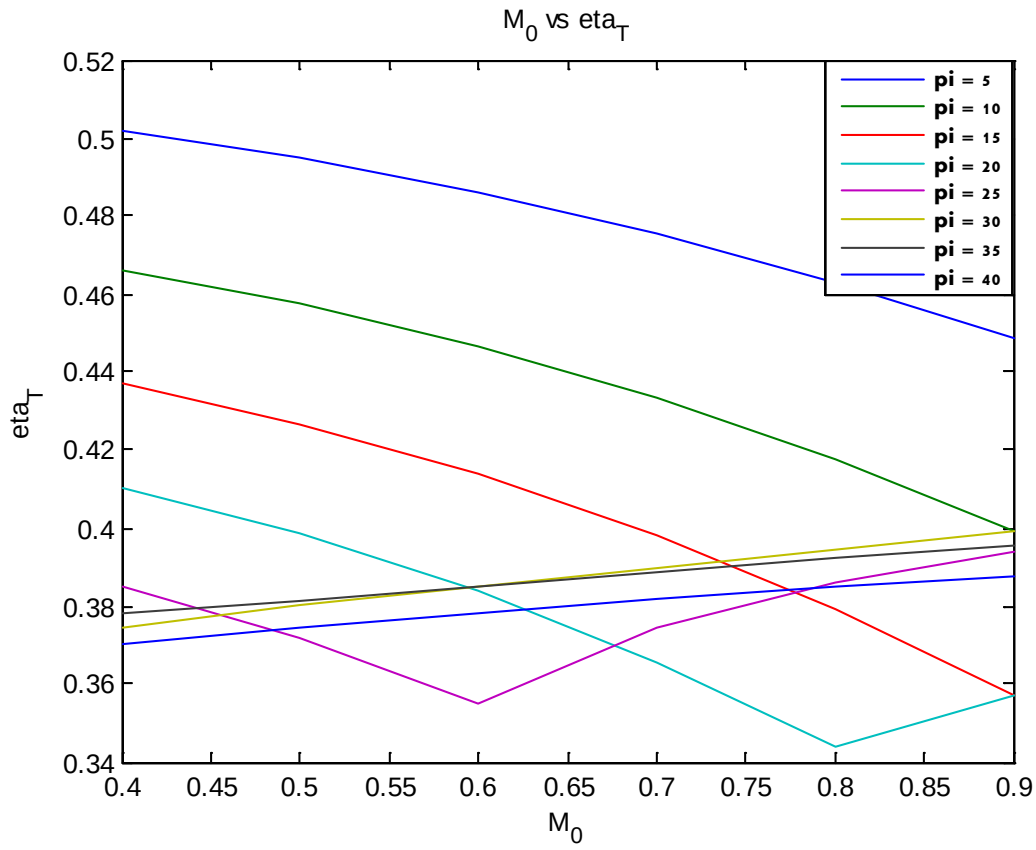

Fig 4.5 Variation of the thermal efficiency (η_T) with (M_0) at varying compressor pressure ratios

Fig 4.5 reveals that the thermal efficiency decreases on increasing the Mach number for a particular pressure though the efficiency increases for a pressure beyond 30. On increasing the Mach number, the fuel-air ratio decreases and the work output co-efficient of propeller (C_{prop}) also decreases. Therefore, thermal efficiency decreases but the thermal efficiency increases on increasing the Mach number for higher range of pressure ratios due to increase in core work output co-efficient (C_c).

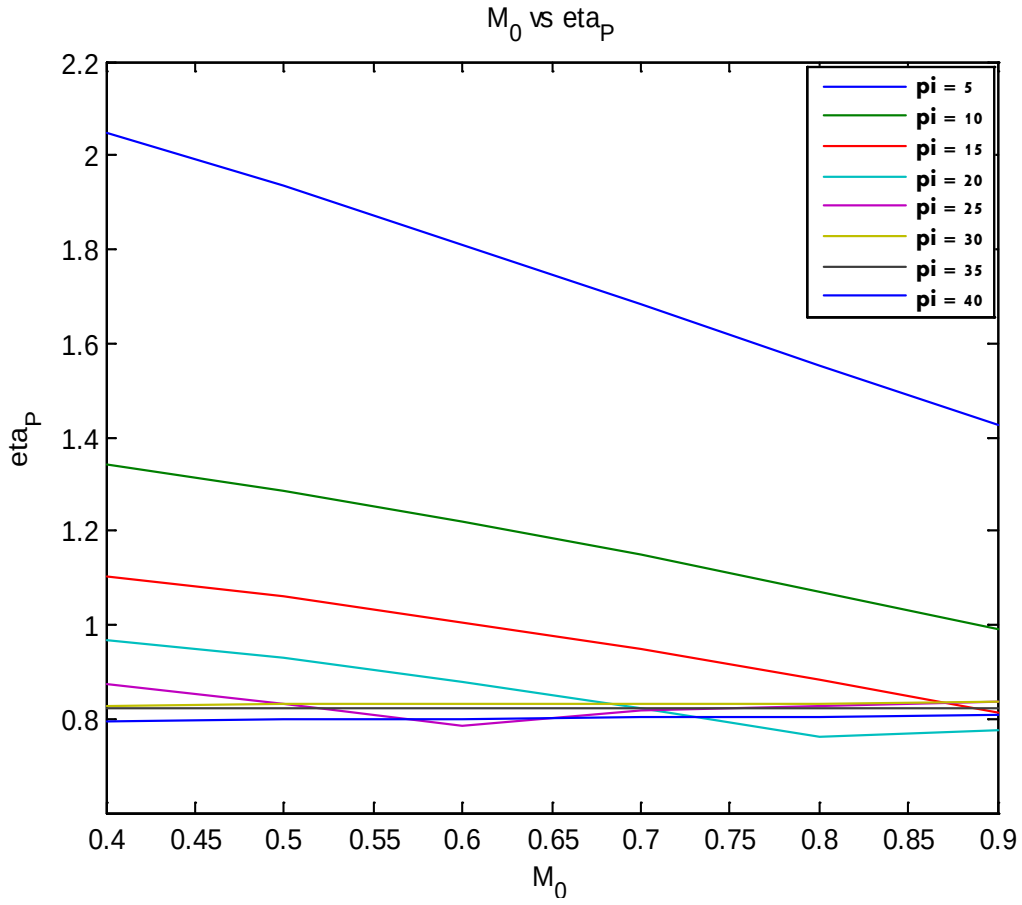

Fig 4.6 Variation of the propulsive efficiency (η_p) with Mach number (M_0) at varying compressor pressure ratios

Fig 4.6 represents the variation of propulsive efficiency (η_p) with Mach no. for a moderate range of compressor pressure ratios. It has been observed that the propulsive efficiency decreases on increasing the Mach no. for a given pressure ratio. Though, the propulsive efficiency increases with increase in Mach no. for pressure ratio above 30. It is due to the fact that Mach number, work output co-efficient of core (C_c) increases and the work output co-efficient of propeller (C_{prop}) decreases. The propulsive efficiency (η_p) shows the relevant values for the pressure above 20. The pressure ratio below 20

gives the value of propulsive efficiency (η_p) unjustified. It may be due to less increase in temperature in the compressor.

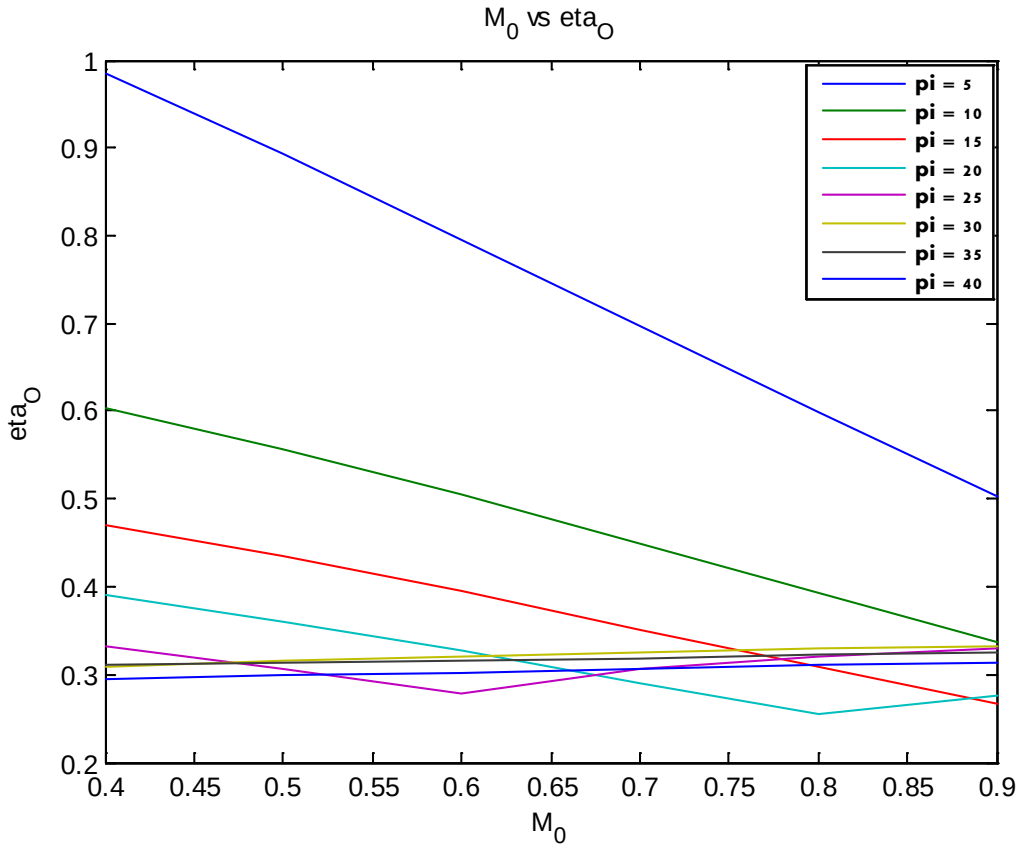

Fig 4.7 Variation of the overall efficiency (η_o) with Mach number (M_0) at varying compressor pressure ratios

Fig 4.7 represents the variation of the overall efficiency (η_o) with the Mach no. for different compressor pressure ratio. It is appeared from the figure that the overall efficiency (η_o) decreases on increasing the Mach number for low range of pressure ratio i.e. upon 20 while above compressor pressure ratio 20, the overall efficiency (η_o) increases on increasing the Mach number. It is due to fact that propulsive efficiency (η_p) and thermal efficiency (η_T) both decreases on increasing the compressor pressure ratios.

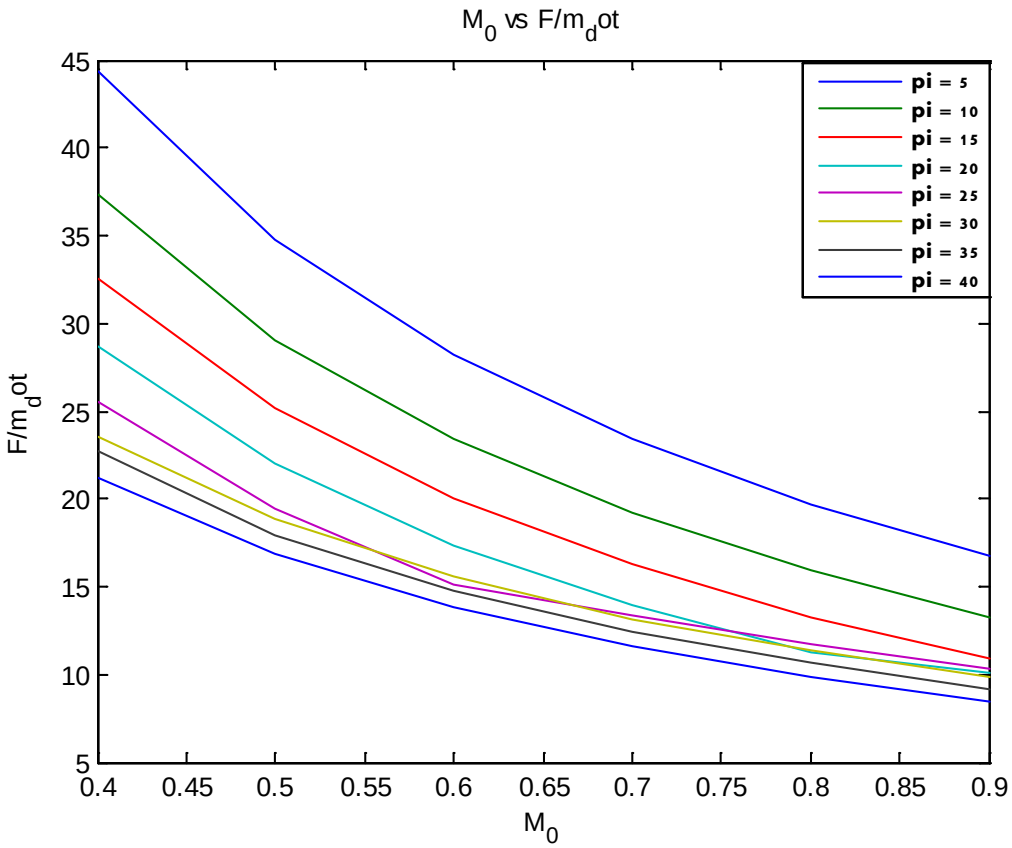

Fig 4.8 Variation of specific thrust ($F/\dot{m}_o$) with Mach number (M_0) at varying compressor pressure ratios

Fig 4.8 shows the variation of specific thrust per unit mass flow rate ($F/\dot{m}_o$) with Mach no. for various compressor pressure ratios. It has been observed that the thrust decreases on increasing the Mach number. This is due to fact that the increase in Mach no. will also increase the absolute velocity of engine. Therefore, there is decrease in specific thrust. It has also been observed from the figure that the specific thrust per unit mass flow rate decreases on increasing the compressor pressure ratio for a given Mach number. This may be the effect of increase in fuel-air ratio due to increase in pressure.

Fig 4.9 represents the variation of work output co-efficient of propeller (C_{prop}) with turbine inlet temperature or burner exit temperature for different compressor pressure ratios (π_c). The figure shows that there is an increase in work output co-efficient of propeller on increasing the burner exit temperature gradually for a fixed compressor pressure ratio. This is due to fact that the burner exit temperature leaves the increase in propeller work output co-efficient. The figure also represents that the value of work output co-efficient of propeller decreases on increasing the pressure ratio for a given burner exit temperature. It is due to the increase in enthalpy ratio with increase in

compressor pressure ratio. The increase in compressor pressure ratio results in higher output temperature of compressor and hence the fuel requirement in the burner is low. So, the turbine output for the propeller will also be increased.

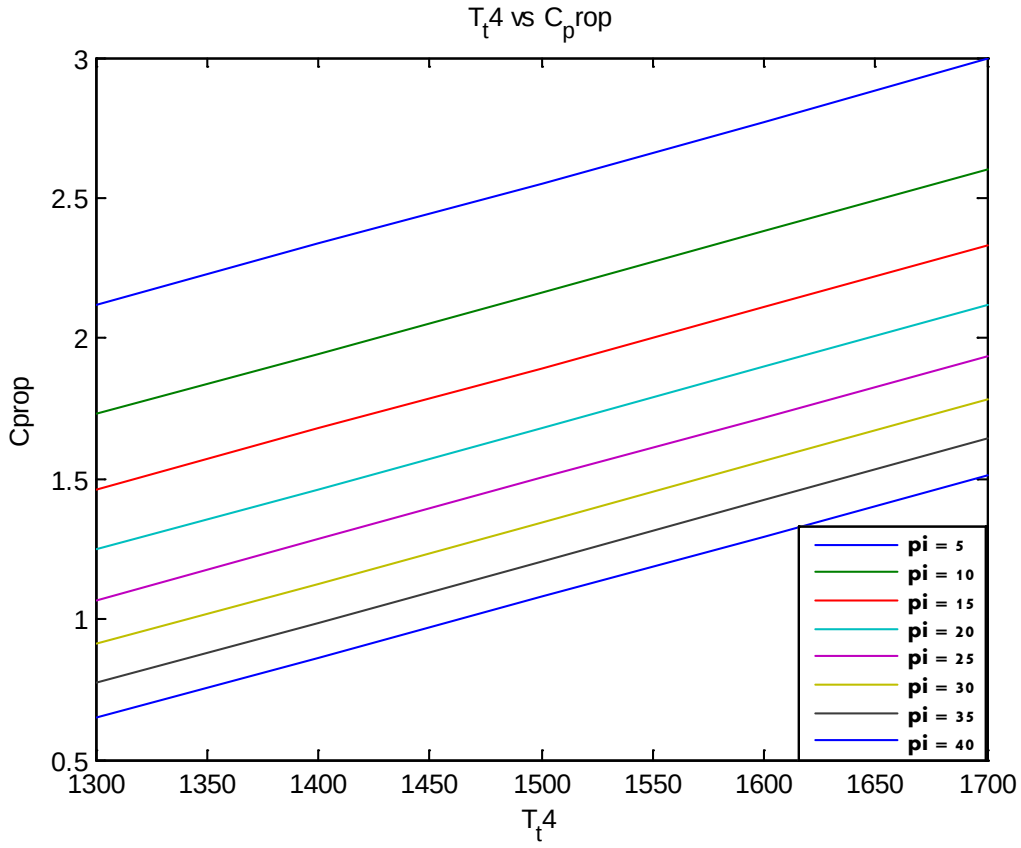

Fig 4.9 Variation of the workoutput co-efficient of propeller (C_{prop}) with turbine inlet temperature (T_{t4}) at varying compressor pressure ratios

Fig 4.10 shows the variation of work output co-efficient of core (C_c) with T_{t4} for various compressor pressure ratios. It has been observed from the figure that the work output co-efficient of core increases on increasing the compressor pressure ratio (π_c) for a given value of T_{t4}. This is due to the fact that the increase in compressor pressure ratio will also increase the exit pressure of compressor so that the fuel consumption decreases. Also, the increase in T_{t4} will require more fuel-air ratio if the pressure at the end of compression is kept constant. Though, the figure reflects that the work output co-efficient of core is considerable for the pressure ratio above 25. The results for the pressure below 25 are absurd. This may be the effect of very low compression and the minimum required pressure of air at the end of compression.

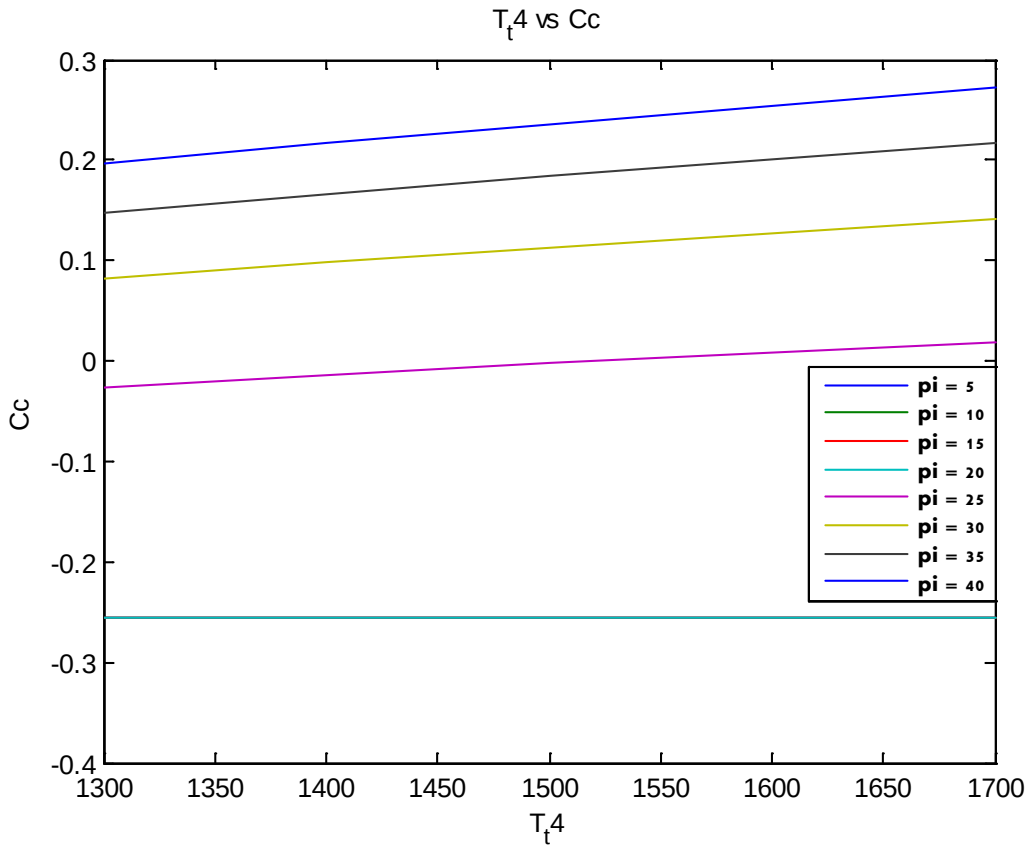

Fig 4.10 Variation of (C_c) with (T_{t4}) at varying compressor pressure ratios

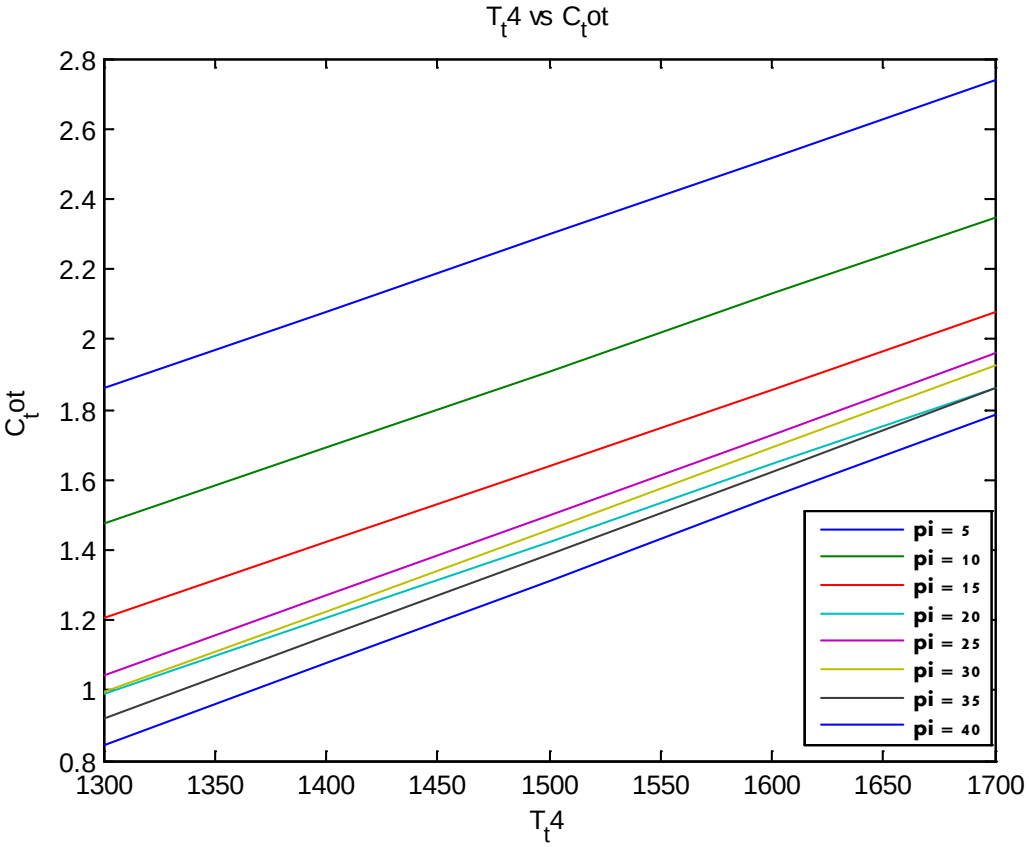

Fig 4.11 Variation of the total workoutput co-efficient (C_{tot}) with turbine inlet temperature (T_{t4}) at varying compressor pressure ratios

Fig 4.11 represents the variation of total work output co-efficient (C_{tot}) with T_{t4} for different compressor pressure ratio. It is shown from the figure that the value of total work output co-efficient increases on increasing the T_{t4} for a given value of pressure ratio but at the same time the total work output co-efficient decreases on increasing the compressor pressure ratio for a given T_{t4}. Though, total work output co-efficient gives the better result at compressor pressure ratio 25 as compared to higher compressor pressure ratio. As we know that total work output co-efficient (C_{tot}) is the sum of work output co-efficient of core (C_c) and work output co-efficient of propeller (C_{prop}). Therefore, increase in T_{t4} will also increase the work output of turbines and hence the total work output co-efficient increases.

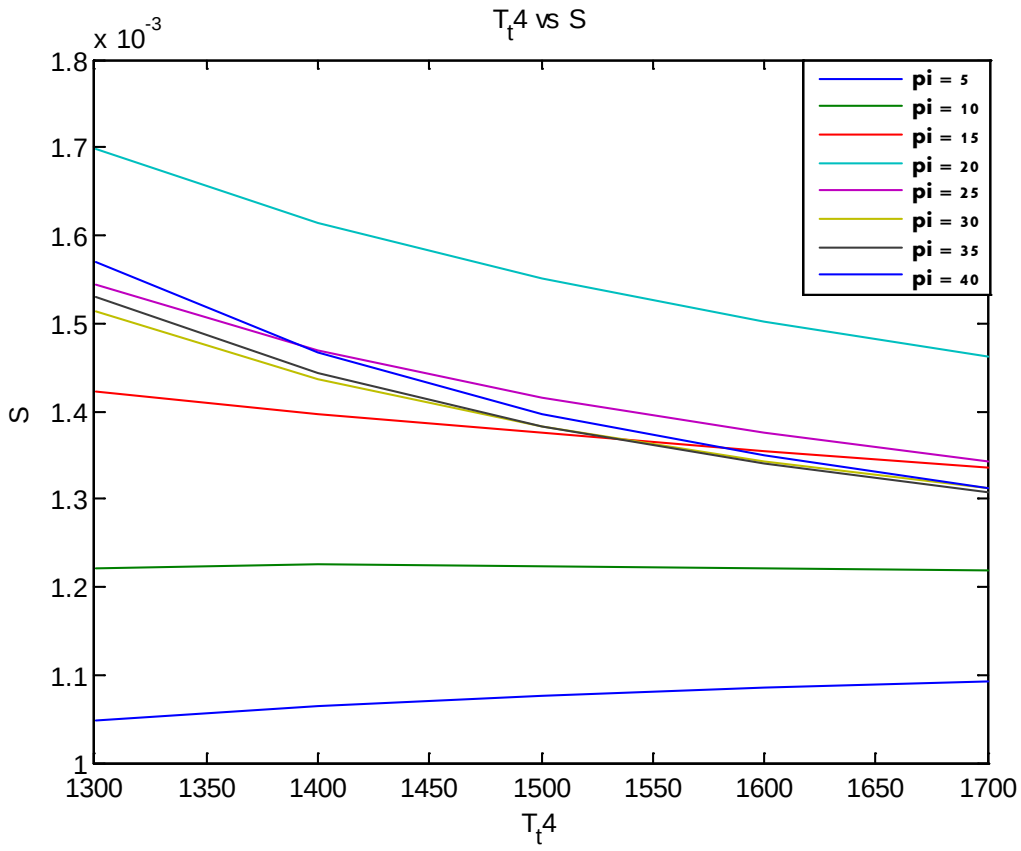

Fig 4.12 Variation of (S) with (T_{t4}) at varying compressor pressure ratios

Fig 4.12 represents the variation of uninstalled thrust specific fuel consumption (S) with T_{t4} for different compressor pressure ratios. The value of S decreases on increasing the T_{t4} for a given compressor pressure ratio. On the other hand, it increases on increasing the compressor pressure ratio for a given T_{t4}. This may be the effect of compression

ratio. As we know that, S is the fuel consumption per unit thrust developed. So, increase in T_{t4} will definitely increase the uninstalled thrust specific fuel consumption.

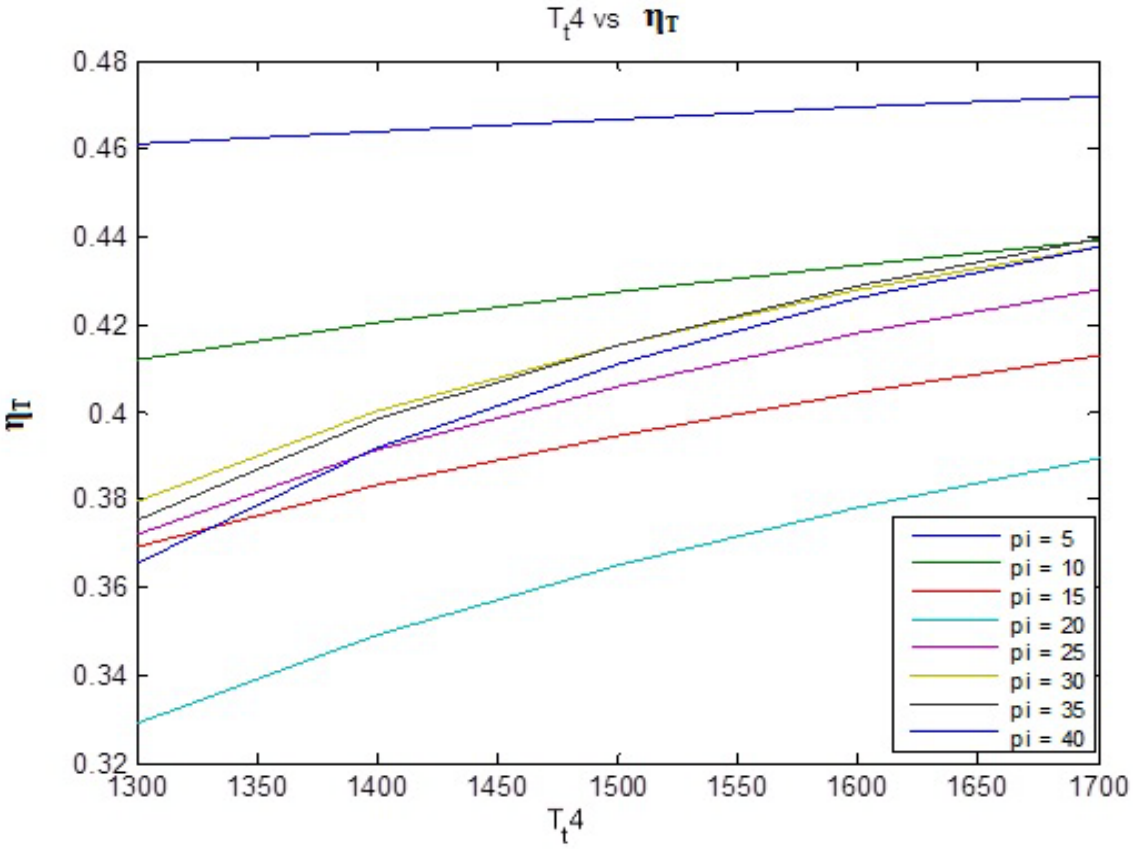

Fig 4.13 Variation of thermal efficiency (η_T) with turbine inlet temperature (T_{t4}) at varying compressor pressure ratios

Fig 4.13 represents the variation of thermal efficiency (η_T) with T_{t4} for various compressor pressure ratios. It is found that the propulsive efficiency increases on increasing the burner exit temperature at a given compressor pressure ratio. This is due to fact that increase in burner exit temperature will increase the fuel-air ratio but the total work output co-efficient also increases rapidly which in turn will result in increase in propulsive efficiency. Though, the value of propulsive efficiency is very high at very low compressor pressure ratio but low compressor pressure ratio will affect the work output of compressor.

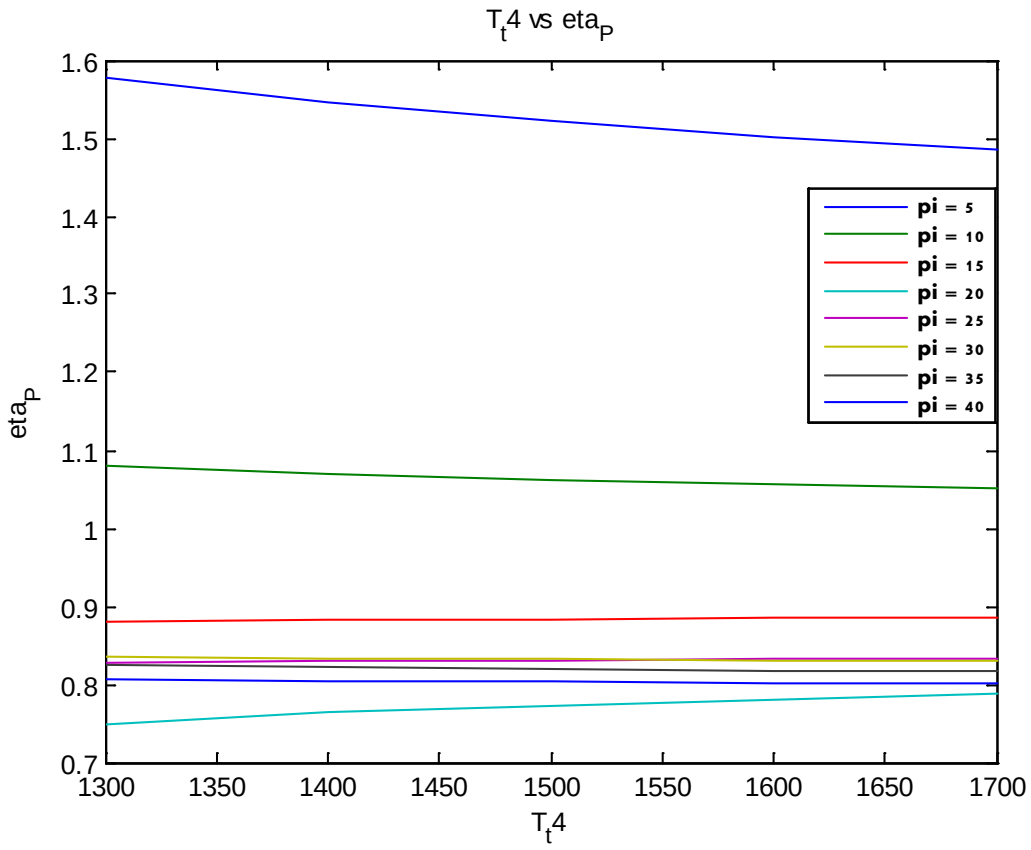

Fig 4.14 Variation of the propulsive efficiency (η_p) with turbine inlet temperature (T_{t4}) at varying compressor pressure ratios

Fig 4.14 represents the variation of propulsive efficiency (η_p) with T_{t4} for different compressor pressure ratio. The propulsive efficiency (η_p) shows the variation in a limited range with increase in T_{t4}. It is due to the fact that the propeller is running with a separate turbine and the pressure ratio effect is very less on the propulsive efficiency.

Fig 4.15 shows the variation of overall efficiency (η_O) with T_{t4} for various compressor pressure ratios. It reveals that the overall efficiency of a turboprop engine varies between 29-32% for the moderate range of pressure ratio. Though, it gives the maximum value for a very low pressure but the drawback of very low compressor pressure ratio is the work developed in high pressure turbine is very low.

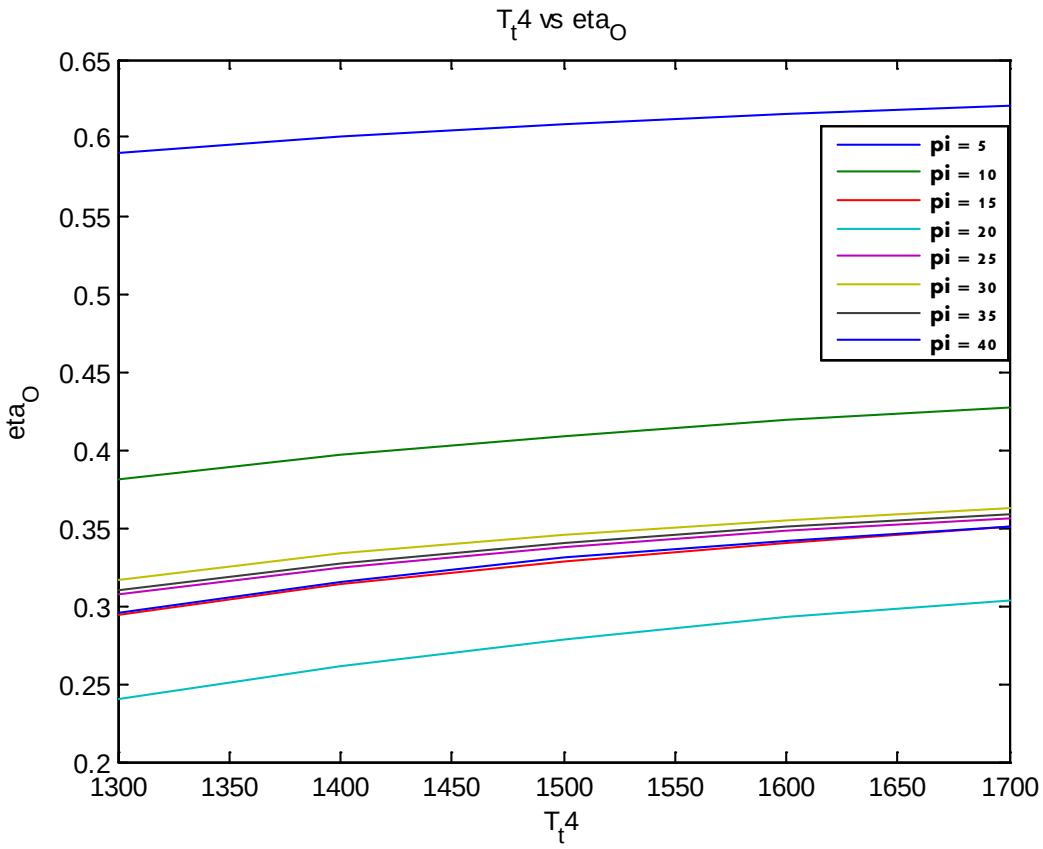

Fig 4.15 Variation of (η_O) with (T_{t4}) at varying compressor pressure ratios

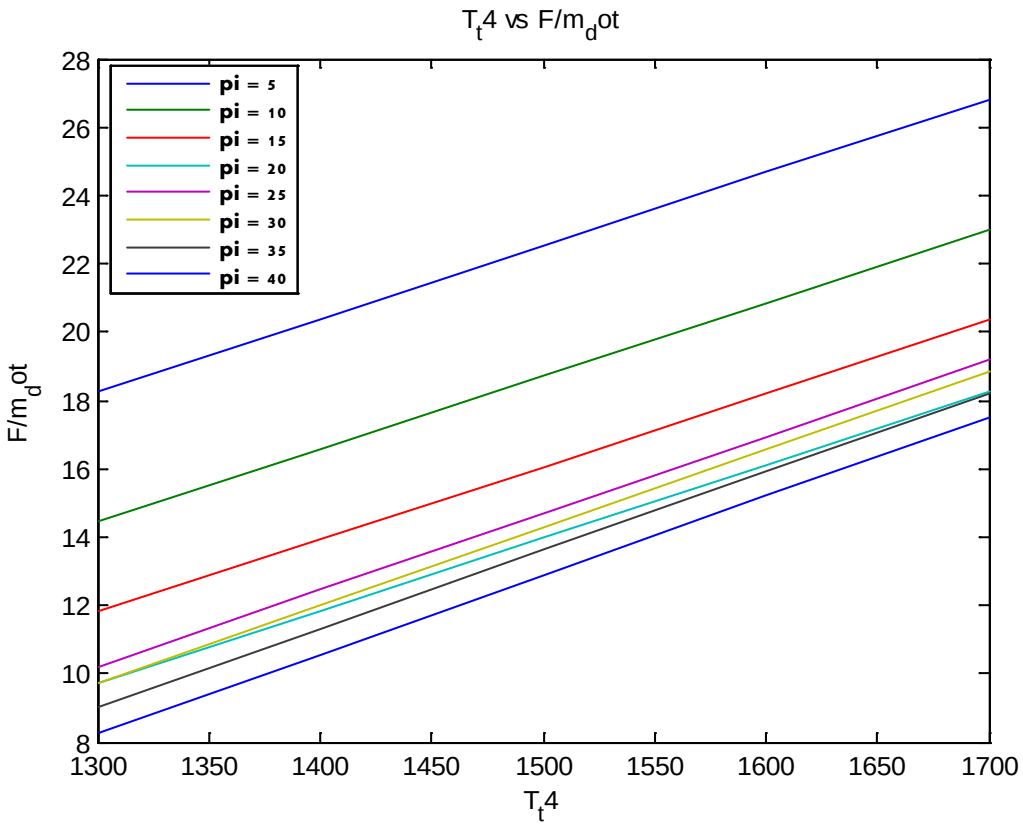

Fig 4.16 Variation of specific thrust ($F/\dot{m}_0$) with turbine inlet temperature (T_{t4}) at varying compressor pressure ratios

Fig 4.16 shows the variation of specific thrust ($F/\dot{m}_0$) with T_{t4} for different compressor pressure ratios. The specific thrust ($F/\dot{m}_0$) increases on increasing the T_{t4} at a particular pressure ratio. At the same time it has also been observed that the specific thrust decreases on increasing the compressor pressure ratio for a fixed value of T_{t4}. This is due to the fact that the increase in T_{t4} will increase in the total work output co-efficient (C_{tot}) and so on specific thrust. Since, in a turboprop engine at a certain height the temperature of air is fixed but uninstalled thrust can be increased with the increase in total work output co-efficient.

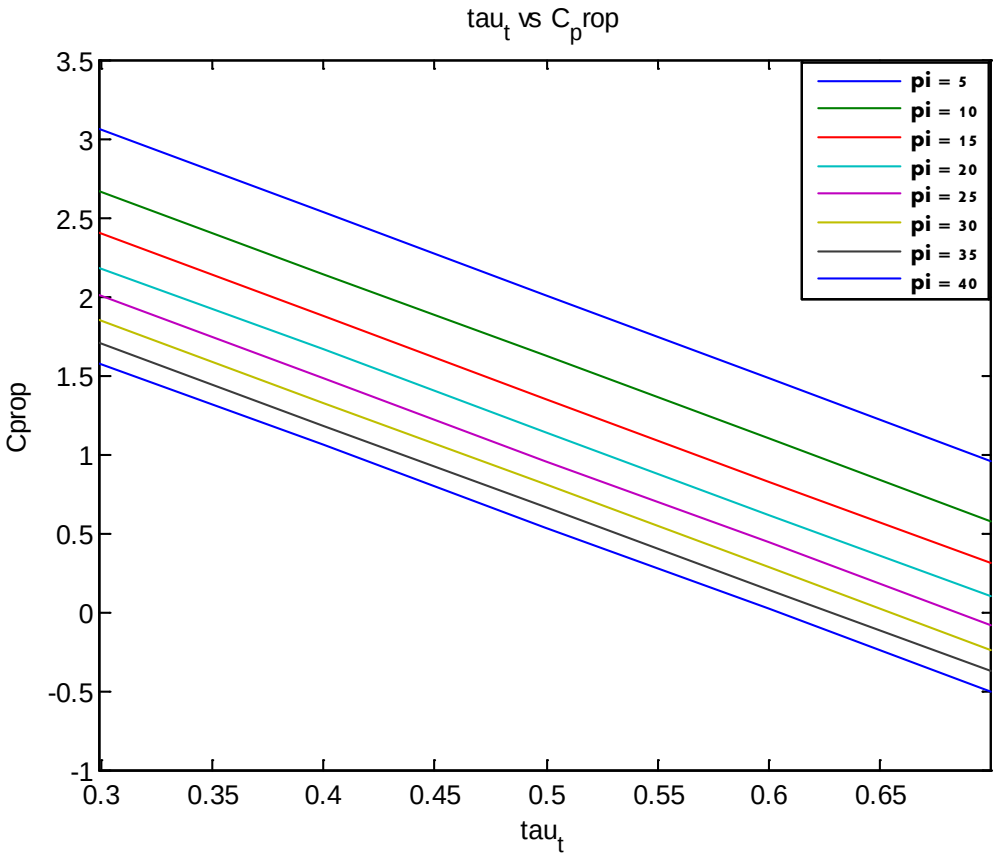

Fig 4.17 Variation of the work output co-efficient of propeller (C_{prop}) with turbine temperature ratio (τ_t) for various compressor pressure ratios

Fig 4.17 represents the variation of work output co-efficient of propeller (C_{prop}) with turbine temperature ratio (τ_t) for various compressor pressure ratios. It is found that work output co-efficient of propeller decreases with increase in turbine temperature ratio for a given value of compressor pressure ratio. The reason behind the work output co-efficient of propeller downfall on increasing the turbine temperature ratio at a given pressure ratio develops the power in the turbine which in turn the output of turbine also

reduces. On the other hand, the high pressure ratio gives the low value of work output co-efficient of propeller due to decrease in temperature ratio of compressor.

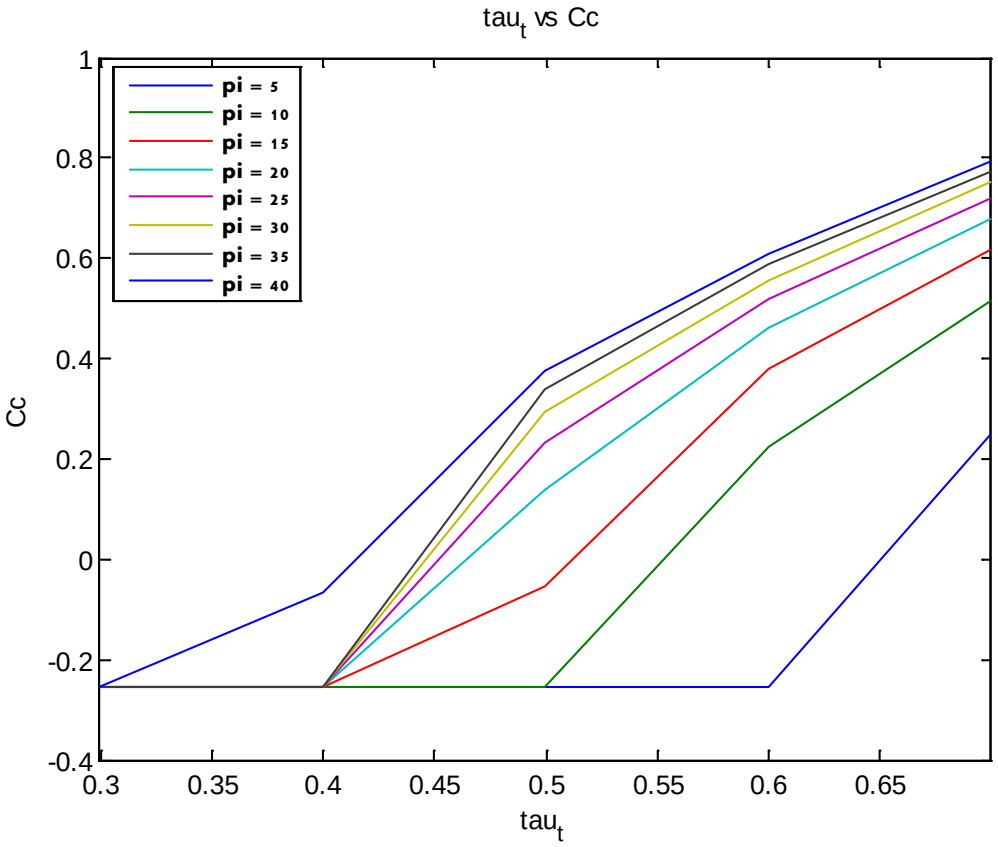

Fig 4.18 Variation of the work output co-efficient of core (C_c) with turbine temperature ratio (τ_t) for various compressor pressure ratios

Fig 4.18 shows the result of work output co-efficient of core (C_c) with the turbine temperature ratio for different compressor pressure ratio. The value of work output co-efficient of core increases on increasing the turbine temperature ratio (τ_t) for the entire range of compressor pressure ratios. Though, the value of work output co-efficient of core at very low pressure and low temperature ratio seems to be similar. This may be due to the design of compressor but for higher range of compressor pressure ratio (above 15) and an optimum range of turbine temperature ratio (> 0.4), work output co-efficient of core would give optimum values. This is due to fact that fuel-air ratio will increase on increasing the turbine temperature ratio for a given compressor pressure ratio.

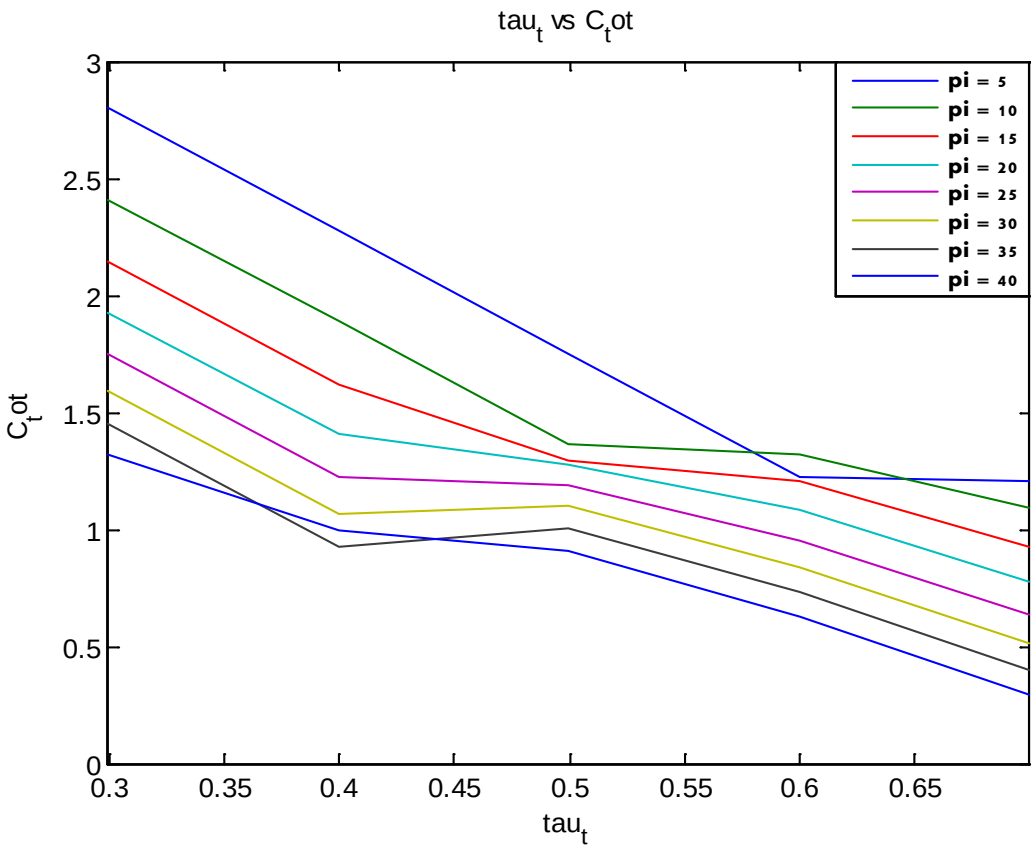

Fig4.19 Variation of the total work output co-efficient (C_{tot}) with turbine temperature ratio (τ_t) for various compressor pressure ratios

Fig 4.19 represents the total work output co-efficient (C_{tot}) with turbine temperature ratio for various compressor pressure ratio. It appears from the figure that the total work output co-efficient decreases on increasing the turbine temperature ratio for almost entire range of pressure ratios. At low pressure ratio and low turbine temperature ratio, it gives the higher values but as long as we go to the lower compressor pressure ratio and turbine temperature ratio, it gives low value. Apart from that, in the middle range of turbine temperature ratio (0.4-0.6), the total work output co-efficient shows the better value.

Fig 4.20 represents the variation of thrust specific fuel consumption (S) with turbine temperature ratio for different compressor pressure ratios. It has been observed from the figure that thrust specific fuel consumption increases on increasing the turbine temperature ratio. The increase in thrust specific fuel consumption on increasing the turbine temperature ratio is due to increase in fuel requirement by the burner. It means that the burner exit temperature increases and turbine exit temperature kept constant.

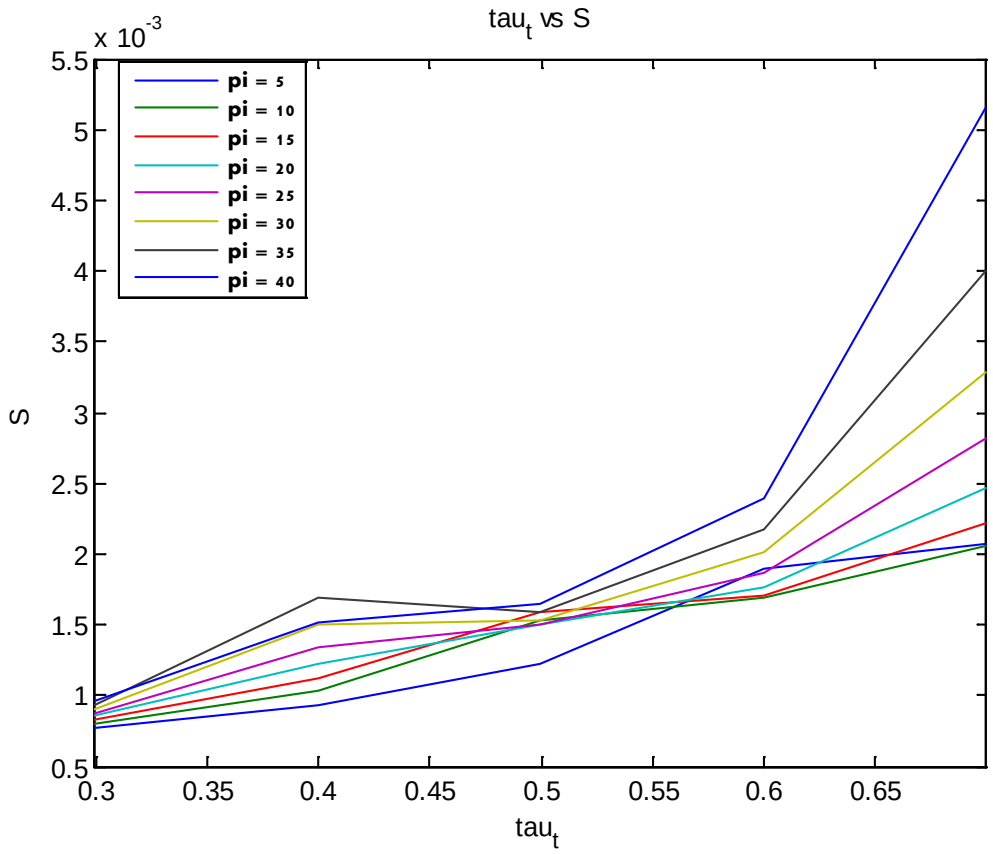

Fig 4.20 Variation of (S) with (τ_t) for various compressor pressure ratios

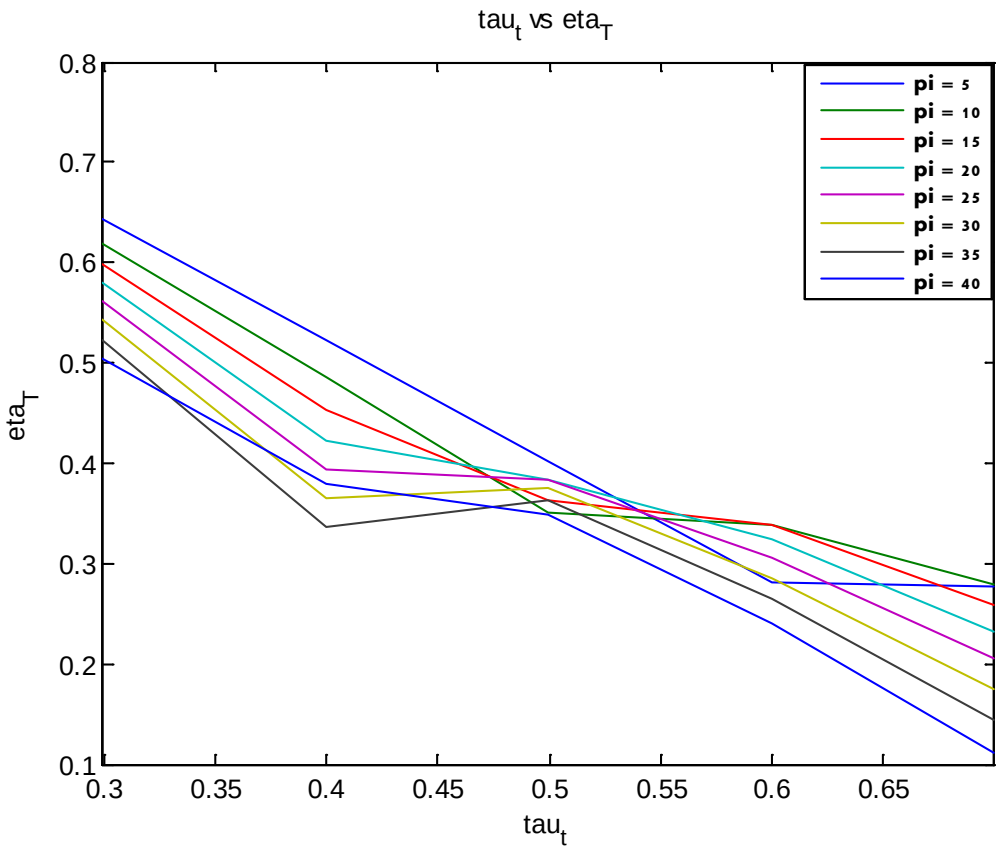

Fig 4.21Variation of (η_T) with (τ_t) for different compressor pressure ratios

Fig 4.21 represents the variation of thermal efficiency (η_T) of a turboprop engine with turbine temperature ratio for different compressor pressure ratio. The thermal efficiency decreases on increasing the turbine temperature ratio. This is due to the fact that the increase in turbine temperature ratio will result in increase in fuel consumption and decrease in power output. In turn it would reduce the thermal efficiency. Though, thermal efficiency has increased at different compressor pressure ratio for turbine temperature (0.4-0.5) but it is only at moderate pressure range of 25-30.

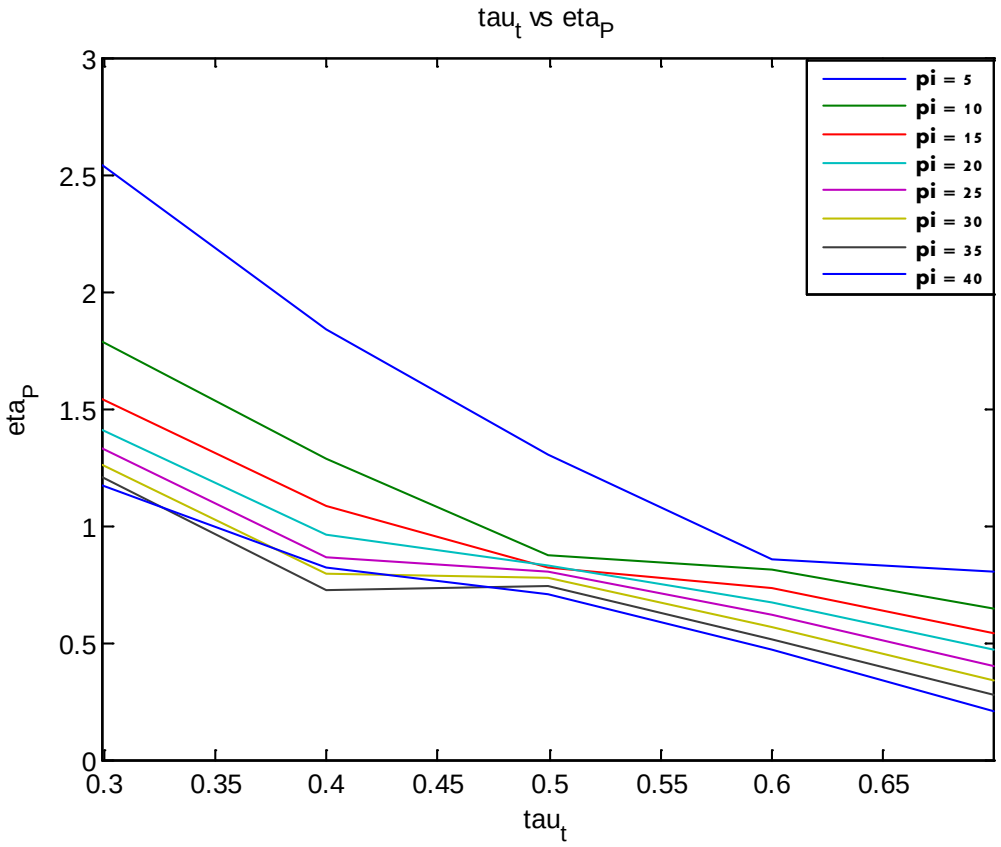

Fig 4.22 Variation of propulsive efficiency (η_p) with turbine temperature (τ_t) for different compressor pressure ratios

Fig 4.22 shows the variation of propulsive efficiency with turbine temperature for different compressor pressure ratio. The propulsive efficiency (η_p) shows the virtual value at very low pressure ratio and at very low turbine temperature ratio. It seems to be that the propulsive efficiency increases slightly on increasing the turbine temperature ratio for the range of 0.4-0.5 at higher pressure ratios (25-40). This is due to fact that the increase in turbine temperature would decrease in the turbine expansion ratio and as such propulsive efficiency decreases.

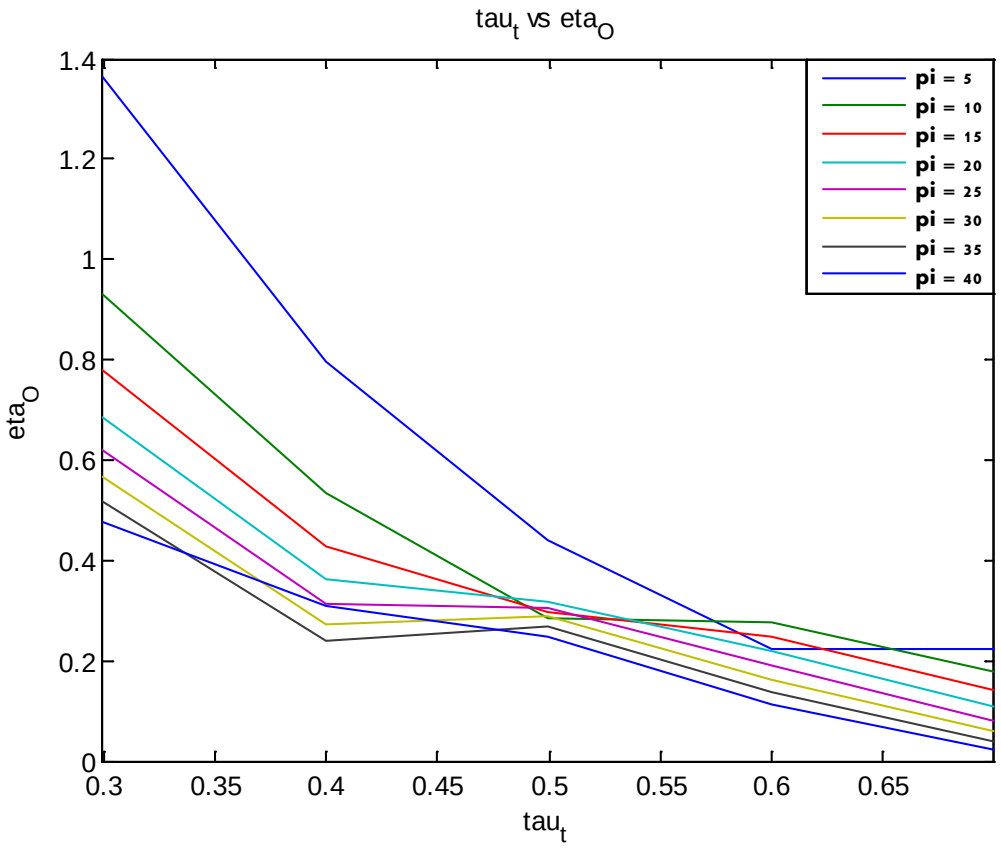

Fig 4.23 Variation of overall efficiency (η_O) with turbine temperature (τ_t) for different compressor pressure ratios

Fig 4.23 represents the variation of overall efficiency (η_O) with turbine temperature ratio for different compressor pressure ratios. Since, the overall efficiency is the sum of the propulsive efficiency (η_p) and thermal efficiency (η_T) and in the last two figures. The propulsive efficiency and thermal efficiency decreases on increasing the turbine temperature ratio. Therefore, the overall efficiency will also decrease with the decrease in turbine temperature ratio for the same reason in the preceding paragraphs.

Fig 4.24 shows the variation of specific thrust ($F/\dot{m}_0$) with turbine temperature ratio at various compressor pressure ratios. The specific thrust decreases on increasing the turbine temperature ratio for a given compressor pressure ratio. This is due to fact that the work output of free turbine decreases on increasing the turbine temperature ratio which in turn results in decrease in specific thrust. It also appears that the turbine temperature ratio has optimum value for the range (0.4-0.5). In this range, the specific thrust increases a little bit for pressure range above 25.

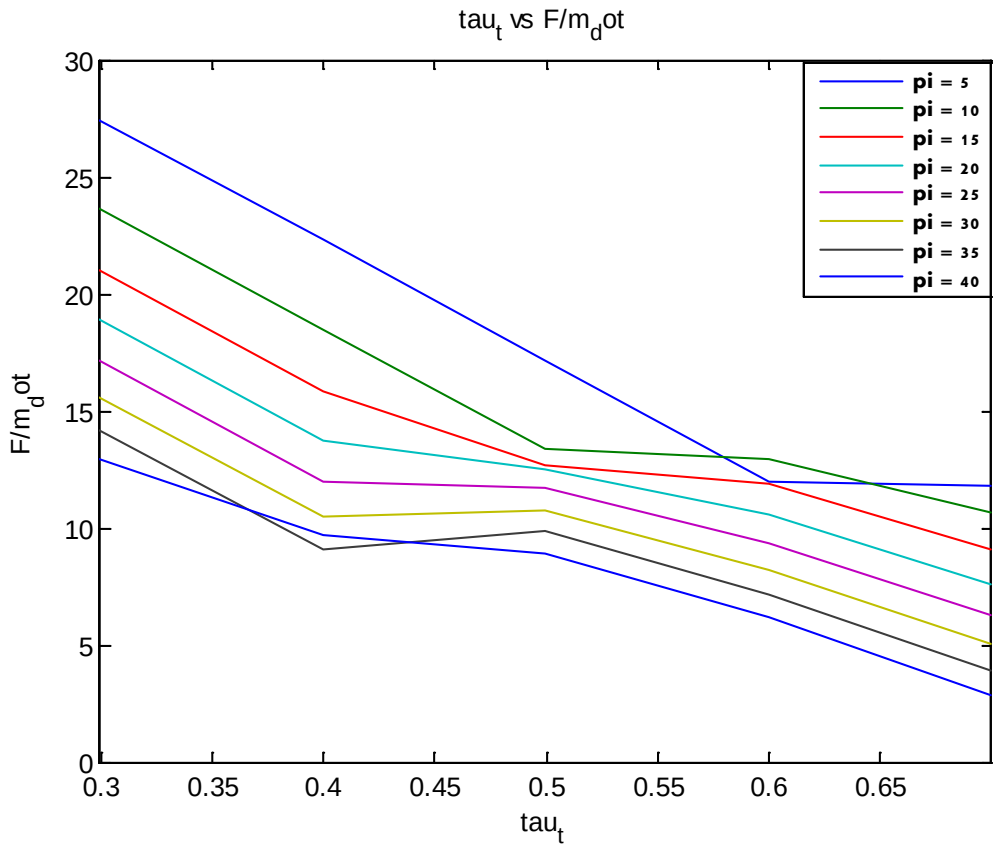

Fig 4.24 Variation of ($F/\dot{m}_0$) with (τ_t) for different compressor pressure ratios

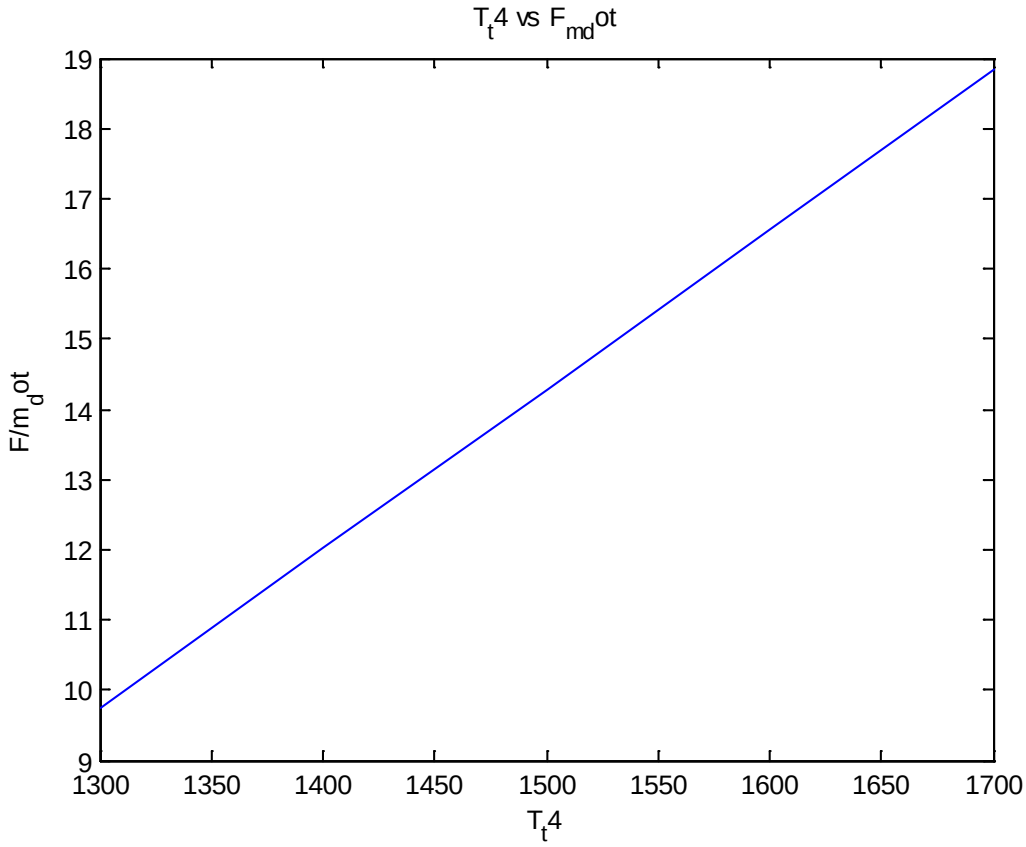

Fig 4.25 Variation of specific thrust ($F/\dot{m}_0$) at varying compressor pressure ratios

Fig 4.25 shows the variation of specific thrust with compressor pressure ratio for a given value of Mach number and burner exit temperature. The figure shows that the specific thrust ($F/\dot{m}_0$) decreases on increasing the compressor pressure ratio consistently from low to high pressure but for the range of compressor pressor ratio (20-25), it has increased slightly. It is due to the fact that on increasing the compressor pressor ratio, the temperature of compressed air will also increase and hence the fuel required into combustor will decrease. The work output co-efficient of propeller (C_{prop}) will decrease and therefore, the specific thrust ($F/\dot{m}_0$) will also decrease.

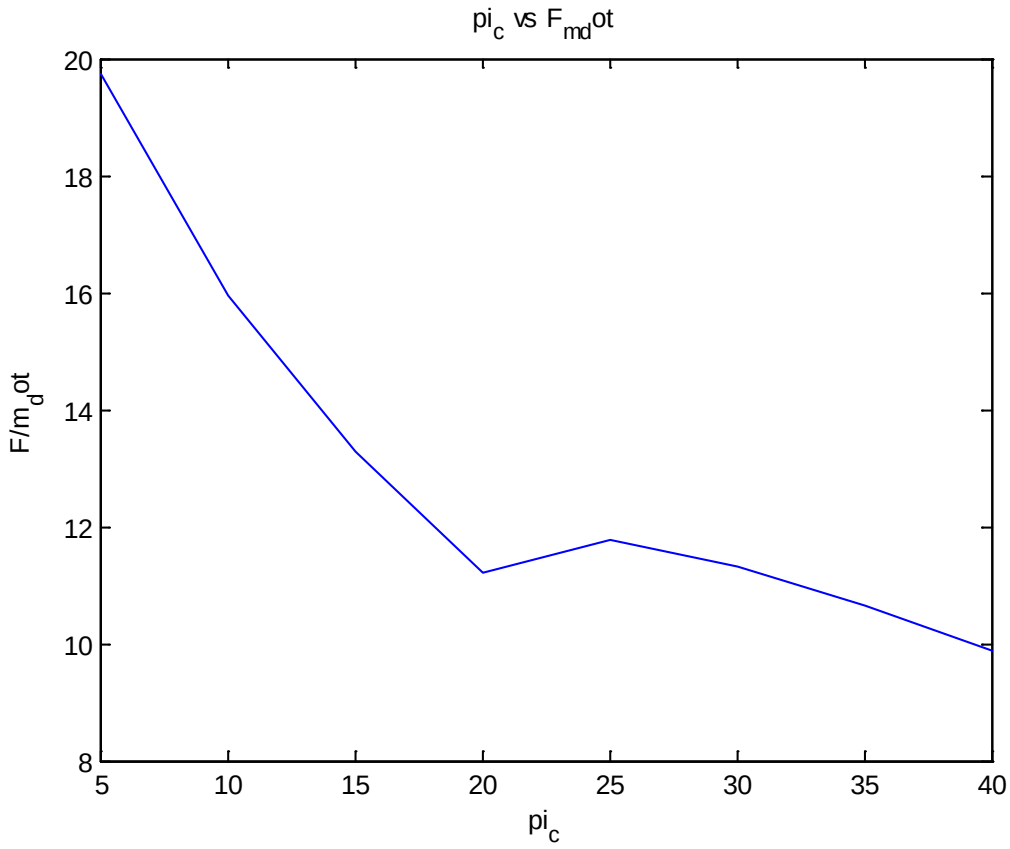

Fig 4.26 Variation of specific thrust ($F/\dot{m}_0$) with turbine inlet temperature (T_{t4}) for different compressor pressure ratios

Fig 4.26 represents the variation of the specific thrust ($F/\dot{m}_0$) with burner exit temperature for a fixed value of Mach number i.e. (0.8) and compressor pressure ratio 30. It has been observed from the figure that the specific thrust gradually increases with increase in T_{t4}. The increase in T_{t4} will require more fuel consumption in the burner. This increase in fuel consumption will result in increase in work output co-efficient of propeller (C_{prop}) and in turn the specific thrust will also be increased.

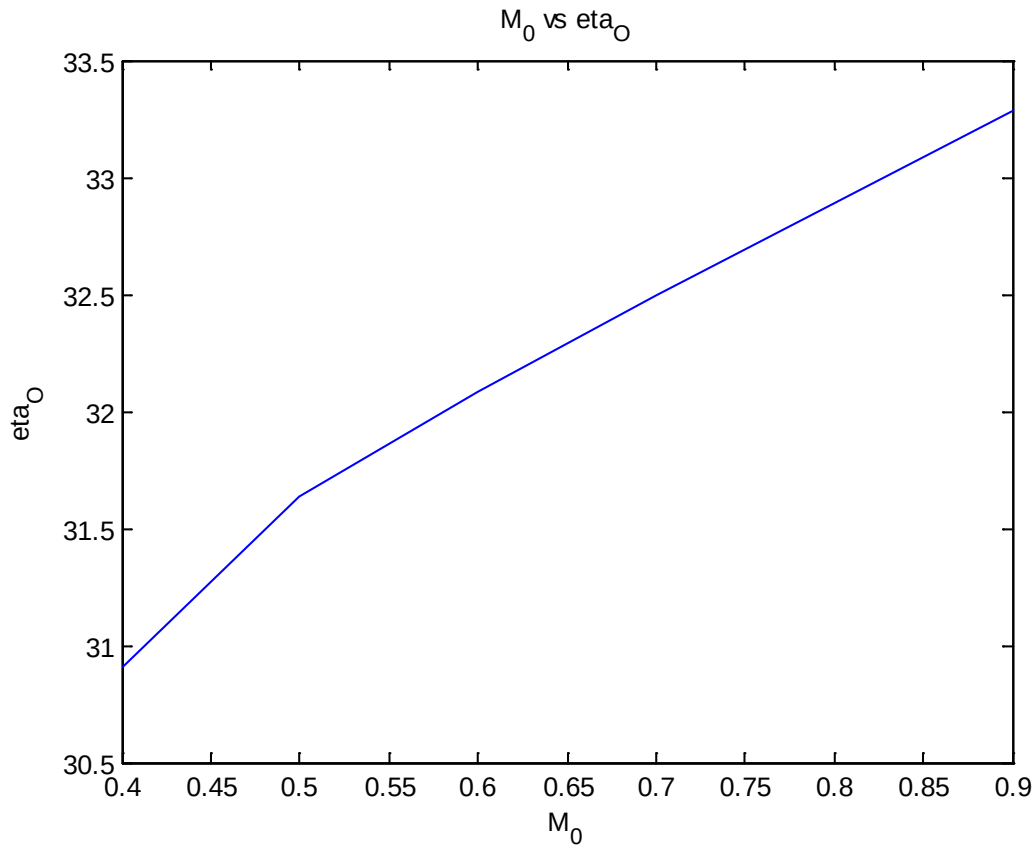

Fig 4.27 Variation of the overall efficiency (η_O) at varying Mach no. (M_0)

Fig. 4.27 shows the variation of the overall efficiency with the varying Mach no. for a given compressor pressure ratio (i.e., 30) and a fixed value of burner exit temperature (1370K). It is observed that the overall efficiency increases with the increase in Mach number.

Fig 4.28 represents the variation of the overall efficiency (η_O) with different compressor pressure ratio for a given value of Mach number (0.8) and burner exit temperature (1370 K). The overall efficiency shows the downtrend with the increase in compressor pressure ratio (up to 20) and hereafter, it increases (up to 30). Then, again it decreases but comparatively at low rate. This is due to the fact that the overall efficiency is the combination of propulsive efficiency (η_p) and thermal efficiency (η_T). Since, the propulsive efficiency decreases at very high rate as compared to thermal efficiency for pressure ratio (upto 20). Further increase in pressure will increase the thermal efficiency more than the propulsive efficiency and therefore, the overall efficiency increases beyond the compressor pressure ratio.

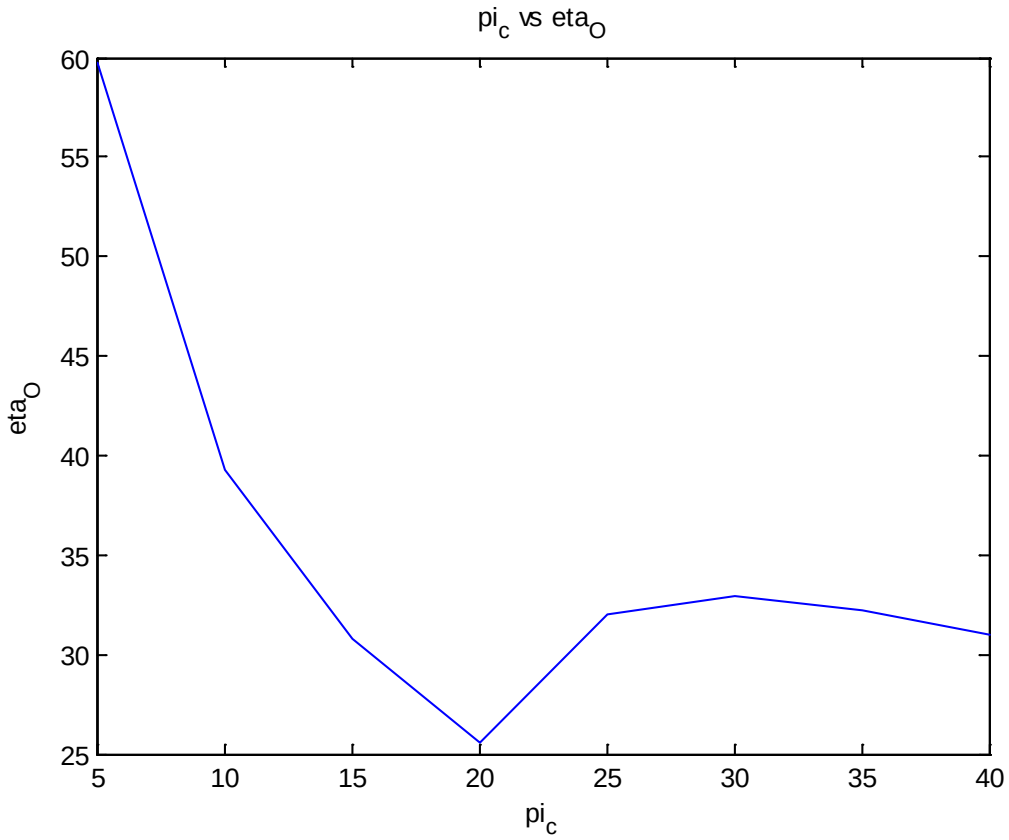

Fig 4.28Variation of (η_O) at varying compressor pressure ratios (π_c)

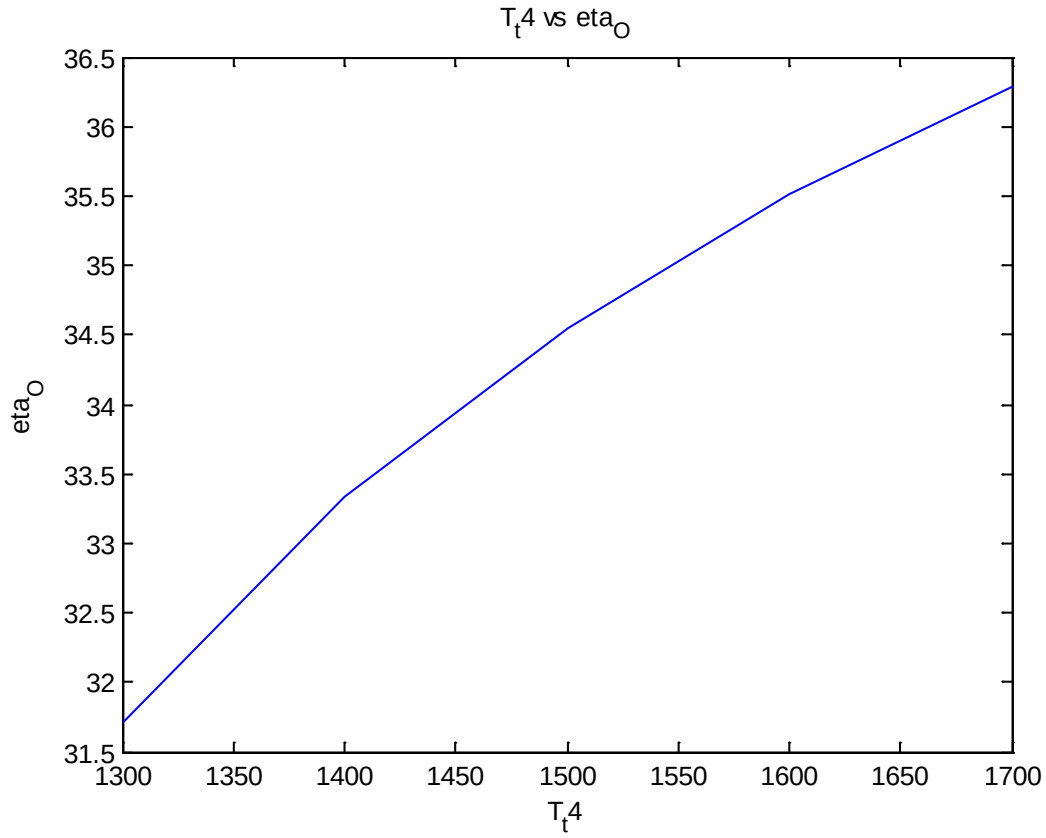

Fig 4.29 Variation of (η_O) at varying burner exit temperature (T_{t4})

Fig 4.29 shows the variation of overall efficiency with burner exit temperature for a given value of compressor pressure ratio and Mach number. The figure reflects the increase in overall efficiency gradually with the increase in T_{t4}. The reason behind this is the increase in the propulsive efficiency and the work output developed by the high pressure turbine.

CHAPTER 5

5. SUMMARY AND CONCLUSIONS

The graphs are plotted for the configuration of turboprop engine represent the effect of component performance on the overall cycle. The work output co-efficient of core stream (C_c) represents the optimum work developed by core section of turboprop engine. The total work output co-efficient (C_{tot}) represents the sum of work output co-efficient of core (C_c) and work output co-efficient of propeller (C_{prop}).

Specific thrust (F) is defined as the force acting on the internal surface of the propulsion system from state 0 to1 in addition with the force acting on the internal surface of the stream from station 1 to 9 which contains the air flowing into the engine. The specific thrust (F) having optimal values in the range of pressure ratio below 25 and M less than 0.6. Though, it has positive values in the entire range of pressure ratios and Mach number. The uninstalled specific fuel consumption, (S) is the mass of fuel needed to provide the net thrust for a given period. Specific fuel consumption increases sharply as long as the Mach number increases. At Mach number 0.9, it has maximum values whereas the thrust has minimum value.

Thermal efficiency (η_T) of an engine is another very useful engine performance parameter. Thermal efficiency is defined as the net rate of organized energy (shaft power or kinetic energy) out of the engine divided by the rate of thermal energy available from the fuel in the engine. The available thermal energy of the fuel is equal to the product of mass flow rate ($\dot{m}_f$) of the fuel and the fuel heating value (h_{PR}). The thermal efficiency (η_T), the propulsive efficiency (η_P) and the overall efficiency (η_O) represent the efficiencies of the engine. The overall efficiency has maximum values of above 0.95 at very low pressure ratio (i.e, below 5) and low Mach number (i.e, 0.4). The propulsive efficiency (η_P) of a propulsion system is a measure of how effectively the engine power output ($\dot{W}_{out}$) is used to power the aircraft. Propulsive efficiency is the ratio of the aircraft power (thrust times velocity) to the power out of the engine. The thermal and propulsive efficiencies can be combined to give the overall efficiency (η_O) of a propulsion system. Multiplying propulsive efficiency by thermal efficiency, the ratio of the aircraft power to the rate of thermal energy released in the engine can be found. The propulsive efficiency also represents the ideal limit of the propeller efficiency.

In the foregoing section of chapter 4, the graphs are plotted to optimize the effect of various parameters for different turbine inlet temperature or burner exit temperature for the entire range of compressor pressure ratio (π_c) and Mach number 0.8. The general trends are same as for the ideal cycle which has been validated [40].

5.1 Effect of Mach number (M)

C_c, C_{prop} and C_{tot} are the work output coefficient parameters of turboprop engine cycle. C_{tot} shows the optimum values at Mach number 0.6 and pressure ratio 25. Though the individual values of C_c and C_{prop} at pressure ratio 25 having values -0.15 and 1.30. The values of C_c at pressure ratio 30 at Mach number 0.5 reflect positive values of the engine. Therefore, the optimum values of C_c are considerable at pressure ratio above 30.

5.2 Effect of Turbine Inlet Temperature (T_{t4})

It has been found that C_{tot} is maximum at higher T_{t4} (1700 K) at minimum pressure ratio 5. Though, the trend of the graph is in increasing order with the turbine inlet temperature at any values of pressure ratio. Specific thrust also represents its maximum values at T_{t4} (1700 K) and pressure ratio 5while the specific fuel consumption is minimum at lower T_{t4} (1300 K) and minimum pressure ratio 5. The overall efficiency (η_O) is maximum at low pressure ratio but the optimum range of (η_O) is 30-35% at pressure ratios 15-35. One can take the values of pressure ratio in the range of 15-35 for optimum results of the overall efficiency.

5.3 Variation of Turbine Temperature Ratio (τ_t)

C_{prop} and C_c show downtrend and uptrend of the graph on increasing τ_t respectively. C_{tot} has the optimum value of 1.0-1.6 in the Mach number range 0.4-0.6 of turbine temperature ratio. Specific thrust also shows the values in the τ_t range of 10-15 for the entire range of pressure ratios.

The overall efficiency shows the optimum values in the range of turbine temperature ratio (0.4 – 0.5). The values are in between 20-40%. Though, the values of the overall efficiency (η_O) are around 20% at very low Mach number and low pressure ratio of 10. The important parameter of the engine having optimum values in the range 15-30 of pressure ratio while Mach number below 0.8. It has also been concluded that the

specific thrust and the overall pressure ratio are varying in the range of Mach number 0.4-0.6 but gives relevant values within range.

5.4 Recommendations for the Future Work

The gas turbine technology has been suffering a continuous evolution since its inception. In the last decades, research on automotive gas turbines has focused in raising the operating turbine inlet temperature in order to increase the thermodynamic efficiency, i.e. fuel efficiency

In order to improve the accuracy of the model, the following additional steps are suggested:

1. The model needs to be further optimized around its design points of Max. Cruise and Max. Take-Off with particular attention paid to accurately estimating component level efficiency and internal cooling. The turbine inlet temperatures (TIT) for both cases also need to be verified.

2. The external bleed flow schedule needs to be verified against system specification or flight test data. It is worthwhile to also evaluate impact of air bled from the HP port.

3. Off-design model development is the next priority. This would require a more accurate estimation of the relationships between pressure ratio, TIT, compressor mass flow and stage efficiencies as a function of power setting or gas generator speed. The idle power setting is an important operating point.

4. The accurate accounting of installation effects e.g. propeller and intake effects and a better means of calculating residual thrust power would enable installed performance to be better represented.

5. Ultimately, an aircraft operator is interested in total fuel burn on a particular mission, so the development of an integrated aircraft and engine model to permit evaluation of a complete flight would be useful.

While gas turbine performance software such as GASTURB is readily available, it is hoped that the results of this PW120A simplified model will provide operators of aircraft powered by this engine a better understanding of the engine's fuel efficiency as a function of the operational parameters of throttle setting, altitude, static air

temperature, external bleed air, compressor fouling and turbine wear. This model could form part of an analytical toolbox that operators could employ to further optimize their flight operations.

REFERENCES

1. **Abdul-Nabe, R. A. and Tariq, M. (2014)** "Thermal Analysis Of A Gas Turbine Cycle For A Turbojet Engine", *International Journal of Advanced Research in Engineering and Technology, Volume 5, Issue 10, Pages 21-33.*
2. **Ahmed, A. M. and Tariq, M. (2013)** "Thermal Analysis of A Gas Turbine Power Plant To Improve Performance Efficiency", *International Journal of Mechanical Engineering and Technology, Volume 4, Issue 6, Pages 43-54.*
3. **Al- Attab, K. A. and Zainal, Z. A. (2010)** "Performance of high-temperature heat exchangers inbiomass fuel powered externally fired gas turbine systems", *Renewable Energy, Volume 35, Issue 5,Pages 913–920.*
4. **Andriani, R. and Ghezzi, U. (2011)** "Parametric Thermal Analysis of Regenerated and Intercooled Turboprop Engine", *47th AIAA/ASME/SAE/ASEE Joint Propulsion Conference & Exhibit, 31 July - 03 Augusts, San Diego, California.*
5. **Armendariz, I., Olarrea, J. and García-Martínez, J. (2015)** "Parametric analysis of a highly dynamical phenomena caused by a propeller blade loss", *Engineering Failure Analysis, Volume 57, November, Pages 528-43.*
6. **Badran, O. O. (1999)** "Gas-turbine performance improvements", *Applied Energy Volume 64, Issues 1, Pages 263–273.*
7. **Banach, J. H. and Reynolds, N. C. (1984)** "Turboprop engine propulsion for the 1990's", *Journal of Aircraft, Volume 21, Issue 4, Pages 238-243.*
8. **Barinyima, N. (2013)** "Performance assessment of simple and modified cycle turbo shaft gas turbines", *Propulsion and Power Research, Volume 2, Issue 2, Pages 96-106.*
9. **Basha, M., Shaahid S. M. and Al-Hadhrami, L. (2012)** "Impact of Fuels on Performance and Efficiency of Gas Turbine Power Plants", *Energy Procedia, Volume 14, Pages 558–565.*
10. **Basrawi, F., Yamada, T., Nakanishi, M. and Naing, S. (2011)** "Effect of ambient temperature on the performance of micro gas turbine with cogeneration system in cold region", *Applied Thermal Engineering, Volume 31, Issues 6, Pages 1058–1067.*

11. **Bassily, A. M. (2004)** "Performance improvements of the intercooled reheat recuperated gas turbine cycle using absorption inlet-cooling and evaporative after-cooling", *Applied Energy, Volume 77, Issue 3, Pages 249–272.*
12. **Becker, M. G. (1991)** "Testing a modern turboprop propulsion system", *AIAA/SAE/ASME/ASEE 27th Joint Propulsion Conference, June 24-26.*
13. **Bedecarrats, J.P. and Strub, F. (2009)** "Gas turbine performance increase using an air cooler with a phase change energy storage", *Applied Thermal Engineering, Volume 29, Issues 5, Pages 1166–1172.*
14. **Bencze, D. P., Dugan, J. F. and Williams, I. J. (1977)** "Advance Turboprop Technology Development", *AIAA Aircraft systems and technology meeting Seattle, Washington/August 22-24.*
15. **Bonaccorsi, A. and Giuri, P. (2000)** "When shakeout doesn't occur: The evolution of the turboprop engine industry", *Research Policy, Volume 29, Issues 7–8, August, Pages 847-870.*
16. **Bowles, D. M. and Dawson, P. V. (1998)** "The Advanced Turboprop Project: Radical Innovation in a Conservative Environment", *from engineering science to big science - The NACA and NASA Collier Trophy Research Project Winners, Pages 321-342.*
17. **Boyce, M. P. (2012)** "Theoretical and Actual Cycle Analyses", *Gas Turbine Engineering Handbook (4th Edition), Pages 89–137.*
18. **Cao, W. and Zheng, D. (2006)** "Exergy regeneration in an O_2/CO_2 gas turbine cycle with chemical recuperation by CO_2 reforming of methane", *Energy Conversion and Management, Volume 47, Issues 18, Pages 3019–3030.*
19. **Carapellucci, R. and Milazzo, A. (2005)** "Thermodynamic optimization of a reheat chemically recuperated gas turbine", *Energy Conversion and Management, Volume 46, Issue 19, Pages 2936–2953.*
20. **Chena, L., Lia, Y., Suna, F. and Wub, C. (2004)** "Power optimization of open-cycle regenerator gas-turbine power-plants", *Applied EnergyVolume 78, Issue 2, Pages 199–218.*
21. **Clemente, S., Micheli, D., Reini, M. and Taccani, R. (2013)** "Bottoming organic Rankine cycle for a small scale gas turbine: A comparison of different solutions", *Applied Energy, Volume 106, Pages 355–364.*
22. **Crane, K., Medeiros, E. S., Cliff, R. and Mulvenon, J. C. (2005)** "A new direction for china's defence industry" *Rand Corporation Publication.*

23. **El-Maksoud, R. M. A. (2014)** "Gas turbine with heating during the expansion in the stator blades", *Energy Conversion and Management, Volume 78, Pages 219–224.*
24. **El-Masri, M. A. (1986)** "On Thermodynamics of Gas Turbine Cycles: Part 3-Thermodynamic Potential and Limitations of Cooled Reheated-Gas-Turbine Combined Cycles," *ASME Journal of Engineering for Gas Turbine and Power, Voume.108, Pages 160-169.*
25. **Erbaya, L. B., Göktun, S. and Yavuz, H. (2001)** "Optimal design of the regenerative gas turbine engine with isothermal heat addition", *Applied Energy Volume 68, Issue 3, March 2001, Pages 249–264.*
26. **Garg, V. K. (2002)** "Heat transfer research on gas turbine airfoils at NASA GRC", *International Journal of Heat and Fluid Flow, Volume 23, Issue 2, Pages 109–136.*
27. **Gearhart, W. S. (1983)** "Efficiency Improved Turboprop", *AlAA 21st Aerospace Sciences Meeting, January 10-13, Reno, Nevada.*
28. **Geels, F. W. (2006)** "Co-evolutionary and multi level dynamics in transitions: the transformation of aviation systems and the shift from propeller to turbojet, Technovation, Volume 26, Issue 9, September 2006, Pages 999-101.
29. **Ghenaiet, A. and Boulekraa, T. (2009)** "Optimal Design of Turboprop Engines Using Generic Algorithm", *Journal of Power and Propulsion, Volume 25, Issue 6.*
30. **Giampaolo, T. (2006)** Gas Turbine Handbook: Principles and Practices, *3rd Edition, Pages 23-39.*
31. **Gudmundsson, S. (2014)** "The Anatomy of the Propeller", *General Aviation Aircraft Design, Pages 581-659.*
32. **Haberland. C. H., Kokorniak, M., Schneegans, A., Xie, X. and Kranz. O. (1996)** "Application of an aircraft design tool for the conceptual design of turboprop transport aircraft", *ISASTI, Jakarta.*
33. **Harvey, S. and Kane, N. (1997)** "Analysis of a reheat gas turbine cycle with chemical recuperation using Aspen", *Energy Conversion and Management, Volume 38, Issue 15, Pages 1671–1679.*
34. **Heppenstall, T. (1998)** "Advanced gas turbine cycles for power generation: a critical review", *Applied Thermal Engineering, Volume 18, Issues 9, Pages 837–846.*

35. **Hirschkron, R. and Russo, C. J. (1986)** "Small Turbo shaft/Turboprop Engine Technology Study", *AIAA/ASME/SAE/ASEE 22nd Joint Propulsion Conference, June 16-18.*
36. **Horlock J. H. (1998)** "Heat exchanger performance with water injection (with relevance to evaporative gas turbine (EGT) cycles)", *Energy Conversion and Management, Volume 39, Issues 16–18, Pages 1621–1630.*
37. **Horlock, J. H. (2003)** "Advance Gas Turbine Cycles", *Elsevier Sci. Ltd.*, UK
38. **Kerr, C. I. and Ivey, P.C. (2003)** "The Engineering Doctorate model of consultant/ researcher/ innovator/ entrepreneur for new product development- A gas turbine instrumentation case study", *Tech innovation, Volume 23, Issue 2, Pages 95- 102.*
39. **Kim, T. S., Chang, H. O. and Ro, S. T. (1994)** "Comparative analysis of the off design performance for gas turbine cogeneration systems", *Heat Recovery Systems and CHP, Volume 14, Issue 2, Pages 153–163.*
40. **Kima, K. H. and Perez-Blancob, H. (2007)** "Potential of regenerative gas-turbine systems with high fogging compression", *Applied Energy, Volume 84, Issue 1, Pages 16–28.*
41. **Kong, C., Ki, J. and Chung, S. (2002)** "Performance simulation of a turboprop engine for basic trainer", *KSME International Journal, June, Volume 16, Issue 6, pp 839–850.*
42. **Kong, C., Ki, J., and Kim, T. (2003)** "Optimal Measurement Parameter Selection of Turboprop Engine Using GPA Approach", *International Journal of Turbo & Jet Engines; 20, 171-182.*
43. **Kraft, G. and Strack, W. (1975)** "Preliminary study of advanced turboprops for low energy consumption", *Lewis Research Centre, Cleveland, Ohio - 44135*.
44. **Langston, L. S. (2013)** "The Adaptable Gas Turbines", *Reference Module in Earth Systems and Environmental Science, Volume 101, Pages 264-267.*
45. **Lee, J. J., Kang, D. W. and Kim, T. S. (2011)** "Development of a gas turbine performance analysis program and its application", *Energy Procedia, Volume 36, Issue 8, Pages 5274–5285.*
46. **Lopez-Diez, A. Ruiz-Calavera, L. Castillo-Calvo, J. and Prieto-Ibanez, R. F. (2005)** "Front End optimization of High Speed Turboprop Engines", *41st AIAA/ASME/SAE/ASEE Joint Propulsion Conference & Exhibit 10 - 13 July, Tucson, Arizona.*

47. **Manuela. M., Gonzáleza, P., Javier, F., Garcíaa, F., Ramona, I. S. and Rocesb, H. S. (2006)** "Experimental thermal behavior of a power plant reheater", *Energy Volume 31, Issue 5, Pages 665–676.*
48. **Mathur, M. L. and Sharma, R. P. (2012)** "Gas turbine and jet Rocket Propulsion", *Second edition: Dhanpat Rai & Co., Pages 2.1-2.28.*
49. **Mattingly, J. D. (1996)** "Element of Gas Turbine Propulsion", *McGraw–Hill, New York.*
50. **McDonald, C. F. and Wilsont, D. G. (1996)** "The Utilization of Recuperated and Regenerated Engine Cycles for High-Efficiency Gas Turbines in the 21st Century", *Applied Thermal Engineering, Volume 16, Pages 635-453.*
51. **Mclntire, W. L. (1985)** "A New Generation T56 Turboprop Engine, *International Journal of Turbo & Jet Engine; 2,189-197.*
52. **Meherwan P. Boyce (2006)** "Performance and mechanical standards", *Gas turbine engineering handbook (3rd edition), Pages 139-175.*
53. **Memona, A. G., Memona, R. A., Harijana, K. and Uqailib M. A. (2014)** "Thermo-environmental analysis of an open cycle gas turbine power plant with regression modeling and optimization", *Journal of the Energy Institute, Volume 87, Pages 81-88.*
54. **Mohammed, M. J. and Tariq, M. (2014)** "Analysis of a Combined Regenerative and Reheat Gas Turbine Cycle using MATLAB", *International Journal of Scientific Engineering and Technology Research, ISSN 2319-8885, Volume 3, Issue 4, Pages 665-672.*
55. **Neema, V. K and Tariq, M. (2011)** "Performance Evaluation of Turbojet and Turbofan Engines with and without an Afterburner", Ph.D. Dissertation.
56. **Nethercote, W. C. E., Hally, D., Mackay, M., Noble, D. J. and Spongale, N. C. (1992) "**DREA's propeller design and analysis experience", MARIN jubilee workshop.
57. **Nishida, K. (2005)** "Regenerative steam-injection gas-turbine systems", *Applied Energy, Volume 81, Pages 231–246.*
58. **Nitzsche, F. (1991)** "Insights on the Whirl-Flutter Phenomena of Advanced Turboprops and Prop fans", *Journal of Aircraft, 28(7), 463-470.*
59. **Nitzsche, F. (1994)** "Whirl-Flutter Suppression in Advanced Turboprops and Prop fans by Active Control Techniques", *Journal of Aircraft, 31(3), 713-719.*

60. **Palsson, J., Selimovicand, A. and Sjunnesson, L. (2000)** "Combined solid oxide fuel cell and gas turbine systems for efficient power and heat generation", *Journal of Power Sources, Volume 86, Issues 2, Pages 442–448.*
61. **Pathak, M., Kumar, P. S. and Saha, U. K. (2005)** "Prediction of Off-Design Performance Characteristics of a Gas Turbine Cycle using Matching Technique", *International Journal of Turbo & Jet Engines, 22,103-119.*
62. **Polyzakisa, A. L., Koroneosband C. and Xydisb, G. (2008)** "Optimum gas turbine cycle for combined cycle power plant", *Energy Conversion and Management, Volume 49, Issue 4, Pages 551–563.*
63. **Povazan, J., Andoga, R., Fozo, L., Judicak, J. and MAdarasz, L. (2012)** "Introduction to advanced modeling and control of turboprop engines", *IEEE-16th International Conference of Intelligent Engineering Systems, June 13-15*, Lisbon, Portugal.
64. **Price, M., Raghunathan, S. and Curran, R (2006)** "An integrated system engineering to aircraft design", *Progress in Aerospace Sciences, Volume 42, Issue 4, Pages 331-376.*
65. **Rahman, M. M., Ibrahim, T. K. and Abdalla, A. N. (2011)** "Thermodynamic Performance Analysis of Gas Turbine Power Plant", *International Journal of the Physical Sciences, Volume 6(14), pp.3539-3550.*
66. **Razak, A. M. Y. (2013)** "Gas turbine performance modeling, analysis and optimization", *Modern Gas Turbine Systems, Pages 423-51*.
67. **Richard L. F. and Hopkins, J. P. (1977)** "Potential of turboprop power plants for fuel conservation", *Acta Astronautica, Volume 4, Issues 1–2, January–February, Pages 53-75.*
68. **Ryerson, M. S. and Hansen, M. (2010)** "The potential of turboprops for reducing aviation fuel consumption", *Transportation Research Part D: Transport and Environment, Volume 15, Issue 6, August, Pages 305-314.*
69. **Sanjay, Singh O., Prasad, B. N. (2008)** "Comparative performance analysis of cogeneration gas turbine cycle for different blade cooling means", *International Journal of Thermal Sciences, Volume 48, Pages 1432–1440.*
70. **Saravanamuttoo, H. I. H. (1987)** "Modern turboprop engines", *Progress on aerospace sciences, Volume 24, Issue 3, Pages 225-24.*
71. **Sforza, P. M. (2012)** "Chapter 10 - Propellers", *Theory of Aerospace Propulsion, Pages 409-437.*

72. **Sheng, H., Zhang, T. and Zhang, Y. (2016)** "Real-time Simulation of Turboprop Engine Control System", *International Journal of Turbo & Jet Engine; pp: 1-11.*
73. **Spencer, R. L. and Ware, M. (2000)** "Introduction to MATLAB", Brigham Young University.
74. **Stevens, T. and Baelmans, M. (2008)** "Optimal pressure drop ratio for micro-recuperators in small sized gas turbines", *Applied Thermal Engineering, Volume 28, Issues 1, Pages 2353–2359.*
75. **Stoten, M. D. and Harvey, R. A. (1983)** "Regional Airline Turboprop Engine Technology", *AIAA/SAE/ASME 19th Joint Propulsion Conference June 27-29, 1983/Seattle, Washington.*
76. **Tariq, M. (2014)** "Analysis of a Regenerative Gas Turbine Cycle for Performance Evaluation", *International Journal of Engineering Research and General Science, Volume 2, Issue 4, June- July*.
77. **Treager, I. E. (1995)** "Aircraft Gas Turbine Technology", *3rd edition, McGraw–Hill, New York.*
78. **Ujam, A.J. (2013)** "Parametric Analysis of a Turbojet engine with reduced inlet pressure to the compressor", *IOSR Journal of Engineering, ISSN: 2250-3021, Volume 3, Issue 8, Pages 29-37.*
79. **Vecchia, P. D. and Nicolosi, F. (2014)** "Aerodynamic guidelines in the design and optimization of new regional turboprop aircraft", *Aerospace Science and Technology, Volume 38, Pages 88-104.*
80. **Walsh, P. and Fletcher, P. (2004)** "Gas Turbine Performance", *2nd edition, Wiley–Blackwell, Fairfield, NJ, pp. 227–282.*
81. **Walsh, P., and Fletcher, P. (1998)** "Gas turbine Performance", *Blackwell Science ltd.*
82. **Wana, K., Zhanga, S., Wanga, J. and Xiaoa, J. (2010)** "Performance of humid air turbine with exhaust gas expanded to below ambient pressure based on micro-turbine", *Energy Conversion and Management, Volume 51, Issue 11, Pages 2127–2133.*
83. **Wang, F. J. and Chiou, J. S. (2002)** "Performance improvement for a simple cycle gas turbine genset", *Applied Thermal Engineering Volume 22, Issue 10, Pages 1105–1115.*

84. **Yuan-Hu, C., Ji, H. W., Di-Yi, T. and Zhi-Wei, L. (1995)** "A New Method for Predicting Performance of Axial-Flow Compressor", *International Journal of Turbo & Jet Engine; 12, 21-28.*

85. **Zhang, X., Li, J., Li, G. and Feng, Z. (2007)** "Cycle analysis of an integrated solid oxide fuel cell and recuperative gas turbine with an air reheating system", *Journal of Power Sources Volume 164, Issue 2, Pages 752–760*.

APPENDIX - A

New_plot1

```
figure,plot(M_0,C_prop_arr(1:6),M_0,C_prop_arr(7:12),M_0,C_prop_ar
r(13:18),M_0,C_prop_arr(19:24),M_0,C_prop_arr(25:30),M_0,C_prop_ar
r(31:36),M_0,C_prop_arr(37:42),M_0,C_prop_arr(43:48));
xlabel('M_0');
ylabel('Cprop');
title('M_0 vs C_prop');
legend('pi = 5','pi = 10','pi = 15','pi = 20','pi = 25','pi =
30','pi = 35','pi = 40');


figure,plot(M_0,C_c_arr(1:6),M_0,C_c_arr(7:12),M_0,C_c_arr(13:18),
M_0,C_c_arr(19:24),M_0,C_c_arr(25:30),M_0,C_c_arr(31:36),M_0,C_c_a
rr(37:42),M_0,C_c_arr(43:48));
xlabel('M_0');
ylabel('Cc');
title('M_0 vs Cc');
legend('pi = 5','pi = 10','pi = 15','pi = 20','pi = 25','pi =
30','pi = 35','pi = 40');


figure,plot(M_0,C_tot_arr(1:6),M_0,C_tot_arr(7:12),M_0,C_tot_arr(1
3:18),M_0,C_tot_arr(19:24),M_0,C_tot_arr(25:30),M_0,C_tot_arr(31:3
6),M_0,C_tot_arr(37:42),M_0,C_tot_arr(43:48));
xlabel('M_0');
ylabel('C_tot');
title('M_0 vs C_tot');
legend('pi = 5','pi = 10','pi = 15','pi = 20','pi = 25','pi =
30','pi = 35','pi = 40');

figure,plot(M_0,S_arr(1:6),M_0,S_arr(7:12),M_0,S_arr(13:18),M_0,S_
arr(19:24),M_0,S_arr(25:30),M_0,S_arr(31:36),M_0,S_arr(37:42),M_0,
S_arr(43:48));
xlabel('M_0');
ylabel('S');
title('M_0 vs S');
legend('pi = 5','pi = 10','pi = 15','pi = 20','pi = 25','pi =
30','pi = 35','pi = 40');


figure,plot(M_0,eta_T_arr(1:6),M_0,eta_T_arr(7:12),M_0,eta_T_arr(1
3:18),M_0,eta_T_arr(19:24),M_0,eta_T_arr(25:30),M_0,eta_T_arr(31:3
6),M_0,eta_T_arr(37:42),M_0,eta_T_arr(43:48));
xlabel('M_0');
ylabel('eta_T');
title('M_0 vs eta_T');
legend('pi = 5','pi = 10','pi = 15','pi = 20','pi = 25','pi =
30','pi = 35','pi = 40');

figure,plot(M_0,eta_P_arr(1:6),M_0,eta_P_arr(7:12),M_0,eta_P_arr(1
3:18),M_0,eta_P_arr(19:24),M_0,eta_P_arr(25:30),M_0,eta_P_arr(31:3
6),M_0,eta_P_arr(37:42),M_0,eta_P_arr(43:48));
xlabel('M_0');
ylabel('eta_P');
title('M_0 vs eta_P');
```

```
legend('pi = 5','pi = 10','pi = 15','pi = 20','pi = 25','pi =
30','pi = 35','pi = 40');

figure,plot(M_0,eta_O_arr(1:6),M_0,eta_O_arr(7:12),M_0,eta_O_arr(1
3:18),M_0,eta_O_arr(19:24),M_0,eta_O_arr(25:30),M_0,eta_O_arr(31:3
6),M_0,eta_O_arr(37:42),M_0,eta_O_arr(43:48));
xlabel('M_0');
ylabel('eta_O');
title('M_0 vs eta_O');
legend('pi = 5','pi = 10','pi = 15','pi = 20','pi = 25','pi =
30','pi = 35','pi = 40');

figure,plot(M_0,ratio_F_m_dot_arr(1:6),M_0,ratio_F_m_dot_arr(7:12)
,M_0,ratio_F_m_dot_arr(13:18),M_0,ratio_F_m_dot_arr(19:24),M_0,rat
io_F_m_dot_arr(25:30),M_0,ratio_F_m_dot_arr(31:36),M_0,ratio_F_m_d
ot_arr(37:42),M_0,ratio_F_m_dot_arr(43:48));
xlabel('M_0');
ylabel('F/m_dot');
title('M_0 vs F/m_dot');
legend('pi = 5','pi = 10','pi = 15','pi = 20','pi = 25','pi =
30','pi = 35','pi = 40');
```

APPENDIX - B

New _plot2

```
figure,plot(T_t4,C_prop_arr(1:5),T_t4,C_prop_arr(6:10),T_t4,C_prop
_arr(11:15),T_t4,C_prop_arr(16:20),T_t4,C_prop_arr(21:25),T_t4,C_p
rop_arr(26:30),T_t4,C_prop_arr(31:35),T_t4,C_prop_arr(36:40));
xlabel('T_t4');
ylabel('Cprop');
title('T_t4 vs C_prop');
legend('pi = 5','pi = 10','pi = 15','pi = 20','pi = 25','pi =
30','pi = 35','pi = 40');


figure,plot(T_t4,C_c_arr(1:5),T_t4,C_c_arr(6:10),T_t4,C_c_arr(11:1
5),T_t4,C_c_arr(16:20),T_t4,C_c_arr(21:25),T_t4,C_c_arr(26:30),T_t
4,C_c_arr(31:35),T_t4,C_c_arr(36:40));
xlabel('T_t4');
ylabel('Cc');
title('T_t4 vs Cc');
legend('pi = 5','pi = 10','pi = 15','pi = 20','pi = 25','pi =
30','pi = 35','pi = 40');


figure,plot(T_t4,C_tot_arr(1:5),T_t4,C_tot_arr(6:10),T_t4,C_tot_ar
r(11:15),T_t4,C_tot_arr(16:20),T_t4,C_tot_arr(21:25),T_t4,C_tot_ar
r(26:30),T_t4,C_tot_arr(31:35),T_t4,C_tot_arr(36:40));
xlabel('T_t4');
ylabel('C_tot');
title('T_t4 vs C_tot');
legend('pi = 5','pi = 10','pi = 15','pi = 20','pi = 25','pi =
30','pi = 35','pi = 40');

figure,plot(T_t4,S_arr(1:5),T_t4,S_arr(6:10),T_t4,S_arr(11:15),T_t
4,S_arr(16:20),T_t4,S_arr(21:25),T_t4,S_arr(26:30),T_t4,S_arr(31:3
5),T_t4,S_arr(36:40));
xlabel('T_t4');
ylabel('S');
title('T_t4 vs S');
legend('pi = 5','pi = 10','pi = 15','pi = 20','pi = 25','pi =
30','pi = 35','pi = 40');


figure,plot(T_t4,eta_T_arr(1:5),T_t4,eta_T_arr(6:10),T_t4,eta_T_ar
r(11:15),T_t4,eta_T_arr(16:20),T_t4,eta_T_arr(21:25),T_t4,eta_T_ar
r(26:30),T_t4,eta_T_arr(31:35),T_t4,eta_T_arr(36:40));
xlabel('M_0');
ylabel('T_t4');
title('T_t4 vs eta_T');
legend('pi = 5','pi = 10','pi = 15','pi = 20','pi = 25','pi =
30','pi = 35','pi = 40');

figure,plot(T_t4,eta_P_arr(1:5),T_t4,eta_P_arr(6:10),T_t4,eta_P_ar
r(11:15),T_t4,eta_P_arr(16:20),T_t4,eta_P_arr(21:25),T_t4,eta_P_ar
r(26:30),T_t4,eta_P_arr(31:35),T_t4,eta_P_arr(36:40));
xlabel('T_t4');
ylabel('eta_P');
title('T_t4 vs eta_P');
```

```
legend('pi = 5','pi = 10','pi = 15','pi = 20','pi = 25','pi =
30','pi = 35','pi = 40');

figure,plot(T_t4,eta_O_arr(1:5),T_t4,eta_O_arr(6:10),T_t4,eta_O_ar
r(11:15),T_t4,eta_O_arr(16:20),T_t4,eta_O_arr(21:25),T_t4,eta_O_ar
r(26:30),T_t4,eta_O_arr(31:35),T_t4,eta_O_arr(36:40));
xlabel('T_t4');
ylabel('eta_O');
title('T_t4 vs eta_O');
legend('pi = 5','pi = 10','pi = 15','pi = 20','pi = 25','pi =
30','pi = 35','pi = 40');

figure,plot(T_t4,ratio_F_m_dot_arr(1:5),T_t4,ratio_F_m_dot_arr(6:1
0),T_t4,ratio_F_m_dot_arr(11:15),T_t4,ratio_F_m_dot_arr(16:20),T_t
4,ratio_F_m_dot_arr(21:25),T_t4,ratio_F_m_dot_arr(26:30),T_t4,rati
o_F_m_dot_arr(31:35),T_t4,ratio_F_m_dot_arr(36:40));
xlabel('T_t4');
ylabel('F/m_dot');
title('T_t4 vs F/m_dot');
legend('pi = 5','pi = 10','pi = 15','pi = 20','pi = 25','pi =
30','pi = 35','pi = 40');
```

APPENDIX - C

New_plot3

```
figure,plot(tau_t,C_prop_arr(1:6),tau_t,C_prop_arr(7:12),tau_t,C_p
rop_arr(13:18),tau_t,C_prop_arr(19:24),tau_t,C_prop_arr(25:30),tau
_t,C_prop_arr(31:36),tau_t,C_prop_arr(37:42),tau_t,C_prop_arr(43:4
8));
xlabel('tau_t');
ylabel('Cprop');
title('tau_t vs C_prop');
legend('pi = 5','pi = 10','pi = 15','pi = 20','pi = 25','pi =
30','pi = 35','pi = 40');


figure,plot(tau_t,C_c_arr(1:6),tau_t,C_c_arr(7:12),tau_t,C_c_arr(1
3:18),tau_t,C_c_arr(19:24),tau_t,C_c_arr(25:30),tau_t,C_c_arr(31:3
6),tau_t,C_c_arr(37:42),tau_t,C_c_arr(43:48));
xlabel('tau_t');
ylabel('Cc');
title('tau_t vs Cc');
legend('pi = 5','pi = 10','pi = 15','pi = 20','pi = 25','pi =
30','pi = 35','pi = 40');


figure,plot(tau_t,C_tot_arr(1:6),tau_t,C_tot_arr(7:12),tau_t,C_tot
_arr(13:18),tau_t,C_tot_arr(19:24),tau_t,C_tot_arr(25:30),tau_t,C_
tot_arr(31:36),tau_t,C_tot_arr(37:42),tau_t,C_tot_arr(43:48));
xlabel('tau_t');
ylabel('C_tot');
title('tau_t vs C_tot');
legend('pi = 5','pi = 10','pi = 15','pi = 20','pi = 25','pi =
30','pi = 35','pi = 40');

figure,plot(tau_t,S_arr(1:6),tau_t,S_arr(7:12),tau_t,S_arr(13:18),
tau_t,S_arr(19:24),tau_t,S_arr(25:30),tau_t,S_arr(31:36),tau_t,S_a
rr(37:42),tau_t,S_arr(43:48));
xlabel('tau_t');
ylabel('S');
title('tau_t vs S');
legend('pi = 5','pi = 10','pi = 15','pi = 20','pi = 25','pi =
30','pi = 35','pi = 40');


figure,plot(tau_t,eta_T_arr(1:6),tau_t,eta_T_arr(7:12),tau_t,eta_T
_arr(13:18),tau_t,eta_T_arr(19:24),tau_t,eta_T_arr(25:30),tau_t,et
a_T_arr(31:36),tau_t,eta_T_arr(37:42),tau_t,eta_T_arr(43:48));
xlabel('tau_t');
ylabel('eta_T');
title('tau_t vs eta_T');
legend('pi = 5','pi = 10','pi = 15','pi = 20','pi = 25','pi =
30','pi = 35','pi = 40');

figure,plot(tau_t,eta_P_arr(1:6),tau_t,eta_P_arr(7:12),tau_t,eta_P
_arr(13:18),tau_t,eta_P_arr(19:24),tau_t,eta_P_arr(25:30),tau_t,et
a_P_arr(31:36),tau_t,eta_P_arr(37:42),tau_t,eta_P_arr(43:48));
xlabel('tau_t');
ylabel('eta_P');
```

```
title('tau_t vs eta_P');
legend('pi = 5','pi = 10','pi = 15','pi = 20','pi = 25','pi =
30','pi = 35','pi = 40');

figure,plot(tau_t,eta_O_arr(1:6),tau_t,eta_O_arr(7:12),tau_t,eta_O
_arr(13:18),tau_t,eta_O_arr(19:24),tau_t,eta_O_arr(25:30),tau_t,et
a_O_arr(31:36),tau_t,eta_O_arr(37:42),tau_t,eta_O_arr(43:48));
xlabel('tau_t');
ylabel('eta_O');
title('tau_t vs eta_O');
legend('pi = 5','pi = 10','pi = 15','pi = 20','pi = 25','pi =
30','pi = 35','pi = 40');

figure,plot(tau_t,ratio_F_m_dot_arr(1:6),tau_t,ratio_F_m_dot_arr(7
:12),tau_t,ratio_F_m_dot_arr(13:18),tau_t,ratio_F_m_dot_arr(19:24)
,tau_t,ratio_F_m_dot_arr(25:30),tau_t,ratio_F_m_dot_arr(31:36),tau
_t,ratio_F_m_dot_arr(37:42),tau_t,ratio_F_m_dot_arr(43:48));
xlabel('tau_t');
ylabel('F/m_dot');
title('tau_t vs F/m_dot');
legend('pi = 5','pi = 10','pi = 15','pi = 20','pi = 25','pi =
30','pi = 35','pi = 40');
```

APPENDIX - D

Calculate_turboprop

```
g_c = 9.8;
T_9 = 240;


R_c = ((gamma_c - 1)/gamma_c).*C_pc;
fprintf('\n R_c = %d',R_c);

R_t = ((gamma_t - 1)/gamma_t).*C_pt;
fprintf('\n R_t = %d',R_t);

a_0 = sqrt(gamma_c.*R_c.*g_c.*T_0);
fprintf('\n a_0 = %d',a_0);

V_0 = a_0.*M_0;
fprintf('\n V_0 = %d',V_0);

tau_r = 1 + (((gamma_c - 1)/2).*(M_0.^2));
fprintf('\n tau_r = %d',tau_r);

pi_r = tau_r.^((gamma_c)/(gamma_c-1));
fprintf('\n pi_r = %d',pi_r);

if M_0<=1

eta_r =1;
fprintf('\n eta_r = %d',eta_r);

else
eta_r = 1 - 0.0075.*((M_0-1).^(1.35));
fprintf('\n eta_r = %d',eta_r);


end

pi_d = pi_d_max.*eta_r;
fprintf('\n pi_d = %d',pi_d);

tau_lambda = ((C_pt.*T_t4)./(C_pc.*T_0));
fprintf('\n tau_lambda = %d',tau_lambda);


tau_c = pi_c.^((gamma_c - 1)./(gamma_c.*e_c));
fprintf('\n tau_c = %d',tau_c);

eta_c  = ( (pi_c.^((gamma_c - 1)./(gamma_c))) - 1)./(tau_c - 1);
fprintf('\n eta_c = %d',eta_c);

f = (tau_lambda - (tau_r.*tau_c))./((eta_b.*h_PR)./((C_pc.*T_0) -
tau_lambda));
```

```
fprintf('\n f = %d',f);

tau_tH = 1 - ((tau_r.*(tau_c -1))./(eta_mH.*(1+f).*tau_lambda));
fprintf('\n tau_tH = %d',tau_tH);

pi_tH = tau_tH.^((gamma_t)./((gamma_t - 1).*e_tH));
fprintf('\n pi_tH = %d',pi_tH);

eta_tH = (1 - tau_tH)./(1-(tau_tH.^(1./e_tH)));
fprintf('\n eta_tH = %d',eta_tH);

tau_tL  = (tau_t./tau_tH) ;
fprintf('\n tau_tL = %d',tau_tL);

pi_tL = tau_tL.^((gamma_t)./((gamma_t - 1).*e_tL));
fprintf('\n pi_tL = %d',pi_tL);

eta_tL = (1 - tau_tL)./(1- (tau_tL.^(1./e_tL)));
fprintf('\n eta_tL = %d',eta_tL);

ratio_Pt9_P0 = pi_r.*pi_d.*pi_c.*pi_b.*pi_tH.*pi_tL.*pi_n;
fprintf('\n Pt9/P0 = %d',ratio_Pt9_P0);


if ratio_Pt9_P0 > (((gamma_t + 1)/2).^((gamma_t)./(gamma_t - 1)))

    M_9 = 1;
fprintf('\n M_9 = %d',M_9);


    ratio_Pt9_P9 = (((gamma_t + 1)/2).^((gamma_t)./(gamma_t -
1)));
fprintf('\n Pt9/P9 = %d',ratio_Pt9_P9);

    ratio_P0_P9 = (ratio_Pt9_P9 )./(ratio_Pt9_P0) ;
fprintf('\n P0/P9 = %d',ratio_P0_P9);



else

    M_9 = sqrt((2./(gamma_t - 1)).*(((ratio_Pt9_P0).^((gamma_t -
1)/gamma_t)) - 1));
fprintf('\n M_9 = %d',M_9);

    ratio_Pt9_P9 = ratio_Pt9_P0;
fprintf('\n Pt9/P9 = %d',ratio_Pt9_P9);


    ratio_P0_P9 = 1;
fprintf('\n P0/P9 = %d',ratio_P0_P9);


end

%ratio_V9_a0 = V_9/a_0
```

```
ratio_V9_a0 = sqrt(((2.*tau_lambda.*tau_tH.*tau_tL)/(gamma_c -
1)).*(1 - ratio_Pt9_P9.^((1 - gamma_t)/(gamma_t))));
fprintf('\nV9/a0 = %d',ratio_V9_a0);

C_prop = eta_prop.* eta_g.*eta_mL.*(1+f).*tau_lambda.*tau_tH.*(1 -
tau_tL);
fprintf('\n C_prop = %d',C_prop);

C_c = ((gamma_c - 1).*M_0).*(((1+f).*ratio_V9_a0) - M_0 + (1+f).*
(R_t./R_c).*((T_9./T_0)./ratio_V9_a0).*((1 -
ratio_P0_P9)./(gamma_c)));
fprintf('\n C_c = %d',C_c);

C_tot = C_prop + C_c;
fprintf('\n C_tot = %d',C_tot);

ratio_F_m_dot = ((C_tot.*C_pc.*T_0)./ (V_0));
fprintf('\n F/m_dot = %d',ratio_F_m_dot);

S  = f./ratio_F_m_dot;
fprintf('\n S = %d',S);


ratio_W_dot_m_dot = (C_tot ).*((f.*(h_PR))./(C_pc.*T_0));
fprintf('\n W_dot/m_dot = %d',ratio_W_dot_m_dot);


S_P = f./(C_tot.*C_pc.*T_0);
fprintf('\n S_P = %d',S_P);

eta_T = C_tot .*((f.* h_PR ).*(C_pc.*T_0));
fprintf('\n eta_T = %d',eta_T);

eta_P = C_tot .*((C_prop./eta_prop) + ((gamma_c - 1)./2).*((1+
f).*((ratio_V9_a0).^2) - (M_0.^2)));
fprintf('\n eta_P = %d',eta_P);

eta_O = (eta_P .* eta_T);
fprintf('\n eta_O = %d',eta_O);
```

APPENDIX - E

Plot_turboprop_new

```
%********* Parameter Conditions*****************
M_0_arr = [0.4 0.5 0.6 0.7 0.8 0.9];
pi_c_arr = [5 10 15 20 25 30 35 40];
tau_t_arr = [0.4 0.5 0.6 0.7 0.8 0.9];
T_t4_arr = [1300 1400 1500 1600 1700];

%************Output Parameters*****************
C_prop_arr = [];
C_c_arr = [];
C_tot_arr = [];
S_arr = [];
eta_T_arr = [];
eta_P_arr = [];
eta_O_arr = [];
ratio_F_m_dot_arr = [];


for k = 1:8

pi_c = pi_c_arr(k);
    M_0 = M_0_arr;
calculate_turboprop;
C_prop_arr = [C_prop_arrC_prop];
C_c_arr = [C_c_arrC_c];
C_tot_arr = [C_tot_arrC_tot];
S_arr = [S_arr S];
eta_T_arr = [eta_T_arreta_T];
eta_P_arr = [eta_P_arreta_P];
eta_O_arr = [eta_O_arreta_O];
ratio_F_m_dot_arr = [ratio_F_m_dot_arrratio_F_m_dot];

end

new_plot1;

C_prop_arr = [];
C_c_arr = [];
C_tot_arr = [];
S_arr = [];
eta_T_arr = [];
eta_P_arr = [];
eta_O_arr = [];
ratio_F_m_dot_arr = [];

for k = 1:8

    M_0 = 0.6;
tau_t = 0.45;
pi_c = pi_c_arr(k);
    T_t4 = T_t4_arr;
calculate_turboprop;
C_prop_arr = [C_prop_arrC_prop];
C_c_arr = [C_c_arrC_c];
```

```
C_tot_arr = [C_tot_arrC_tot];
S_arr = [S_arr S];
eta_T_arr = [eta_T_arreta_T];
eta_P_arr = [eta_P_arreta_P];
eta_O_arr = [eta_O_arreta_O];
ratio_F_m_dot_arr = [ratio_F_m_dot_arrratio_F_m_dot];

end

new_plot2;

C_prop_arr = [];
C_c_arr = [];
C_tot_arr = [];
S_arr = [];
eta_T_arr = [];
eta_P_arr = [];
eta_O_arr = [];
ratio_F_m_dot_arr = [];




for k = 1:8

    M_0 = 0.6;
    T_t4 = 1370;
pi_c = pi_c_arr(k);
tau_t = tau_t_arr;
calculate_turboprop;
C_prop_arr = [C_prop_arrC_prop];
C_c_arr = [C_c_arrC_c];
C_tot_arr = [C_tot_arrC_tot];
S_arr = [S_arr S];
eta_T_arr = [eta_T_arreta_T];
eta_P_arr = [eta_P_arreta_P];
eta_O_arr = [eta_O_arreta_O];
ratio_F_m_dot_arr = [ratio_F_m_dot_arrratio_F_m_dot];


end

new_plot3;

    M_0 = 0.6;
    T_t4 = 1370;
pi_c = pi_c_arr;
tau_t = 0.45;
calculate_turboprop
figure,plot(pi_c,ratio_F_m_dot);
xlabel('pi_c');
ylabel('F/m_dot');
title('pi_c vs F_m_dot');

    M_0 = 0.6;
    T_t4 = T_t4_arr;
pi_c = 30;
tau_t = 0.45;
calculate_turboprop
```

```
figure,plot(T_t4,ratio_F_m_dot);
xlabel('T_t4');
ylabel('F/m_dot');
title('T_t4 vs F_m_dot');

    M_0 = 0.6;
    T_t4 = 1370;
pi_c = 30;
tau_t = 0.45;

    M_0 = M_0_arr;
    T_t4 = 1370;
pi_c = 30;
tau_t = 0.45;
calculate_turboprop
figure,plot(M_0,eta_O);
xlabel('M_0');
ylabel('eta_O');
title('M_0 vs eta_O');


    M_0 = 0.6;
    T_t4 = 1370;
pi_c = pi_c_arr;
tau_t = 0.45;
calculate_turboprop
figure,plot(pi_c,eta_O);
xlabel('pi_c');
ylabel('eta_O');
title('pi_c vs eta_O');

    M_0 = 0.6;
    T_t4 = T_t4_arr;
pi_c = 30;
tau_t = 0.45;
calculate_turboprop
figure,plot(T_t4,eta_O);
xlabel('T_t4');
ylabel('eta_O');
title('T_t4 vs eta_O');
```

APPENDIX - F

Get_turboprop

```
M0 = 0;
T0 = 0;
gamma_c = 0;
C_pc = 0;
gamma_t = 0 ;
C_pt = 0;
h_PR = 0;
pi_d_max = 0;
pi_b = 0;
pi_n = 0;
e_c = 0;
e_tH = 0;
e_tL = 0;
eta_b = 0;
eta_g = 0;
eta_mH = 0;
eta_mL = 0;
eta_prop = 0;
T_t4 = 0;
pi_c = 0;
tau_t = 0;

M_0 = input('Enter M_0 = ');
T_0 = input('Enter T_0 = ');
gamma_c = input('Enter gamma_c = ');
C_pc = input('Enter C_pc = ');
gamma_t = input('Enter gamma_t = ');
C_pt = input('Enter C_pt = ');
h_PR = input('Enter h_PR = ');
pi_d_max = input('Enter pi_d_max = ');
pi_b = input('Enter pi_b = ');
pi_n = input('Enter pi_n = ');
e_c = input('Enter e_c = ');
e_tH = input('Enter e_tH = ');
e_tL = input('Enter e_tL = ');
eta_b = input('Enter eta_b = ');
eta_g = input('Enter eta_g = ');
eta_mH = input('Enter eta_mH = ');
eta_mL = input('Enter eta_mL = ');
eta_prop = input('Enter eta_prop = ');
T_t4 = input('Enter T_t4 = ');
pi_c = input('Enter pi_c = ');
tau_t = input('Enter tau_t = ');
```